



TAMPEREEN TEKNILLINEN YLIOPISTO  
TAMPERE UNIVERSITY OF TECHNOLOGY

TEEMU SALO  
ALTERNATIVE MANUFACTURING AND TESTING METHODS OF  
STRETCHABLE ELECTRONICS

Master of Science Thesis

Examiners: prof. Jukka Vanhala  
asst. prof. Mikko Kanerva  
Examiner and topic approved on 27<sup>th</sup>  
September 2017

## ABSTRACT

**TEEMU SALO:** Alternative Manufacturing and Testing Methods of Stretchable Electronics

Tampere University of Technology

Master of Science Thesis, 97 pages

September 2018

Master's Degree Programme in Materials Engineering

Major: Materials Technology

Examiner: Professor Jukka Vanhala, Assistant Professor Mikko Kanerva

Keywords: Stretchable electronics, module assembly, failure mechanisms, reliability testing

Stretchable electronics are used in wearable applications to implement intelligent features. The main characteristic of stretchable electronics is stretchability enabling deformation required in wearable objects such as bandages and clothes. In this thesis, the stretchable electronics consist of elastic substrates, printed stretchable interconnections, adhesives and rigid modules with traditional electronic components. The modules on the elastic substrate form rigid islands that allow the substrate to stretch.

Stretchable electronics can endure only a specific amount of elongation before their electrical interconnections fail. Adhesion and deformation mechanisms in the joint and in the joint area of the module and the substrate affect elongation. The durability of stretchable electronics can be improved by improving adhesion and controlling the deformations via optimizing the structure of the joint and the joint area.

In this thesis, the stretchable electronics were studied on several levels. A thermoplastic polyurethane (TPU) film was used as the elastic substrate. Wettability and effectiveness of pre-treatments on wettability were examined. The substrate was investigated by measuring contact angles of droplets with a drop shape analyzer. Adhesion and peel behavior of non-conductive adhesives between the TPU-film and the rigid substrates were studied with a floating roller peel test setup. Finally, tensile testing was used to investigate deformations and elongation of the fabricated stretchable electronics samples. In the tensile test samples, width of the interconnection, the amount of the conductive adhesive and the use of a supportive frame structure were varied.

The tests presented new results that can be adopted alone or as whole. The wettability of the TPU-film improved most with a plasma pre-treatment that decreased the contact angles up to 63 percent. The peel tests showed that the sample with one cyanoacrylate adhesive with a primer had the highest momentary bond strength (0,5 N/mm). The high bond strength made the TPU-film elongate during the peeling test. Unlike the tested structural adhesives, an elastic transfer tape adhesive had the most even peeling force during the tests (between 0,2 – 0,3 N/mm) and was the easiest adhesive to process.

According to the stress peaking concept, in the tensile testing, when the samples elongated, stress concentrated close to the attached module and broke the samples. The strongest interconnection elongated 91,7 % before failure. The referred sample type had the supportive frame and conductive adhesive only under the contacts. Similarly, according to the concept, the stress exerted on this sample was more uniform compared to the other tensile test samples, which explains the good results.

## TIIVISTELMÄ

**TEEMU SALO:** Venyvän elektroniikan vaihtoehtoiset valmistus- ja tutkimusmenetelmät

Tampereen teknillinen yliopisto

Diplomityö, 97 sivua

Syyskuu 2018

Materiaalitekniikan diplomi-insinöörin tutkinto-ohjelma

Pääaine: Materials Technology

Tarkastaja: professori Jukka Vanhala, tenure-track tutkija Mikko Kanerva

Avainsanat: venyvä elektroniikka, moduulin kiinnittäminen, hajoamismekanismit, luotettavuuden testaus

Venyvää elektroniikkaa käytetään puettavissa ratkaisuisissa, joissa halutaan lisätä älykkäitä käyttöominaisuuksia. Venyvyys on venyvän elektroniikan pääpiirre, joka mahdollistaa elektroniikan myötäilyä puettavissa tuotteissa kuten laastareissa ja vaatteissa. Tämän diplomityön venyvä elektroniikka koostuu elastisesta substraatista, printatuista venyvistä johtimista, liimoista ja kovista moduuleista, joihin on kiinnitetty elektroniikkakomponentit. Kiinnitetyt moduulit elastisessa kalvossa luovat kiinteitä saarekkeita, jotka eivät estä kalvon venymistä.

Venyvä elektroniikka kestää vain rajatun määrän venytystä, ennen kuin sähköiset johtimet rikkoutuvat. Adheesio ja muodonmuutosmekanismit moduulin ja substraatin liitoksessa ja liitosalueella vaikuttavat venyvyyteen. Venyvän elektroniikan kestävyyttä voidaan parantaa lisäämällä adheesiota ja rajoittamalla muodonmuutoksia muokkaamalla liitoksen ja liitosalueen rakennetta.

Työssä tutkittiin venyvää elektroniikkaa monella eri tasolla. Elastisena substraattina käytettiin termoplastista polyuretaani (TPU) kalvoa. TPU-kalvon vettymistä ja pintakäsittelyiden vaikutusta vettymiseen tutkittiin kontaktikulmalaitteella, jolla mitattiin pisaroiden kontaktikulmia. Ei-johtavien liimojen adheesiota ja kuoriutumista TPU-kalvon ja kovien substraattien välissä tarkasteltiin  $45^\circ$  kulman kuoriutumistestillä. Viimeiseksi valmistettiin venyvän elektroniikan rakenteen sisältäviä näytteitä, joiden venymistä ja muodonmuutoksia tutkittiin vetotesteillä. Vetotestinäytteissä johtimien leveys, sähköä-johtavan liiman määrä ja kehys-tukirakenteen käyttö vaihtelivat.

Testit osoittivat uusia tuloksia, joita voidaan soveltaa erikseen tai yhdessä. TPU-kalvon vettymisen parantui eniten plasmakäsittelyllä, joka pienensi pisaroiden kontaktikulmia jopa 63 %. Kuoriutumistesteissä näytteellä, jossa käytettiin syanoakrylaattiliimaa pohjustusaineen kanssa, oli suurin hetkellinen liitoslujuus (0,5 N/mm). Korkea liitoslujuus venytti TPU-kalvoa kuoriutumisen aikana. Toisin kuin rakenneliimoilla, elastisella liimakalvolla oli tasaisin kuoriutumisljuuus (välillä 0,2 – 0,3 N/mm) ja se oli kaikista liimoista helpoin käsiteltävä.

Kehitetyn kuormittumiskonseptin mukaan vetotesteissä koekappaleiden venyessä jännitys keskittyi moduulin ja kalvon liitosalueelle, mikä rikkoi näytteet. Kestävin johdin venyi 91,7 % ennen rikkoutumista. Kyseisessä näytteessä käytettiin kehys-tukirakennetta ja sähköä-johtavaa liimaa vain kontaktien alueella. Vastaavasti kuormituskonseptin mukaan jännitys jakautui näytteessä tasaisemmin kuin muissa vetotestinäytteissä, mikä selittää hyvät tulokset.

## PREFACE

This Master's thesis was written at Department of Electronics and Communications Engineering at Tampere University of Technology. The material for the thesis was collected in EETU project, which was funded by Tampere University of Technology, the Regional Council of Satakunta, the Town of Kankaanpää and Clothing Plus Oy.

I would like to thank my thesis examiners Professor Jukka Vanhala and Assistant Professor Mikko Kanerva for support and guidance. In addition, I want to thank M.Sc. Aki Halme and M.Sc. Pekka Iso-Ketola from TUT Personal Electronics Group and people of Clothing Plus Oy for guidance and the great work atmosphere. I would also like to thank M.Sc. Malin Kraft, M.Sc. Sanna Siljander and others from Department of Material Science at Tampere University of Technology for valuable cooperation. Moreover, I thank Anne Mäkiranta and rest of Forciot Ltd for advices and feedback.

Lastly, I want to thank my family and friends in Renko and in Tampere for endless support during this work and over the years.

Kankaanpää, 29.08.2018

Teemu Salo

## CONTENTS

1.	INTRODUCTION .....	1
2.	STRETCHABLE ELECTRONICS .....	2
2.1	Stretchable interconnections .....	2
2.1.1	Conductive inks.....	5
2.1.2	Substrates .....	7
2.2	Modules.....	11
3.	ATTACHMENT OF ELECTRONICS .....	12
3.1	Structural adhesives.....	12
3.1.1	Epoxies.....	12
3.1.2	Polyurethanes .....	14
3.1.3	Cyanoacrylates .....	15
3.1.4	Electrical connection with NCA .....	16
3.2	Elastic adhesives .....	16
3.3	Conductive adhesives.....	17
3.3.1	Isotropic conductive adhesives .....	17
3.3.2	Anisotropic conductive adhesives.....	19
3.4	Soldering .....	20
3.5	Compression joint .....	21
3.6	Encapsulation .....	22
4.	ADHESION .....	24
4.1	Phenomenological theories of adhesion.....	26
4.1.1	Adsorption theory .....	26
4.1.2	Mechanical theory.....	27
4.1.3	Diffusion theory .....	28
4.2	Deformation mechanisms of polymers .....	29
4.2.1	Amorphous polymers.....	29
4.2.2	Semicrystalline polymers.....	30
4.2.3	Block copolymers .....	31
4.3	Failure of stretchable joint.....	32
4.3.1	Failure patterns.....	32
4.3.2	Interfacial failure.....	34
5.	METHODS .....	37
5.1	Surface treatments and wetting .....	37
5.1.1	Theory of surface tension and energies.....	37
5.1.2	Contact angle measurements.....	38
5.1.3	Roughening .....	40
5.1.4	Plasma pre-treatment.....	41
5.1.5	Heat treatment .....	42
5.2	Peel tests.....	42
5.2.1	Examination of failure mechanisms.....	45

5.3	Tensile testing .....	47
5.3.1	Screen-printing of interconnections .....	47
5.3.2	Modules.....	49
5.3.3	Joining of ACF samples .....	50
5.3.4	3D-printed frames .....	51
5.3.5	Measurement of the samples.....	52
6.	RESULTS .....	56
6.1	Surface treatments and wetting .....	56
6.2	Peel tests.....	57
6.2.1	Average maximum values of peel samples.....	57
6.2.2	Epoxy adhesive samples .....	60
6.2.3	Polyurethane adhesive samples.....	62
6.2.4	Cyanoacrylate adhesive samples.....	65
6.2.5	Pressure sensitive adhesive samples .....	68
6.2.6	Failure modes of peel test samples .....	70
6.3	Tensile testing with modules.....	73
6.3.1	Reading of module test graphs.....	73
6.3.2	Results of tensile tests with modules .....	74
6.3.3	Deformations of tensile test samples .....	79
7.	DISCUSSION.....	82
7.1	Surface treatments and wetting .....	82
7.2	Peel tests.....	82
7.2.1	Epoxy and polyurethane adhesive samples.....	83
7.2.2	Cyanoacrylate adhesive samples.....	84
7.2.3	Pressure-sensitive adhesive tape samples .....	85
7.3	Tensile testing .....	86
7.3.1	Effect of the interconnections to failure of the samples.....	86
7.3.2	Effect of the frame to failure of the samples.....	89
7.3.3	Effect of the ACF to failure of the samples .....	93
8.	CONCLUSIONS AND FOLLOW-UP WORK.....	95
8.1	Conclusions .....	95
8.2	Follow-up work .....	96
	REFERENCES.....	97

## LIST OF SYMBOLS AND ABBREVIATIONS

ACA	anisotropic conductive adhesive
ACF	anisotropic conductive film
CNT	carbon nanotube
CoV	Coefficient of variation
DiCy	dicyandiamide
E-textile	electronic textile
ICA	isotropic conductive adhesive
IPA	isopropyl alcohol
NCA	non-conductive adhesive
PCB	printed circuit board
PU	polyurethane
SD	standard deviation
SMD	surface-mount sevice
$T_g$	glass transition temperature
TPU	thermoplastic polyurethane
VOC	volatile organic compounds
$\Delta\varepsilon$	change of strain along linear portion
$\Delta\varepsilon_l$	change of strain in longitudinal direction
$\Delta\varepsilon_n$	change of strain in perpendicular direction
$\Delta\sigma$	change of stress
$\Delta L_0$	change of length
$\dot{\gamma}$	strain rate
$\gamma_{LV}$	tension of liquid and vapor interface
$\gamma_{SL}$	tension of solid and liquid interface
$\gamma_{SV}$	tension of solid and vapor interface (surface tension)
$\gamma_{LV}^D$	dispersion portion of the liquid and vapor interface
$\gamma_{LV}^P$	polar component of the liquid and vapor interface
$\gamma_{SV}^D$	dispersion component of the solid and vapor interface
$\gamma_{SV}^P$	polar component of the solid and vapor interface
$\sigma$	engineering stress
$\varepsilon$	strain
$\eta$	viscosity
$\theta$	angle of peel
$\theta_{eq}$	contact angle of equilibrium point of the three interfaces
$\mu$	Poisson's ratio
$\rho$	material resistivity
$\tau$	shear stress
$A$	area
$b$	width
$c$	intersection of a line and y-axis
$E$	tensile modulus (Young's modulus)
$F$	force (load)
$G_p$	momentary peel strength
$I$	current

$L$	length
$L_0$	original length
$m$	slope of a line
$R$	resistance
$R_1$	resistance of surface mount resistor
$R_2$	resistance of printed interconnection
$V$	voltage
$V_1$	output voltage of system
$V_2$	voltage over printed interconnection
$W$	work of adhesion
$x$	$x$ coordinate
$y$	$y$ coordinate



# 1. INTRODUCTION

The stretchable electronics are one integration level of electronics, which are widely used in wearable applications. The stretchable electronics are originally evolved because the traditional electronics are rigid and are not easily compatible with wearable materials. As a matter of fact, first wearable electronics were clothes that had standard electronic components sewed in them. Like the snowmobile suit prototype by Reima-Tutta in 2000, the electronics textile (e-textile) was already multifunctional at that time. However, the electronics and textile had low integration level and washability and power supply were recognized issues. [1] [2]

Nowadays, e-textiles have better usability because the stretchable electronics have increased the integration level. The stretchable electronics comply tens of percent stretching, and can be used alone on the skin as bandages or as more permanent applications in clothes. There are many methods to produce the stretchable electronics. The stretchable system can solely consist of stretchable components, or there can be small rigid islands on elastic substrate. The systems are complex and mechanical properties of components commonly vary inside the systems. The mechanical differences can lead to premature breakup of stretchable electronics, where cracks and weak adhesion accomplice failure mechanisms. [2] [3] [4] [5]

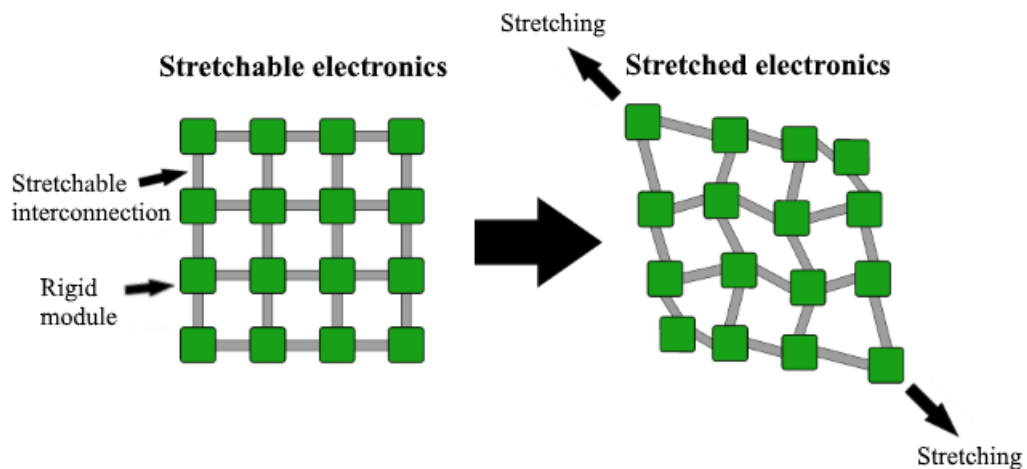
The failure mechanisms of stretchable electronics can be studied in various levels. The properties of single components can be inspected separately and adhesion of adhesives can be tested. In addition, durability of whole stretchable electronics can be studied by following electrical properties of the system under loading.

In this study, wetting properties of elastic substrate before and after pre-treatments are studied with a drop shape analyzer. Later on, adhesion between the substrate and adhesives are examined with a floating roller peel test setup. Finally, strain tests are conducted to series of stretchable electronics structures to investigate how printed interconnections, amount of adhesion and reinforcing of the structures affect to durability. From the series, the most elongating stretchable electronics structure before electrical failure is founded.

This thesis focus on stretchable electronics that consist of rigid islands and elastic substrate, which are discussed in Chapter 2. Chapter 3 introduces existing attachment methods of the rigid islands on the substrate, and Chapter 4 considers adhesion and failure of stretchable electronics. Chapter 5 review the used methods and Chapter 6 shows the results. Finally, Chapter 7 presents conclusions about the results.

## 2. STRETCHABLE ELECTRONICS

Stretchable electronics are electronic devices that can stretch and return to their original shape without breaking up [3]. There are few approaches to make stretchable electronics where one way is to use rigid modules and stretchable interconnections. Modules are component islands, which are small enough not to influence negatively to the stretchability. The interconnections are conductive pathways between the modules and make the device stretchable, as seen in Figure 1. [4]



*Figure 1. Stretching behavior of stretchable electronics.*

The benefits of these kinds of stretchable electronics are compatibility with existing manufacturing methods and the possibility to use off-the-shelf electronic components to make complex modules [4]. The modules and stretchable interconnections can be done with standard printed circuit board (PCB) technology, which requires no further adaption to make PCB based modules. In addition, the interconnections can also be fabricated with printing or textile manufacturing methods like screen-printing or knitting [4] [6] [7].

### 2.1 Stretchable interconnections

In the stretchable electronics, interconnections are conducting wires between rigid modules where the interconnections can stretch tens of percent over their original length. There are two principles to realize stretchable interconnections, where the other way is to use stretchable conductive materials and another is to shape the interconnections to a stretchable form. Furthermore, it is possible to shape highly stretchable material to a stretchable shape. [4] [8]

Stretchable conductive inks and pastes are one solution to make interconnections stretchable. They consist of stretchable polymer matrix and conductive filler or polymer [9] [10] [11]. Under stretching, the matrix of the ink elongate with the substrate, which makes it possible to print versatile patterns without shaping the interconnections. However, the elongation increases the length of the interconnections, which further increases the resistance of linear conductors according Formula 1:

$$R = \frac{\rho L}{A}, \quad (1)$$

where  $R$  is the resistance of a track,  $\rho$  is material resistivity of the track,  $L$  is length of the track and  $A$  is area of track's cross-section. [12] Moreover, the elongation also shrinks the cross-section area and deforms tracks internal structure, which also affect to resistance of the track. [8]

Other way to make interconnections stretchable is to modify the shapes of the tracks. They can be shaped as two-dimensional springs that open up during stretching. There are designed 2D-patterns, where the meander horseshoe shape is the most stretchable interconnection shape. [6] The stretchable shape allows the use of non-stretchable materials in the interconnections because of the elongation aims first to straighten the meandering shape before too much straining the material. This allows different materials and manufacturing methods than printable conductive inks. For instance, copper film is widely used material for meandering interconnections [4] [5]. The benefits of copper film are low resistance values and the possibility to use lamination, soldering or other conventional electronic fabrication methods that require higher temperatures. [5] However, stretchability of the copper meander rely only on the meander shape and has more design restrictions compared to printed interconnections.

Third method to create stretchable interconnections between modules is to use conductive yarns in wearable electronics. The conductive yarns can be fabricated with many ways, where a coating with silver is a widely used method. Also, conductive fillers like carbon nanotubes (CNTs) can be blended to raw material of the yarn during a spinning. In addition, fibers can be entirely made from conductive material, such as stainless-steel fibers. [13]

An advantage of conductive yarns is that they can be added to the fabric during normal production to make conductive fabric. A conventional fabric can be also enhanced with conductive yarns with sewing or embroidery finishes. The conductive yarns are used as interconnections but they can be used as sensors, for example strain sensors have been done with knitted silver-coated yarns. [7] [13] Table 1 shows an example about knitted interconnections, screen-printed and laminated interconnections and how they behave during straining:

**Table 1.** Stretching behavior of different interconnections.



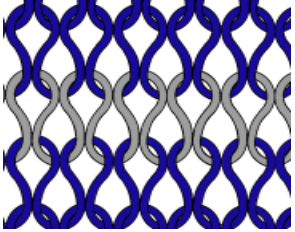
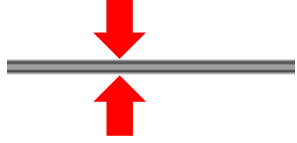

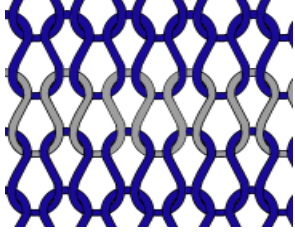
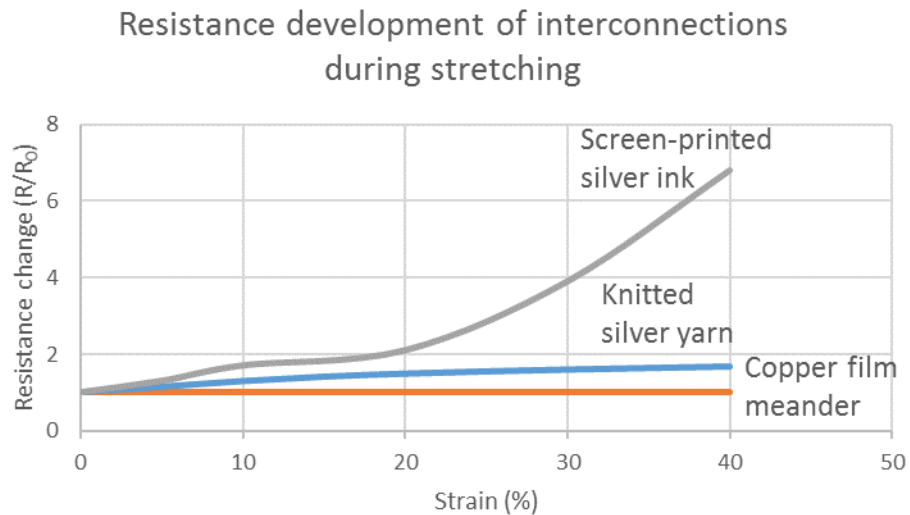
	Screen-printed silver ink	Copper film meander	Knitted silver yarn
Substrate	Elastomer film	Elastomer film	Knitted fabric
Not Stretched			
Stretched			

Table 1 shows that the shape of screen-printed interconnections change only little by small narrowing. The copper meander and knitted yarn geometries are spread and wavy structures have opened up. [4] [7] [14] Because of the shape and elongation of interconnections affect resistance values, it is important to know resistance-strain response. Figure 2 presents the relative resistance increase in relation to strain.



**Figure 2.** Resistance change during straining of interconnections [4] [7] [14]

As seen in Table 1 and in Figure 2, the shape of printed silver ink interconnection is stable and the elongation increases resistance during stretching [14]. In lower elongations the structure of the ink elastically stretches and the resistance does not increase permanently. In higher elongations, the interconnection undergoes permanent deformation and cracks are created perpendicularly to the strain direction. The cracks increase the resistance and finally cause the failure. [8] However, after the release of strain the interconnection shrinks back to its original measures and the cracks are pressed together, which further can recreate conductivity in the interconnection. With some conductive inks cracked interconnection can be recovered with annealing [11].

During stretching of copper meanders, the meander shapes straighten up without major bulk deformations. In addition, the resistance of the meanders stays constant as long as the meanders can stretch with the substrate. After the critical point when the meanders cannot straighten up anymore, they start to crack and quickly break. [4]

The interconnection from silver-coated yarn is knitted as consecutive loops in the knitted fabric. A knitted structure shapes the conductive yarn to a meandering row, where the loops have contact with each other. Stretching separates the loops of conductive yarn, which affect to conductivity of the interconnection. The loops in separation form for interconnection which resistance stays approximately constant like for the copper meander interconnection. [7]

When different stretchable interconnections are compared, the printed interconnects are the most multifunctional ones. The printing does not limit the shape of interconnections and there are various kinds of conductive inks and substrates available. [6] [13] Furthermore, after printing, the stretchable films with conductive patterns are laminated over textile substrate to create electronic textiles (e-textiles) [5]. In this thesis, the stretchable interconnections are screen-printed with conductive silver ink on elastic thermoplastic polyurethane (TPU) film.

### **2.1.1 Conductive inks**

There are various kinds of conductive inks in the market, which have different compositions. The composition depends mainly on the printing method of the ink. For instance, conductive inks for screen-printing are very viscous to prevent excess spreading in the process. Generally, main composition of screen-printing inks consists of polymer resin, conductive fillers, solvent and additives. [13] [15]

Polymer resin is used as a binder in conductive ink to create a polymer matrix. The polymer matrix works as “backbone structure” and dominates in mechanical properties of the ink. The matrix is cured in a heat treatment, which is done after printing. The cured matrix can go through high deformations by elongating viscoelastically. It binds conductive filler particles of the ink inside the matrix which are further formed to conductive pathways.

The conductive pathways deform with the matrix that induce the viscoelastic behavior also to the conductivity of the ink. [14] [11]

Fillers in conductive inks are the components that make the inks conductive. These fillers are made from highly conductive materials, such as silver, graphene or CNTs. Especially silver fillers are used in the inks and pastes because of excellent optical and electrical properties. Furthermore, it is less expensive conductive filler material than other highly conductive metals. [9] [16] The shape of fillers vary and they can be designed like flakes or round particles in different sizes. For example, screen-printable inks have micro-size conductive fillers for which size varies between  $2\mu\text{m}$  –  $20\mu\text{m}$  [8]. There are either one type of conductive filler in ink [10] or more than only one kind, which can improve conductivity of ink [11].

Solvents are used in conductive inks to decrease viscosity and make the inks more homogenous and processable. Liquids such as water, glycerol, ethanol and other volatile organic compounds (VOCs) are used as solvents, which are evaporated away during the heat treatment after printing. Time and temperature of the heat treatment vary because solvents have different evaporation properties. Furthermore, solvents can be absorbed into surface of the substrate, which may influence adhesion between the ink and substrate. [8] [15]

A wide amount of additives are used to improve properties of conductive inks. There are for instance stabilizing agents that prevent premature agglomeration of the conductive fillers that further increases the useful life of the inks [15]. In another case, conductivity and stretchability of polyvinyl alcohol (PVA) based conductive inks are increased by adding phosphoric acid ( $\text{H}_3\text{PO}_4$ ) to the polymer blend [9].

In this thesis, stretchable interconnections are made from conductive silver ink CI-1036, manufactured by ECM. The CI-1036 ink is polyurethane (PU) based ink that is highly conductive and flexible, and it is designed for creasable circuit traces [17] [18]. More detailed properties of the conductive ink CI-1036 are listed in Table 2:

**Table 2.** *Properties of conductive silver ink CI-1036. [18]*

Viscosity (cP)	10000
Total solids content (%)	66
Electrical resistance (ohms/square, 25,4 microns)	<0,010
Typical curing time (min)	10

Typical curing temperature (°C)	120
Amount of VOC (g/l)	703,8

From Table 2 can be noticed that a high amount of VOC based solvent are used in the conductive ink CI-1036. In spite of that, viscosity of the ink can be compared to thick syrup [19]. The total solids content describes how much conductive silver flakes ink has, which is 66 % here. Some conductive inks have clearly higher amount of conductive fillers and better conductive properties. However, the amount of conductive filler is commonly trade-off between conductive and mechanical properties, which means that the ink CI-1036 is designed mechanically better and more stretchable.

After the printing, the conductive inks are heat treated. During the heat treatment, solvents are evaporated and polymer resin starts to cross-link. The cross-linking causes strong (chemical) bonds between the binder polymers, filler particles and surface of the substrate and affect greatly the adhesion between the ink and substrate. [8] [13]

During the heat treatment of conductive inks, the conductivity is often formed at low temperatures (<150 °C), which are enough for polymer to form the matrix and fillers to aggregate and sinter. The low temperatures also make it possible to use plastics or other sensitive substrates. However, the low temperatures require correspondingly longer heat treatments. For example, printed TPU-films are heat treated at 130 °C for 30 min in a heating chamber. [6] [13] [20]

The sintering is a phenomenon where metal particles are diffused together due to heat. At low temperatures, the silver particles in the conductive ink are sintered at grain boundary level, which requires less heat than total bulk level diffusion. The sintering is especially related to conductive inkjet inks because they do not have strengthening polymer resin matrix and electrical and mechanical properties only rely on sintering. [21]

### 2.1.2 Substrates

Substrate is the bulkiest component in stretchable electronics and dominate how stretchable the system is. The electronics itself can be rigid islands or flexible films, which are added over the stretchable substrate. Interconnections can be printed on the substrate using stretchable inks, for which elongation and recovery is after all determined by substrate. Total stretchability and other mechanical and chemical properties of the substrate are essential for stretchable electronics because of the rest of the stretchable electronics is built over it. [3] [14]

All substrates that can deform elastically are not stretchable. Substrates such as some fabrics and plastics are classified as stretchable because they can elastically deform more

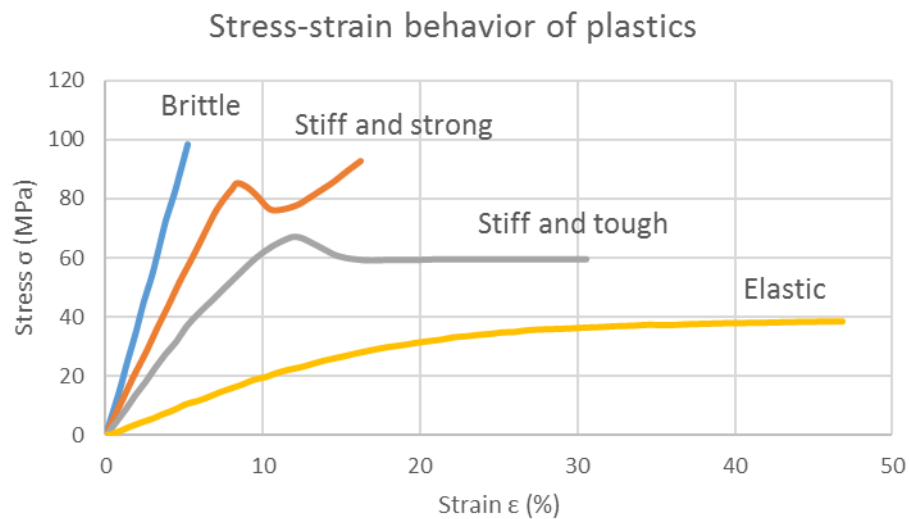
than few percent. Some substrates are not truly stretchable and are categorized as bendable substrates. [3] The stretchability is often determined with a tensile test and finally stress-strain curves, where parameters stress and strain are used:

$$\sigma = \frac{F}{A}, \quad (2)$$

where  $\sigma$  is the engineering (nominal) stress,  $F$  means force and  $A$  is the initial cross-sectional area of the sample. Strain can be estimated during tensile test as:

$$\varepsilon = \frac{\Delta L_0}{L_0}, \quad (3)$$

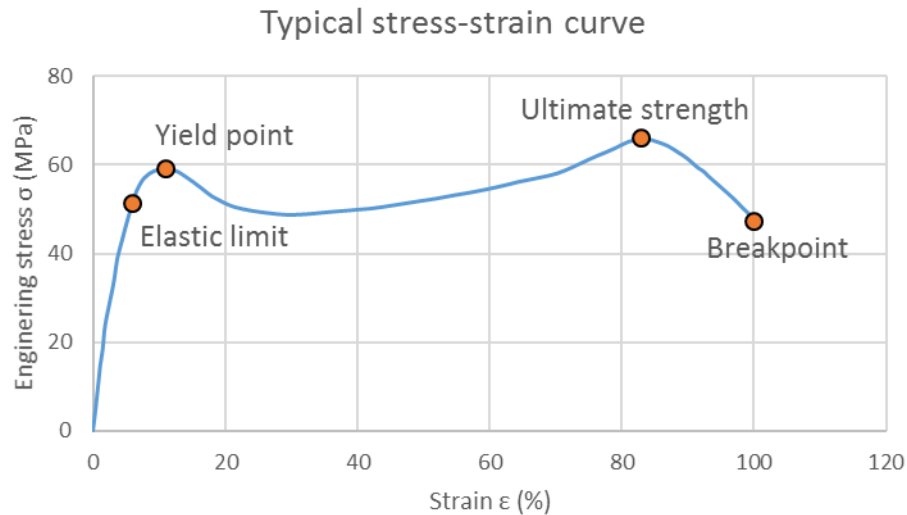
where  $\varepsilon$  is the strain,  $L_0$  is original length of the sample and  $\Delta L_0$  is the change in the sample's length. [22] Plastics have different stress-strain behavior because of different relations between the stress and the strain components. Example curves are presented in Figure 3.



**Figure 3.** Stress-strain behavior of different plastics.

The behavior of plastics varies from brittle to hyper-elastic, which can be observed in stress-strain curves in Figure 3. Brittle plastic endure stress well but break fast at low strain. On the contrary, elastic plastics elongate tens of percent by a low amount of stress. Generally, processable hard thermoset plastics are brittle and elastomers are highly elastic. Between brittle and non-linear stress-strain curves, there are irregular curves that indicate moderate non-linearity. Usually, multiple times processable thermoplastic polymers have a yield point, which is shown in more detail in Figure 4.





**Figure 4.** Typical stress-strain curve of thermoplastic polymer.

In Figure 4, there is a typical engineering stress-strain curve of thermoplastic polymer. The curve shows some specific points during a tensile test; elastic limit, yield point, ultimate strength and breakpoint. At small strains the plastic has linear elasticity and behaves elastically until the elastic limit. After the elastic limit elastic deformation changes to plastic deformation and covers the yield point. Definition of the elastic limit and yield point vary and in some cases they can be understood to be the same. Elastic deformation is reversible and the plastic deformation is irreversible, which is the reason why a stretchable substrate should be linear or non-linear elastic. [3] [22] [23] Tensile modulus (Young's modulus) and Poisson's ratio are used to describe elasticity of plastic:

$$E = \frac{\Delta\sigma}{\Delta\epsilon}, \quad (4)$$

where  $E$  is the tensile modulus,  $\Delta\sigma$  is the elastic change of the stress and  $\Delta\epsilon$  is the change of the strain along linear portion [22] [23]. Generally, plastics have high strain at low stress values and, hence, low tensile modulus [3]. Poisson's ratio is defined the following way:

$$\mu = -\frac{\Delta\epsilon_n}{\Delta\epsilon_l}, \quad (5)$$

where  $\mu$  is the Poisson's ratio,  $\Delta\epsilon_n$  is a change of strain in a selected perpendicular direction and  $\Delta\epsilon_l$  is an increase of strain in a selected longitudinal direction. Poisson's ratio of elastomers is around 0,5, which means that perpendicular dimension can change half amount of the increase in the longitudinal direction. [22] [24] In some stretchable electronics applications, the Poisson's effect during stretching can decrease the resistance of

interconnections by improving electrical contacts inside the interconnections in the lateral direction directions. [13]

After reaching the yield point, plastics have plastic deformation. Thermoplastic plastic undergoes neck formation and cold drawing, where structure of plastic is thinned and elongated. The first elongation phase is followed by strain hardening that strengthen the plastic. Due to the deformation, plastic reaches ultimate strength point, where it reaches the maximum amount of stress. Later on after the ultimate strength point the plastic quickly fails at breakpoint. [22] [23] [25]

Substrates are made from various plastics, for example polyvinyl chloride, polyimide, polydimethylsiloxane, and thermoplastic polyurethane (TPU) are used [4] [13]. The chosen substrate in the thesis is highly stretchable TPU-film Platilon U 4201 AU by Epurex Films. Generally, TPU films are heat laminable, biocompatible and cost-effective. Because of their properties, TPU substrates are widely used in stretchable electronics studies. Furthermore, TPU film is already used in the traditional textile industry in the manufacturing of wet proof clothing. [5] [6] [20]

Chemically, TPU is categorized as copolymer. It is composed of alternating hard and soft segments for which the ratio defines how rigid or flexible the film is. The hard crystalline segments are achieved by urethane linkages between di-isocyanates and diols or diamine chain extenders. The soft amorphous segments are opposite and are diols. For instance, ester or ether diols are often used, which affects mechanical properties of a film. For instance, diols with ether groups are used for elastic TPU films. [26] [27]

The TPU-film Platilon U 4201 AU by Epurex Films is blow-molded ether grade TPU-film that has excellent hydrolysis resistance and thermoformability. Its thickness is 100  $\mu\text{m}$  and it does not contains plasticizers. Further properties of the substrate are shown in Table 3:

**Table 3.** *Properties of TPU-film Platilon U 4201 AU [28].*

Density ( $\text{g}/\text{cm}^3$ )	1,15
Softening Range ( $^{\circ}\text{C}$ )	155-185
Hardness (Shore A)	87
Tensile Stress at Break (MPa)	60
Tensile Stress at 50 % Strain (MPa)	5-7
Tensile Strain at Break (%)	550

The TPU-film has relative high softening range, which makes it compatible with conductive ink CI-1036. The film has higher softening range than the curing temperature of the ink. Also, the film can elongate even 550 % before break, which ensures that the film does not limit the stretchability of printed patterns. [28]

## 2.2 Modules

Modules are intelligent islands in stretchable electronics that are made from rigid two-sided PCBs. The top side of PCBs are loaded with integrated circuits (ICs) or other electronic components. On the other side, there are contact pads that are attached on stretchable interconnections on substrate. Multiple small modules, which each are designed for specific applications, work together and create a highly functional PCB matrix. [4] [5]

Typical PCB is made from FR4 composite board that is based on epoxy resin and glass fiber, which makes it heat resistant and an electrical insulator. The board is in the most cases covered with an additional solder mask layer for which the purpose is to limit spreading of molten solder and prevent short circuits between contacts. Commonly, the solder mask is made from epoxy resin that is screen printed on the board. [29] Because of the solder mask prevents excess leaking of liquid solder, it can be also somewhat inactive with other liquids. The passivity of the solder mask can affect flowing and the attachment properties of adhesives and further the amount of adhesion.

The modules are also tuned by changing their shapes. The shape is an appearance matter but also affects durability of the stretchable electronics matrix. During stretching of matrix, the strain concentrates close to the module and the local stress in the boundary area is higher than elsewhere. Areas under higher stresses break earlier than areas that have lower stress. There are many possibilities to shape the modules and decrease the stress concentration phenomenon. For example, round shaped modules [5] and clover shaped structures [30] are used to minimize mechanical stresses in the matrix.

### 3. ATTACHMENT OF ELECTRONICS

Nature of the module and substrate are very different and still they have to be attached together. Because of the differences, stress concentrations are formed around the modules and makes the transition area of the module and the substrate vulnerable to break [5]. The durability of the boundary area can be increased by making a joint endure more stress or distribute the stress over a wider area. The both solutions can be realized by using non-conductive adhesives (NCAs) in the joint. The joint is made stiff with non-conductive structural adhesives that fasten modules and a stretchable substrate together. On the other hand, the stress is transmitted over a wider area with non-conductive elastic adhesives. In addition to NCAs, the module can be mechanically attached with a compression joint that uses screws, bolts, rivets or other fasteners. [31] [32] [33]

While the module is attached firmly on the substrate, also electrical connections between the module and printed interconnections must be created. The electrical connections can be formed by locking contact pads together with NCAs or compression joint. More refined electrical connections are made with conductive adhesives and soldering. However, the conductive adhesives and solders have poor mechanical properties and they require non-conductive adhesives (NCAs) to be used with them. [5] [32] [33]

After attachment of the module on the substrate, the module and the surrounding area need to be protected from mechanical and electrical damage. The encapsulation is done with low viscose adhesive or polymer resin that forms a bubble over the module. Another way is to make casing with other manufacturing methods like 3D printing or injection molding. [32] [34]

#### 3.1 Structural adhesives

Structural adhesives are categorized from other adhesives by their ability to endure high static and dynamic loads. Because of their durability, they can be the only load bearing component in the joint. Structural adhesives are one or two-component thermoset plastics, which are, for example anaerobic adhesives, epoxies, polyurethanes, or cyanoacrylates. [35] [36] [37] [38] This thesis is focused on epoxy, polyurethane and cyanoacrylate adhesives.

##### 3.1.1 Epoxies

Epoxy adhesives involve a thermoset epoxy resin for which molecules consist of reactive oxirane rings. The ring is opened with a hardener that cross-links the resin into infusible matrix. The epoxy resin is made from glycidyl epoxy or non-glycidyl epoxy, where diglycidyl ether of bisphenol-A (DGEBA) is the most often used epoxy resin. There are

also many options for the hardener, for which the selection affects physical and chemical properties of epoxies. [38] [39] [40] [41]

The curing reaction of the resin and the hardener happens by either condensation or catalytic reactions. The condensation based curing is especially sensitive, because of the condensation reaction must be carried out completely for a durable matrix. The condensation curing reaction is the reason why mixing and dosing of two-component epoxy adhesive must be precise. There are also one-component epoxy adhesives, where latent hardener dicyandiamide (DiCy) is added to the epoxy resin. The DiCy is insoluble to the epoxy resin at ambient temperatures, but at elevated temperatures starts to react with the resin. [38] [39] [40]

One and two component epoxies are non-sensitive to impurities, which makes them compatible with various additives. Additives such as fillers, plasticizers and accelerators are used to enhance final properties of the epoxies. Epoxies have generally high bond strength and gap-filling properties. They are also heat resistant, which makes them useful in electronics applications. [38] [39] [40] Table 4 shows two different two-component epoxies by Permabond that are used in this thesis:

**Table 4.** *Permabond epoxy adhesives [42] [43].*

	Permabond ET515	Permabond MT382
Adhesive type	Two-component epoxy	Modified two-component epoxy
Handling time (min)	20-30	105-120
Full cure (d)	3	≥3
Curing temperature (°C)	25	25
Hardness (Shore D)	30-50	20-30 (Shore A 55-85)
Elongation at break by ISO37 (%)	20-40	150-200

Table 4 presents two-component epoxy adhesives ET515 and MT382 by Permabond. The ET515 adhesive is transparent, semi-flexible and toughened epoxy adhesive that has max 40 percent elongation before failure. Correspondingly, the MT382 is more elastic black-colored and modified epoxy adhesive. The MT382 has lower shore D hardness value and has to be elongated over 150 percent to break. Furthermore, the MT382 can be also used for sealing purposes. [42] [43]

### 3.1.2 Polyurethanes

Polyurethane (PU) adhesives have a molecular backbone that is based on common polyurethane linkages. Otherwise these polymers can be modified variously like the epoxy adhesives, which makes PU adhesives versatile. PUs are generally made via addition reaction of polyol and isocyanate groups, which does not produce any side products. By choosing between polyester polyols and polyether polyols, PU adhesives are made rigid or flexible. The polyester polyols are used for rigid PUs, which have good adhesion and high hardness. The polyether polyols are used for flexible PUs, which have low modulus. [38]

Commonly used isocyanates with the polyols are methylene diphenyl di-isocyanate (MDI) and toluene di-isocyanate (TDI). In addition to the reaction with polyols, isocyanates tend to react with water molecules to form urea linkages and carbon dioxide, where the generated gas bubbles can weaken the adhesive. However, the reaction with water can be also useful and moisture curing is one way to cross-link the PU adhesives. [38]

By using only diols and di-isocyanates, which have two reactive groups, linear TPU is formed. These TPUs are especially used in stretchable films. Highly cross-linked thermoset PU adhesives are made from by either using an excess amount of isocyanate or using multifunctional polyols and isocyanates. [38]

PU adhesives have high bond strength and excellent gap-filling properties, likewise epoxies do. Furthermore, they are inherently flexible and resistant to moisture after bonding. On the other hand, they are sensitive to moisture during bonding and have poor temperature resistance compared to epoxies. [38] PU adhesives are, for example, used in automotive applications. [38] In this thesis, a PU adhesive Scotch Weld™ DP610 by 3M is used, which is introduced Table 5:

**Table 5.** 3M Scotch Weld DP610 polyurethane adhesive. [44]

	3M Scotch Weld™ DP610
Adhesive type	Two-component polyurethane
Handling time (min)	120
Full cure (d)	7
Curing temperature (°C)	23

The DP610 adhesive is clear and flexible two-component PU adhesive that is suitable for bonding of most plastics, glass and painted or primer treated metal surfaces. DP610 attains its full cure in 7 days, which can prolong with some substrates to even 30 days. [44]

### 3.1.3 Cyanoacrylates

Cyanoacrylates are structural adhesives that are also known as instant glues. They are chemically 2-cyanoacrylates with additional alkyl group like methyl or ethyl. The cyano groups withdraw electrons eagerly, which initiate chain polymerization reaction of the resin. The chain polymerization starts from moisture and realizes in seconds. After the initiation, the polymerization of cyanoacrylate propagates until; the monomers are exhausted, their diffusion is hindered by a high viscosity level or strong acid is brought to the system. [38] [45]

Cyanoacrylates have rather good adhesion over many substrates. Methyl cyanoacrylates are viscous and good for bonding of metal and rigid surfaces. Ethyl cyanoacrylates are other commonly used cyanoacrylates, which are used for plastic and elastomer substrates. For especially difficult materials to bond, there are primers that are applied and dried over bondable surfaces before spreading of the adhesive. The primers enhance the polymerization of the cyanoacrylates and improve adhesion between surface and adhesive. [19] [38]

Cyanoacrylates are fast-curing one-component adhesives with a high bond strength over various substrates, which makes them convenient to use in many applications. However, they are brittle by nature and sensitive to impurities that limits the usage of additives with them. [38] [45] Table 6 presents Loctite 406 instant glue that is used in thesis:

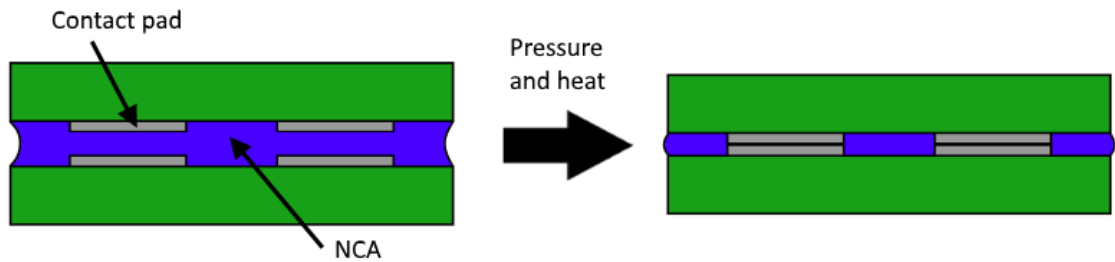
**Table 6.** *Loctite 406 cyanoacrylate adhesive. [46]*

	Loctite 406
Adhesive type	Ethyl cyanoacrylate
Handling time (s)	<5-45
Full cure (d)	$\geq 1$
Curing temperature ( $^{\circ}\text{C}$ )	22

The ethyl cyanoacrylate adhesive Loctite 406 is designed to bond plastics and elastomers. The instant glue reacts with atmospheric moisture and bonds plastics in  $\sim 5$  seconds and steel in  $\sim 45$  seconds. For especially difficult plastics to bond, surfaces can be treated with primer Loctite SF 7239 before the Loctite 406 adhesive. Loctite SF 7239 is an organic amine derivate and is meant for bonding of polypropylene, thermoplastic rubber materials and other low surface energy plastics. After spreading, the primer is let to evaporate and, then, surface is bonded in 10 minutes. [46] [47]

### 3.1.4 Electrical connection with NCA

Structural adhesives are fundamentally inflexible non-conductive adhesives that besides non-conductive bonding, are also used to create electrical interconnections. The joint is realized by covering a substrate thoroughly with the adhesive and pressing substrates over the substrate. The substrate, component and their interconnections are clamped until the adhesive is fully cured and binds the conductive and non-conductive areas together. An example of an NCA joint is presented in Figure 5. [31]



*Figure 5. Forming of an NCA joint.*

Electrical interconnections in NCA joints are purely maintained by compression force that is caused by pressure from fabrication of the joints and shrinking of NCAs. Electrical properties of interconnections depend on the mechanical contact pressure between the contact pads. NCAs prevent short-circuit in the joint because they do not have conductive fillers. With the same reason, they have low cost compared to other adhesives in the electrical industry. [31] [32]

## 3.2 Elastic adhesives

The idea of elastic adhesives in a joint is to tack tightly on surfaces and to follow movement of the surfaces. Elongation of a stretchable substrate is transferred to the adhesive and is decreased near the rigid surface of module. One type of an elastic adhesive that is used in this thesis is pressure-sensitive adhesives (PSAs).

PSAs are viscoelastic-behaving adhesives that are manufactured in form of tapes and films. They have rigid support films that make them possible to cut and easy to apply over a substrate. Furthermore, they are easy to use because they do not require mixing or activation before use. During setting the PSA, light pressing is enough to make the adhesive to flow and adhere with the surfaces. [48] [49]

PSAs can be made by blending tackifier resin and rubber over a rigid support film. Terpenes or petroleum products are used as tackifier resins, where terpenes have the best



properties but are expensive. In addition, various rubbers are added in the adhesives, for example natural rubber and styrene-isoprene-styrene (SIS). Moreover, PSAs are also manufactured merely from acrylates, which have excellent properties and are used in high-quality tapes. [48] [49] [50]

Generally, PSAs have uniform thickness and are easy to apply. Also, bonding can be reversible so that the adhesive can adhere again over the stretched substrate if it is peeled off by excess elongation. However, their peeling and shear strengths are poor compared to structural adhesives and they are unsuitable for rough surfaces. [37] [48] [49] The tested PSA in thesis is adhesive transfer tape 8132LE by 3M, which is introduced Table 7.

*Table 7. Main properties of adhesive transfer tape 8132LE [51].*

	Adhesive transfer tape 8132LE
Adhesive type	High strength acrylic
Adhesive thickness ( $\mu\text{m}$ )	58
Bonding temperature ( $^{\circ}\text{C}$ )	38-54

The 8132LE tape is excellent for bonding low surface energy plastics. It has liners on both sides for selective die-cutting, which also makes it easy to use. The adhesive transfer tape can be bonded at atmospheric temperature, but a higher bonding temperature (between 38  $^{\circ}\text{C}$  and 54  $^{\circ}\text{C}$ ) and firm pressure increase the bond strength. [51]

### 3.3 Conductive adhesives

Conductive adhesives are normal adhesives that are enriched with conductive fillers. The fillers are metallic, carbon or metallized nano or micro particles [16] [32]. The conductive adhesives can be made hard or soft, which is an advantage compared to conventional solders. In addition, the adhesives require low temperatures to form conductive joint, which makes them well compatible with plastic substrates. Based on the amount of conductive fillers, there are isotropic conductive adhesives (ICA) and anisotropic conductive adhesives (ACA). [32]

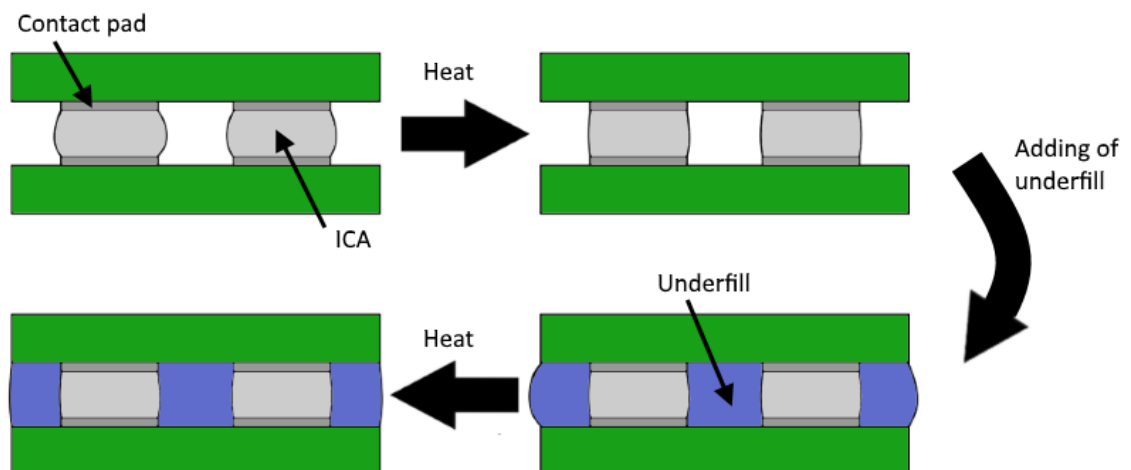
#### 3.3.1 Isotropic conductive adhesives

Isotropic conductive adhesive (ICA) consists of conventional adhesive body that includes conductive fillers. The amount of filler particles in ICA is high, which enables continuous filler network and further the isotropic conductivity. The filler network is a requirement for high conductivity and it is formed after amount of fillers increases over the percolation threshold. The percolation threshold is the point when the conductivity of ICA increase

considerably and the filler network is created. Below the percolation threshold, there is no continuous filler network and conductivity is poor. However, wide filler network decrease the cross-linking potential of adhesive polymers, which decrease the strength of adhesive. The amount of fillers should be limited for a durable adhesive but still high enough over the percolation threshold. In commercial ICAs, the amount of conductive fillers is between 70 and 82 percent by weight. [32] [52]

As in conductive inks, conductive fillers such as gold, silver and CNTs are used in ICAs. [38] [41]. Currently, the most used ICA type includes epoxy adhesive and one-size micro silver flakes [32] [52] [53]. The epoxy has great heat resistance and is compatible with various fillers, which makes it good resin for ICA [38]. The micro silver flakes have good electrical and thermal conductivity and are chemically stable [53]. There are also options to use silver nanoparticles or CNTs with silver flakes, which increase conductivity of adhesives [53] [54]. However, they are not yet commercially used.

Underfill is non-conductive epoxy adhesive that is commonly used in surface mount device (SMD) and flip-chip technologies. The main purpose of the underfill is mechanically support ICA or solder connections in electronics structure. The underfill must be heat treated like ICA, which can be done after establishment of conductive connections. [31] [32] Thermal and chemical properties of underfill and ICA should be compatible to ensure stable joint. Mismatch of thermal or chemical shrinkage of the underfill and the ICA cause cracking, delamination or other premature joint failure. [55] Figure 6 shows the forming of ICA contacts after the ICA and underfill are added between substrates:



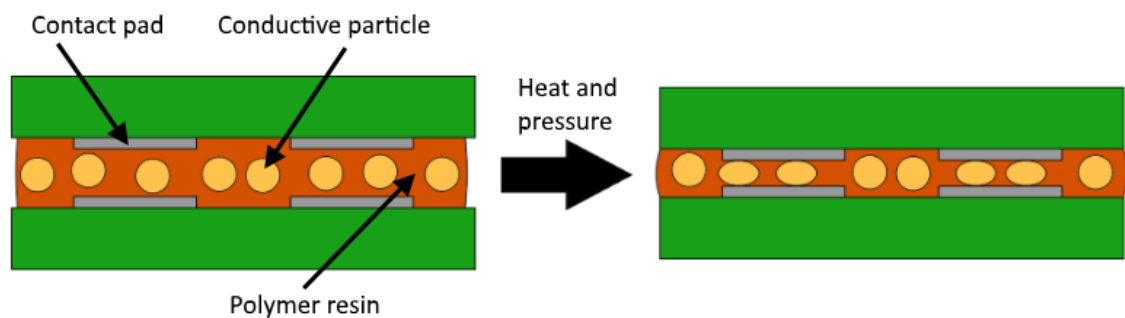
**Figure 6.** The concept of an ICA joint.

Originally ICAs are developed to miniaturize electronics and substitute traditional lead containing solders that are categorized as environmentally hazard problems. The ICAs have low curing temperatures that makes them compatible with more sensitive substrates.

Furthermore, they have simple process steps and are non-conductive until the heat treatment. [31] [53] [56]

### 3.3.2 Anisotropic conductive adhesives

Anisotropic adhesives (ACAs) are adhesives that are selectively conductive. ACAs have an adhesive body and conductive fillers like the ICAs but the amount of conductive fillers is considerably lower. The filler quantity is below the percolation threshold (1-30 percent by weight), which obstructs mutual conductivity of fillers. However, by using uniformly dispersed big size fillers in thin adhesive layer, it is possible to create conductivity to normal direction of adhesive layer (z-direction). The z-direction conductivity is strengthened by firm pressure and heat of the bonding process, which squeezes and locks conductive particles of ACA between contact pads. Figure 7 shows an example about the forming of anisotropic adhesive film joint. [32] [57]



*Figure 7. The concept of an ACF joint.*

ACAs are provided in two different forms. There are anisotropic conductive pastes (ACPs) that are in liquid form and anisotropic conductive films (ACFs) that are in solid film form. Generally, ACPs consist epoxy based resin like ICAs and the ACFs are made from thermoplastic polymer or rubber. Conductive fillers in ACAs are generally fabricated from nickel coated polymer particles that are further coated with gold or silver. The highly conductive coating and polymer core increase plasticity of the filler particles and decrease costs of ACA. [32] [57]

ACAs have many advantages. Joints made with ACA require low bonding temperature and simple equipment. ACA joints are thin and, especially with ACF, the adhesive thickness is well defined. Because of low conductive filler content, they are a low costs application and are used, for example, in electronics industry. [57] In Table 8 is presented ACF tape tesa HAF 8412 that is used as the conductive adhesive in the tests:

**Table 8.** *The tesa HAF 8412 ACF tape properties [58]*

	tesa HAF 8412
Adhesive type	Phenolic resin and nitrile rubber
Thickness ( $\mu\text{m}$ )	45
Lamination temperature ( $^{\circ}\text{C}$ )	180 – 220
Lamination pressure (N)	80 – 130
Lamination time (s)	1,5

The tesa HAF 8412 is designed for one step bonding process to form reliable mechanical and electrical bonds. The main applications of the ACF tape are to embed chip-modules to smart cards, where PCV, ABS and PC based cards are especially suitable. The ACF has support film on the other side, which makes application of the ACF easier. [58]

### 3.4 Soldering

During a soldering process, a small amount of highly conductive metal alloy is melted and placed between two metallic surfaces. Soldering is used in traditional electronic industry and in manufacturing PCBs. Soldering is a fast, precise and inexpensive method to attach components and PCBs together. [29]

Conventional solder materials require high temperatures ( $>180\text{ }^{\circ}\text{C}$ ) to melt, which is a challenge over plastic substrates because most plastics soften or melt before that. However, normal soldering methods can be used in stretchable electronics when temperature-resistant copper film is laminated over the plastic substrate. Especially the solderability is the benefit for laminated horseshoe shaped copper film interconnections. [4] [29]

In addition to conventional solders, there are low-temperature solders that melt at much lower temperatures. For example, solders that contain indium or bismuth have reflow temperatures ranging from  $115\text{ }^{\circ}\text{C}$  to  $180\text{ }^{\circ}\text{C}$ , which allow the usage of plastic substrates and printed interconnections. The main disadvantage of low-temperature solders is high costs compared to traditional soldering materials or conductive adhesives. The expensive-ness of rare metals that the solders requires restricts usage of these solders. [59]

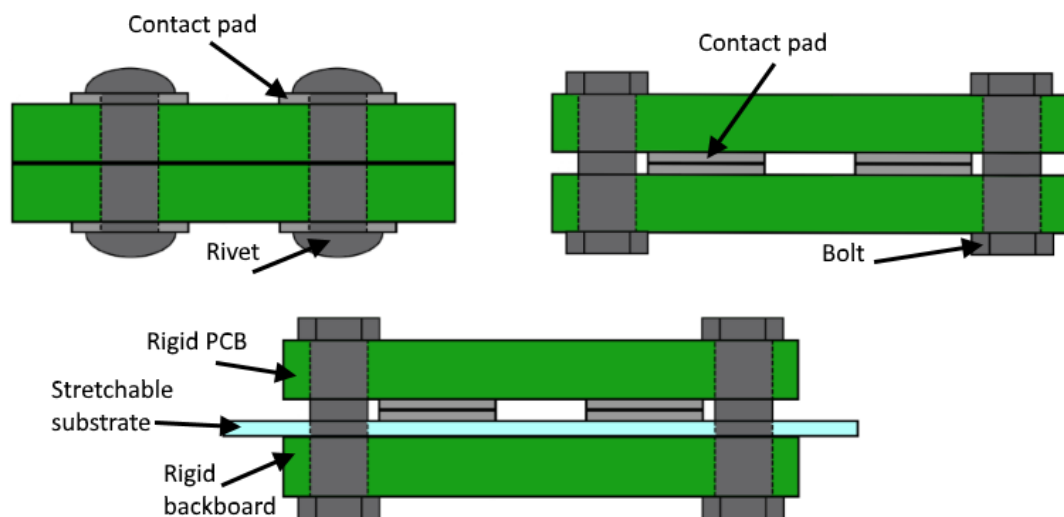
In printed stretchable electronics, the low-temperature soldering is done with furnace soldering. The furnace soldering is a reflow soldering method for complicated and precise components, which are used in SMD applications. In the soldering, the assembled structure with a substrate, components and solid solders is put in the furnace and heated over liquidus temperature of the solders. At elevated temperatures, the solders reflow over contacts and form a joint mechanically and electrically. The process is realized rapidly to

avoid excess grain growth of solders, which decrease strength of the joint. However, the heating and cooling must be slow enough to prevent thermal shock of the components. [29]

### 3.5 Compression joint

A compression joint is purely mechanically formed joint without adhesives. The compression joint is realized by fastening connectable substrates firmly together with fasteners. The joints can be fastened permanently with rivets and nails or temporary with screws and bolts. The reopenable mechanism is one distinctive feature of a compression joint and such as press-buttons are exploited in wearable electronics. [5] [33] [60]

The compression joints can form both non-conductive and conductive contacts. While the non-conductive contacts are simply made with the fasteners, the conductive contacts are more delicate. The conductive contacts are done either by pressing conductive pads together or by using fasteners as connectors, which are presented in Figure 8. [33] [60]



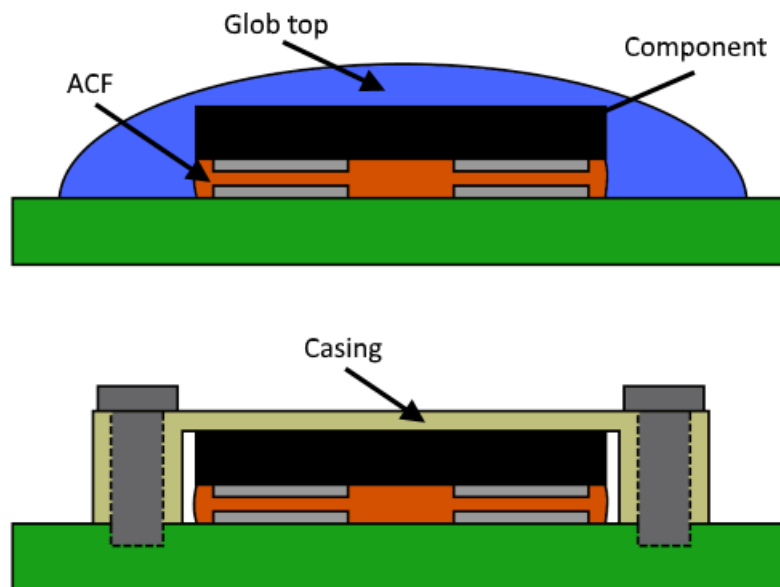
**Figure 8.** Conductive compression joints between two rigid substrates and rigid and stretchable substrates.

In stretchable electronics, the compression joint requires additional rigid backboard because the stretchable substrate tends to compress. Without the backboard, the substrate elongates away under the rigid PCB and the amount of compression is not enough for conductive contacts. The three-layer structure is bulkier than other joints of stretchable electronics. However, the ability to remove and attach rigid PCBs with compressive joints are taken advantage in wearable electronics to provide washability.

### 3.6 Encapsulation

After components are set and electrical contacts are formed, they are vulnerable for external conditions such as moisture and heat. To make the build-up structures durable, they are encapsulated and isolated from environment. The encapsulation is realized with liquid that form glob top or solid that makes casing over the structure. [32] [33]

Glob top is low-viscous non-conductive adhesive that spreads over components and insulates them. Various polymers and adhesives can be used as glob top adhesives, for example MT382 by Permabond. Because of the low viscosity and high surface tension, the glob top adhesives spread and solidify as round shaped dome over the structure. Furthermore, the glob top is used to insulate conductive interconnections outside joints. [32] [34] An example about the glob top is shown in Figure 9:



*Figure 9. The glob top concept and casing of a component.*

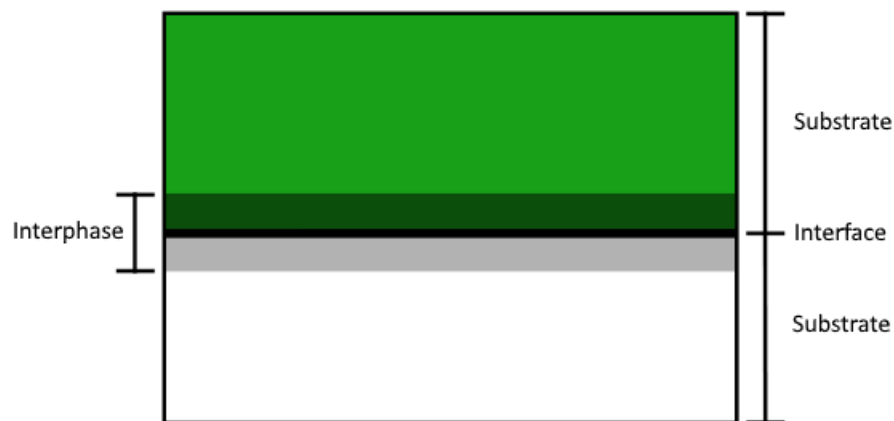
As seen in Figure 9, adhered or mechanically fastened solid casing is an alternative choice for liquid glob top. However, a casing is more complicate and not compatible for protection of interconnections like the easily addable glob top. Also, the casing is not as tight-proof as the glob top and requires holes for fasteners in substrate. On the other hand, the casing does not need heat in the assembly and is removable, which make the casing attractive to use. [33]

When comparing the glob top and the casing in stretchable electronics, the glob top forms much more flexible insulation. The glob top can be used over stretchable interconnections, which makes it practical over whole stretchable electronic system. However, glob

top still affects to total stretchability of the structure. Because of the characteristic spreading of the glob top, the glob top limits the possibilities to control final stretchability of the structure. [32] [34]

## 4. ADHESION

Adhesion is defined as a phenomenon when two bodies stick together [61] [62]. The adhesion is also explained as “state in which two surfaces are held together by interfacial bonds [36]”, what proclaims more precise how the adhesion is created. There are different theories and mechanisms about origin of adhesion, which have aroused since studies of adhesion have started to advance in the 1920s. Some simplified theories exist, for example adsorption theory, mechanical theory, electrostatic theory, diffusion theory and weak boundary layer theory. In general, two substrates have a contact and form a common interface, which is shown in Figure 10:



*Figure 10. Interface and interphase between connected bodies.*

The location of the interface cannot be exactly defined in the joint and is often thought as two-dimensional area between two separate bodies. For many cases, three-dimensional volume around the interface is called an interphase. Depending on materials and the shape of the interface, sometimes the interphase is more important than the interface. There can be the reactions and deformations over a wider volume than just through thin interface plane. For example, mechanical interlocking and diffusion of substrates happen over a thicker interphase. [63] [64]

A durable interface requires good contact between the substrates so that the surfaces can react with each other. The maximum contact is obtained when a liquid spread over a solid substrate and covers the surface. Wetting is a feature for the adhesion and it is affected by various properties. For instance, roughness of the solid surface and the viscosity of the flowing medium affect adhesion. [64] [65] [66] Figure 11 presents an example joint of a module and stretchable substrate:





**Figure 11.** *Conceptual joint of a module and substrate.*

Figure 11 shows that there are three different components in a stretchable structure: a rigid module, stretchable substrate and adhesive layer between them. There are two interfaces in the structure, one with the module and adhesive, and second with adhesive and substrate. The structure requires versatile properties from adhesive because adhesive has to join two different surfaces together. The surface of the module is coated with solder mask that is smooth and hard. On the contrary, the surface of substrate is elastic and soft. Under stretching, the adhesive layer against the module is stagnant, and against substrate, tends to move with the substrate. To solve the problem, the adhesive can be designed either to be strong to endure the stretching or to stretch with the substrate and distribute strains over bigger area. [19] [63]

Because of materials and the topographies of the surfaces, it can be understood that adhesion of stretchable electronics is formed with certain mechanisms. In this case, the adhesion can originate from mechanisms that are specified by adsorption theory, mechanical theory and diffusion theory. The adhesion can be improved with additional surface pre-treatments. Plasma treatment is discussed with adsorption theory and abrasion is mentioned in mechanical theory. Also, the nature of the adhesive affect adhesion.

After the joint is formed, it might fail in some day. The failure of polymer based joints starts as molecular level deformations and further develop to critical failures. The failure type of a joint can be recognized as adhesion failure, cohesive failure and substrate failure. By knowing the failure deformations and the failure pattern of the joint, the potential failure mechanism can be averted and durability of the joint can be improved. [25] [67]

## 4.1 Phenomenological theories of adhesion

The adhesion in stretchable electronics is primarily explained with the absorption theory, mechanical theory and diffusion theory. These are affected by basic parameters of liquid adhesive and solid substrate. The viscosity of the adhesive describes how much it resists flowing:

$$\eta = \frac{\tau}{\dot{\gamma}}, \quad (6)$$

where  $\eta$  is viscosity,  $\tau$  is shear stress and  $\dot{\gamma}$  is strain rate [68]. High viscosity means that liquid is thick and it flows slowly. For comparison, viscosity of water is 1 centipoise (cP) and viscosity of thick syrup is 10000-30000 cP. The difference is about same than between conductive inkjet inks (8-25 cP) and conductive screen printing inks (10000 cP) [18] [69].

Some liquids, for example water, are independent of the strain rate and their viscosity stays always constant. These kind of liquids are called as Newtonian liquids. Also, there are non-Newtonian liquids that do not have constant viscosity. The viscosity of non-Newtonian liquids change with temperature, which is a usable feature to modify the viscosity values. Elevated temperatures decrease the viscosity, which is caused by increasing amount of kinetic energy (Brownian motion) in the liquid. Viscosity is also decreased by evaporative solvents that are used in adhesives and inks. [19]

A low viscosity of liquid eases the wetting over a solid surface. Wetting is also affected by the surface area and surface energy of the solid. The surface area is affected by surface roughness. On smooth or slightly coarse surfaces the surface roughness has very small effect on wetting. On coarse surfaces the effect is significant and hinders wetting. However, the surface roughness increases the surface area, which increases the surface energy and theoretical amount of adhesion. Therefore, the wetting of liquid over solid surface is basis for the adhesion and is considered in all adhesion theories. [64]

### 4.1.1 Adsorption theory

Based on an adsorption theory, molecules of the liquid and solid surfaces have interactions with each other and create adhesion. The amount of interactions is directly proportional to the quantity of adhesion and thus the aim is to maximize the interactions. The amount of interactions is at its maximum when the surfaces have as much common contact area as possible, which is ensured with good wetting of the liquid. The interactions can be chemical bonds or temporary attractions between the molecules. Generally according to the strength of interactions, chemical bonds are called as primary bonds and temporary forces are called as secondary forces. The primary bonds are the strongest interactions and the main source of adhesion. [64] [70] [71]

Hydrogen bonds, covalent bonds and ionic bonds of molecules are categorized as primary bonds. Hydrogen bonds are particular bonds between hydrogen atom and nitrogen, oxygen or fluorine atom. The covalent bonds are established when two atoms share their electrons with each other. Furthermore, the ionic bonds are formed because of electrical attraction of opposite charged ions. Theoretical strength of these primary bonds is around hundreds of kJ/mol. [64] [70]

In addition to stable primary bonds, secondary forces form weaker inconstant attractions. The secondary forces are mainly attractive forces between moving molecules and fluctuates according to the prevailing distance of the molecules. These weak polar forces are commonly called as Van der Waals forces. Magnitude of their bond strength is tens of kJ/mol, which is many times weaker than the primary bonds. [64] [70]

The molecular interactions between surfaces can be improved by surface activating pre-treatments. The plasma treatment is one type of surface treatment where the surface energy of the plastic product is improved by exposing the surface directly to a cloud of ionized gas. The ionized gas changes the surface chemically and creates new active chemical compounds. The plasma treatment is used for solid substrates to increase their interactions with adhesives and inks. [72]

#### **4.1.2 Mechanical theory**

The mechanical theory deals how the topographies of joinable surfaces affect the adhesion. To a certain point, an interface of coarser surfaces can have better adhesion and durability than an interface from smooth surfaces. After a certain point, when the surfaces come rough enough, despite the good adhesion, the durability of the interface and the joint decrease. The interface becomes strong with very rough surface and the failure mechanism changes from adhesive failure to substrate failure. Making surfaces coarser improves the adhesion especially when substrate in the first place has poor adhesion and is difficult to bond. However, with the surfaces that have already good adhesion, the benefit of abrasion is not clear. [19] [64] [71]

Improved adhesion of rougher surfaces can be explained in couple of ways. One approach is to consider the surface on molecular level. On uneven surface, there are molecules that have less bonds than same kind of molecules in the substrate. Because of the smaller amounts of bonds, the surface molecules have more free energy (surface free energy) and are more reactive. [64]

Other approach is to inspect the size of surface area. The rougher surface has larger surface area than a smooth surface. The larger area has higher total amount of surface energy. In addition, wider or longer bonding area increases durability of a joint force-wise. While the bigger joint area is larger in x and y-direction, the coarsening increase the area in z-direction. [64]

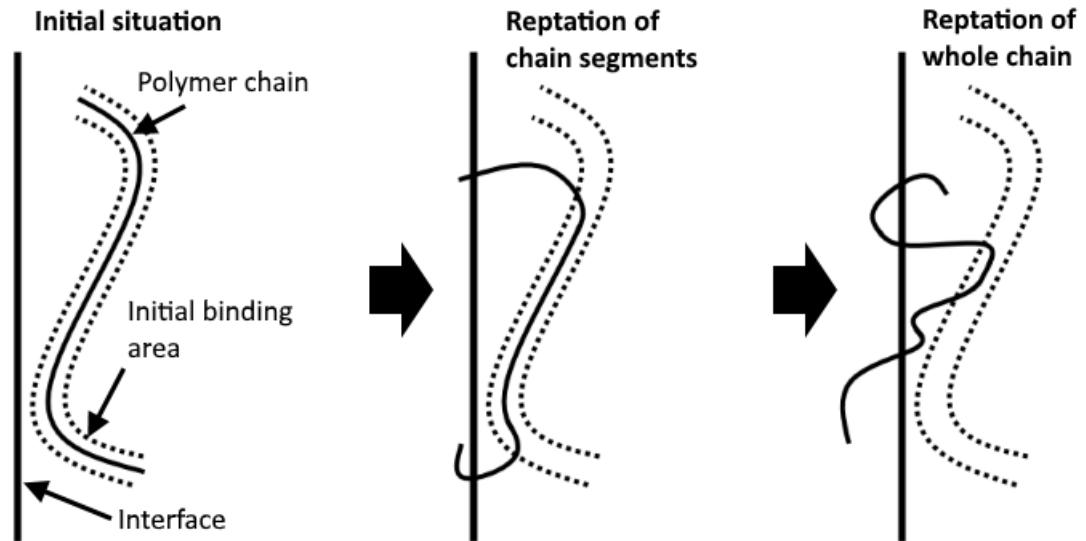
Bonded rough surfaces have also better endurance under tension. A rough surface form wider bond area than smooth surfaces, and transmits loads over larger area. The loading is not subjected only to the joint area but is also carried by substrates through the uneven surfaces. [73]

The roughness of surfaces can be increased by abrading before the bonding. Furthermore, abrasion is used to remove weak or difficult-to-bond surface layers, such as highly crystalline surfaces. The abrasion pre-treatment includes cleaning of surfaces before and after the abrasion, which removes contamination on the surfaces. The abrasion can be done with efficient grit blasting method, laser, or with abrasive paper. [19] [74]

### **4.1.3 Diffusion theory**

The diffusion theory consists of defining two polymer based surfaces that blend and diffuse together. The surfaces form an interphase, where polymer chains from both bodies are mixed and entangled with each other. The entanglements work like knots and bind polymer chains, which increase the adhesion of the joint. In order to polymers to entangle, they must be above their glass transition temperature. Properties such as molecular weight and amorphousness affect how easily polymer chains move inside polymer matrix (reptate) and diffuse over a surface. In addition, process settings like temperature, time and pressure influence to the diffusion of plastics. [64] [75] [76] [77]

The diffusion of polymer substrates happen in steps. According the reptation model, before the diffusion the chains are bound with entanglements in narrow tube like areas. When the diffusion starts, it starts partially. Segments of the chains, minor chains, relax and reptate over the interface and form low depth diffusion. Over the time the whole chains relax and reptate, which leads to reptate diffusion and entanglements of the chains in the interphase. [64] [75] The diffusion steps are also described in Figure 12.



*Figure 12. Development of reptation during diffusion.*

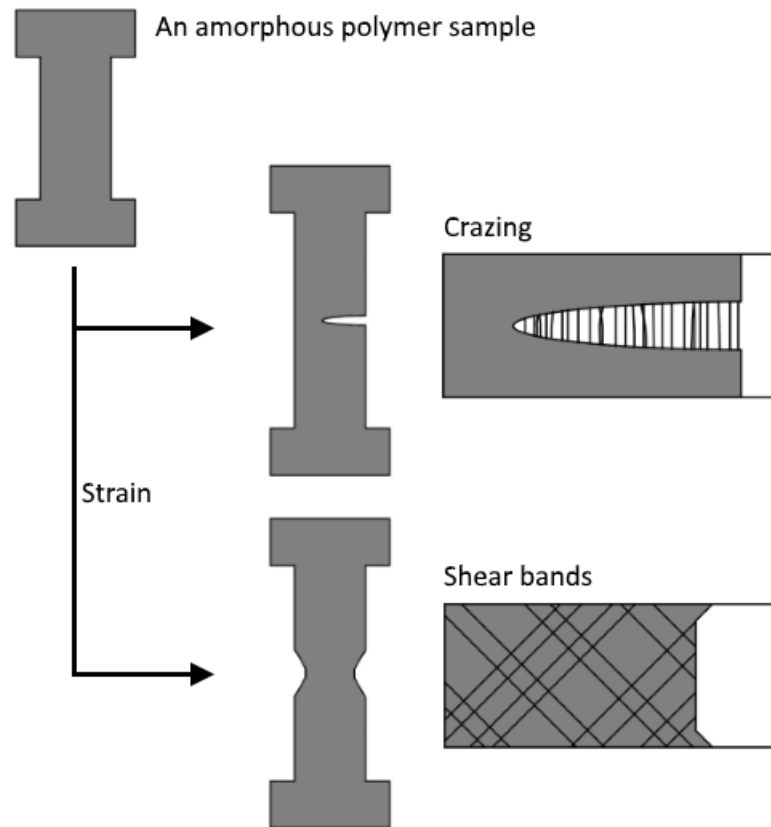
The depth and time of diffusion vary with different polymers. Moreover, polymers can be incompatible with each other and form unstable diffusion that weakens in time. The compatibility is increased by using tailored copolymer compatibilizers, which attract two different polymer substrates together. [64] [75] [78]

## 4.2 Deformation mechanisms of polymers

Under straining, polymers go through deformations that finally lead to failure of the structure. Various parameters such as strain rate, temperature and nature of polymers affect the deformation mechanisms in the structure. Soft and elastic amorphous polymers have different deformation mechanisms than harder semicrystalline polymers. Elastomers like TPUs are commonly copolymers and have two or more dissimilar domains in the structure. [25]

### 4.2.1 Amorphous polymers

Amorphous polymers have randomly oriented amorphous molecular structure that does not have highly ordered configuration. The amorphous structure consists of entangled polymer chains that are the main source of strength of amorphous polymers. Furthermore, there is a certain amount of free volume between randomly oriented chains, which also affects mechanical properties of amorphous polymers. [25] During straining, the amorphous polymers deform and finally form crazes and shear bands, which are presented in Figure 13:



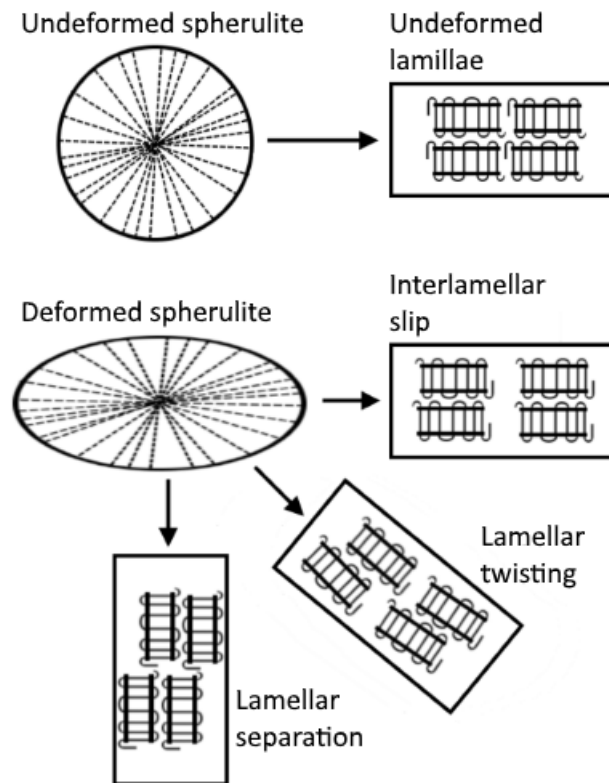
*Figure 13. Strain induced crazing and shear bands in amorphous polymer.*

Crazes and shear bands both consist of strips of linear polymer chains that are organized in sparser area. Crazes are aligned in perpendicular direction to the load and they consist of voids between polymer chains. Shear bands are formed in 45 degrees direction to the load and are densely pressed together. Moreover, the development of crazes requires just elongation of polymer chains contrary to the shear bands that require also slipping of the chains. The both deformations are unwanted because of the more sparse areas are weaker than bulk substrate and are pathways to crack propagation. [25]

#### **4.2.2 Semicrystalline polymers**

Semicrystalline polymers have highly ordered polymer chains that are arranged in a wavy lamellae structure. The lamellae are further oriented to roundish spherulite structures, where the lamellae are packed side by side towards the centre of the spherulites. The semicrystalline polymers have also amorphous phases along the crystalline phases, which exist between lamellae and spherulites. Under straining, initial deformation is mainly controlled by the amorphous phases, which advances to spherulites. The straining deforms spherulites and causes slipping, twisting and separation of lamellae inside the spherulites, which are presented in Figure 14. The spherulite deformations appear as neck formation,

cold drawing and strain hardening of semicrystalline structure and increase ductility of semicrystalline polymers. [25]



*Figure 14. Deformation inside spherulites in polymers.*

The crystalline and amorphous phases consist of defects that guide damage propagation. The defects can be ready in the structure or created by deformations. Because of amorphous phases are softer than oriented crystalline phases, the damage propagation tends to happen along boundaries of spherulites, which leads to brittle behavior. More intensive propagation of damage can advance inside of spherulite, where it first attempts to travel in the amorphous space between lamellae before going through them. The toughness of semicrystalline polymers is directly transversely proportional to the amount of defects and proportional to stiffness of the deformation area. [25]

### 4.2.3 Block copolymers

Block copolymers are made by combining two or more different polymer chains together. The alternating polymer chains with different block copolymers form a polymer structure where distinguishable hard and soft segments exist. The segments are created by incompatibility and glass transition temperature ( $T_g$ ) differences: hard segments are below their  $T_g$  and soft segments are over their  $T_g$  at ambient temperature. Orientation and phase

separation of the block copolymer structure is affected by shape of the polymers (linear or branching) and proportional quantity of the polymers. [25] [27]

Morphology of a block copolymer such as the one in TPU includes hard segments that are oriented to spherulites and soft segments that separate the spherulites. The block copolymers have various deformation manners, which resemble deformations of amorphous and semicrystalline polymers. During straining, the block copolymers can form crazes and deform lamellae. In addition, strain can concentrate towards interface of hard and soft segments, which causes voids and cavities around harder particles. Voids of smaller hard segments or particles increase ductility, but bigger cavities spread and improve cracking. [25] [27]

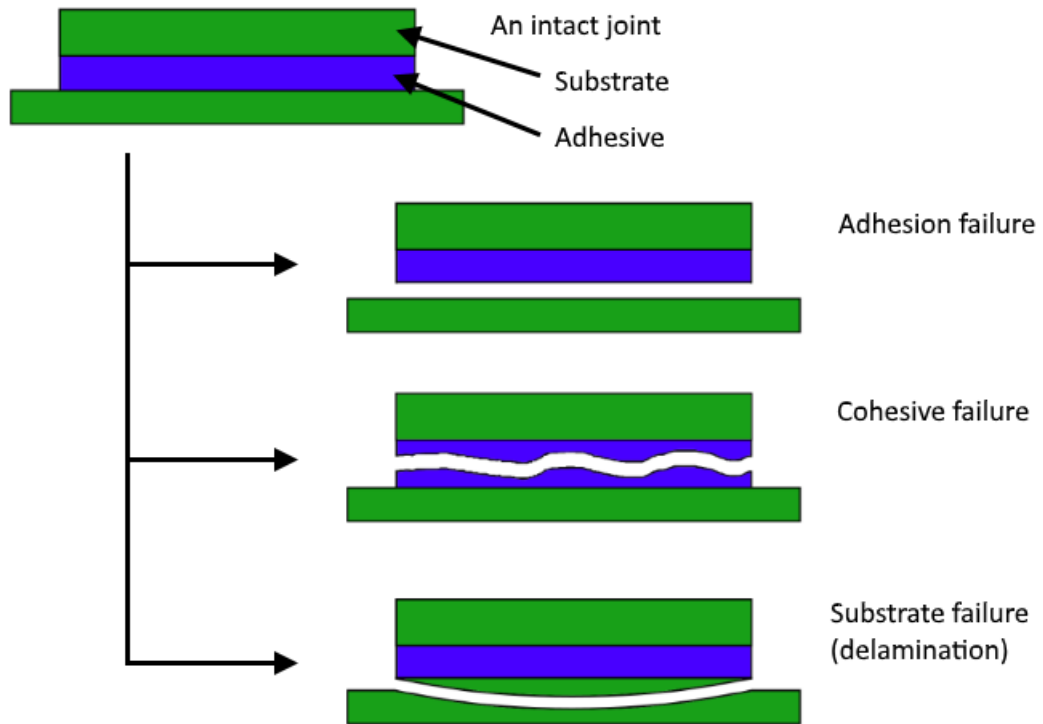
### **4.3 Failure of stretchable joint**

Every adhered joint fails when they are under high enough load. The failure starts as crack initiation and develops when the crack propagates in a joint. Properties such as residual stresses and ductility affect how the crack initiates and propagates in adhesive layer and substrate. Furthermore, failure and propagation of crack depend also on nature of load. [79]

#### **4.3.1 Failure patterns**

On a macro scale, failure in a joint occurs either adhesively or cohesively. It is also possible that a test specimen is locally weaker than the joint and the failure happens solely in the substrate. The failure patterns can be simple such as an adhesive failure on single interface or more complex. The examples about joint failures are presented in Figure 15.





*Figure 15. Failure pattern models.*

The adhesion failure occurs when the adhesion between the substrate and the adhesive fails. The crack initiates at the interface between the substrate and the adhesive and propagates along it. The crack can propagate on one interface or jump over the adhesive layer to the other interface of the adhesive. The crack can change its interface single or multiple times during the propagation. In adhesion failure the adhesion is the weakest link in the joint. The durability of the joint and amount of adhesion can be increased with additional surface pre-treatments. [19] [67] [79]

In the cohesion failure, the interfaces of the joint are stronger than materials and the crack propagates inside the materials. If the crack nucleates at the interface and cannot move along it, it evades and moves to the substrate or to the adhesive layer. The crack can also purely initiate and propagate in the adhesive layer, which is commonly the sign of a too thick adhesive layer. Furthermore, the failure can happen partially cohesively and partially adhesively. [19] [67] [79]

Failure of a structure does not always happen because of a weak joint. The joint can be durable as a whole and the substrate fails. The substrate failures occur outside the joint by snapping or under the joint by cohesive delamination. [19] [67] [79]

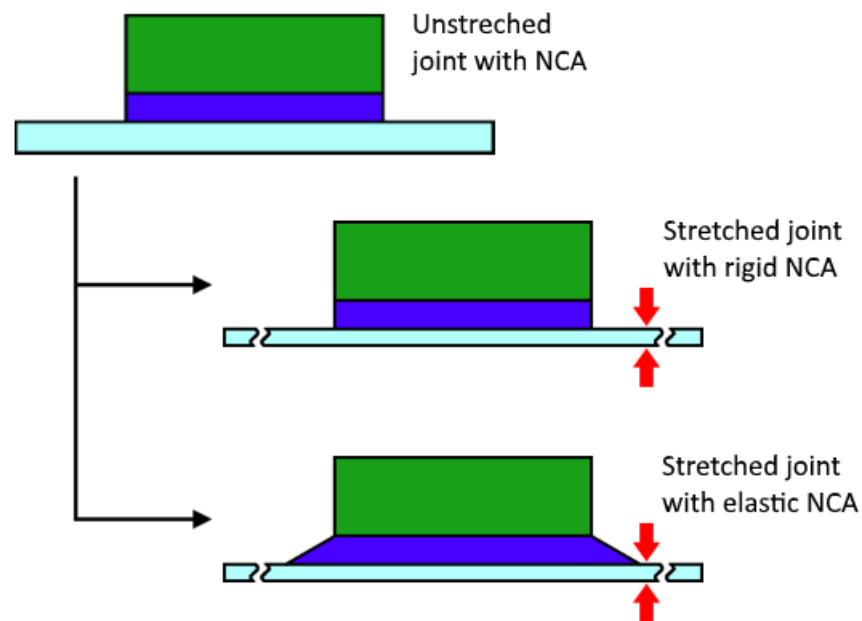
### 4.3.2 Interfacial failure

In stretchable electronics, a rigid module is attached with an adhesive on the elastic substrate. The elastic substrate elongate under the straining, which makes the deformation of the joint and the fracture mechanisms more complex. Figure 16 shows an example stretchable joint that has a module that is bonded with a NCA.



*Figure 16. An attached rigid module on elastic substrate.*

A NCA binds surfaces of rigid module and elastic substrate together and endures mechanical differences of the materials. The NCA can be structural adhesive or elastic adhesive, which deformation behaviour vary in stretchable joint. The rigid NCA endures a load and prevents deformation of the surface of the substrate. On the contrary, the elastic NCA follows elongation of the substrate, which deform the adhesive layer. Figure 17 displays deformations of the NCAs in stretchable joint.

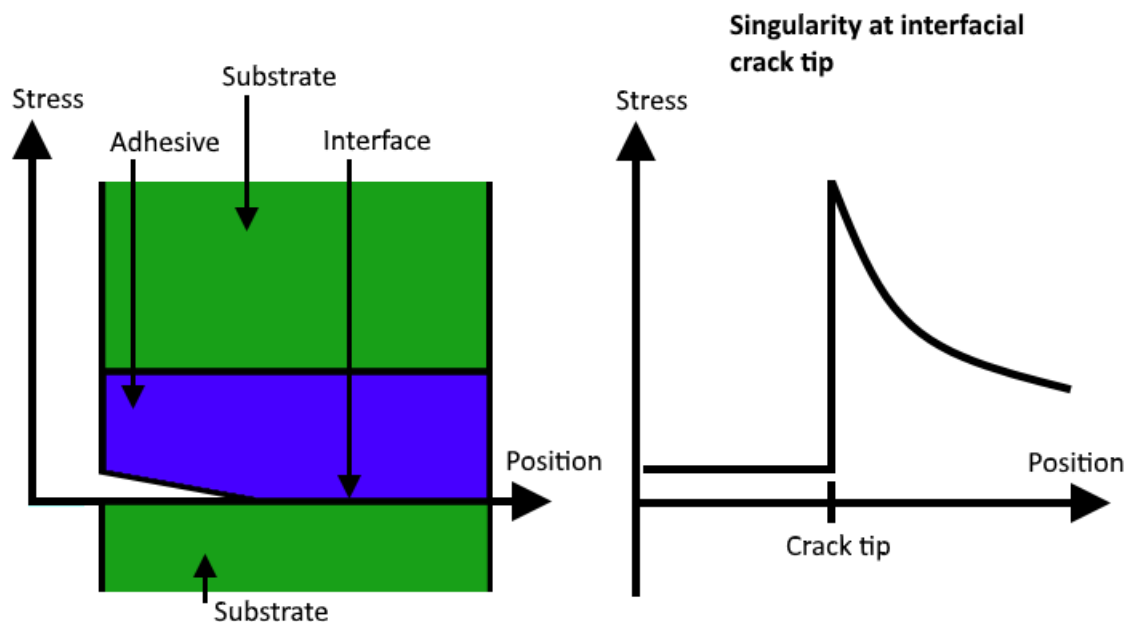


*Figure 17. Stretching of the joint with different NCAs.*

As seen in Figure 17, rigid NCAs, such as structural adhesives, do not deform during elongation. Because of the mechanical differences of the components, stress (and strain) concentrates to the boundary area of the substrate and adhesive. The stress concentration of the boundary area induce higher stresses to outer edges of the adhesive layer and can initiate damage in the adhesive layer. [19] [80]

Contrary to the rigid adhesive, the elastic adhesive, like PSAs, deform with the elongation of the substrate. The elastic adhesives accomplice the movement of the substrate with shearing of the adhesive layer. In the joint, the adhesive gradually elongates around the module, which decrease the deformation differences of the substrate and the adhesive, and further decrease the stress concentration. However, elastic adhesives can elongate under small loads, which makes them shear with low stress concentrations and stand small amount of loads without excess deformations. [19] [80]

The stress concentration in the boundary area can cause failure in two ways; the higher stresses can cause failure of the substrate at the boundary area, or the stress concentration initiates damage in the adhesive layer, which propagates and break the adhesive layer. In the more rigid structural adhesives, the stress concentration is higher than in elastic adhesives, which makes the adhesive layer from the structural adhesive more sensitive to the damaging. [19] [80] Figure 18 presents an example about an interface crack, where stress distribution in the interface of two isotropic elastic substrates is sketched.



**Figure 18.** Singularity and debonding at elastic substrate-adhesive interface.

In the isotropic elastic substrates, the stress concentrates gradually until the tip of the crack and drives the propagation of the crack [80]. However, in the stretchable joint, there

are one rigid (linear-elastic) substrate and one highly non-linear elastic substrate (TPU-film). Distribution of stress concentration in the interface crack is affected by deformations in the TPU-film, which change along stress. Because of this, the interface failure in the stretchable joint is more complex than in Figure 18. For instance, the substrates have different Poisson's ratios. The rigid substrate binds the interface of the highly elastic substrate (that has high Poisson's ratio) and boosts stresses in applied direction in the joint. [24] [80]

The maximum amount of stress in the tip can be enormous. Especially in the internal or external sharp shapes in linearly elastic materials, the theoretical maximum stress in the tips is infinite. These sharp shapes that have mathematically the infinite stress are also called as the stress singularities. The stress singularities are distinguishable in the rigid materials as weak spots that fail prematurely. In the elastic materials, the stress singularities are also the failing areas. However, the elastic materials can have plastic flow around the sharp corners, which somewhat correspond to the stress singularities. [81]

## 5. METHODS

Various methods are used to study stretchable electronics in several levels. Materials, adhesives and joint designs are studied to find the best way to build up the stretchable electronics based on stretchable substrate and rigid islands. In addition to the substrate, adherence of NCAs to rigid surfaces and the TPU-film is tested by floating roller peel-test setup. Failure mechanisms of peel samples are further studied with Fourier transform infrared spectrometer (FTIR).

Finally, complete joints of stretchable electronics are assembled from modules, a substrate and conductive adhesives. The formed joints are reinforced with additional frames that are 3D-printed and attached around the modules with a NCA. The joints are tested by using the tensile testing and the endurance and electrical resistance development are analyzed and compared.

### 5.1 Surface treatments and wetting

Amount of surface energy of the substrate and effect of common surface pre-treatments are inspected by measuring wetting of the substrate with Krüss DSA100 drop shape analyzer.

#### 5.1.1 Theory of surface tension and energies

The surface energy can be understood as excess free energy of the surface that can react with other materials. It is also the required amount of energy, which needs to be focused on the surface to break it. For good adhesion, sufficiently high surface energy is “the must”. Generally, polymers have low surface energies between 18-47 mJ/m<sup>2</sup> because of the satisfied polymer structure. [19] [82] [83]

In addition to the surface energy, also a term surface tension is widely used to describe the activity of surface. The both terms are defined with thermodynamically and are classified as two different parameters. However, on practical level the surface energy and the surface tension are equal and are used often as interchangeable terms. The unit of the surface energy is energy per area (mJ/m<sup>2</sup>) and the unit of surface tension is force per length (mN/m). Young has described the surface tension of solid with the following equation:

$$\gamma_{SV} = \gamma_{SL} + \gamma_{LV} \cos \theta_{eq} , \quad (7)$$

where  $\gamma_{SV}$  is the tension of solid and vapor interface (the surface tension),  $\gamma_{SL}$  is the tension of solid and liquid interface,  $\gamma_{LV}$  is the tension of liquid and vapor interface and  $\theta_{eq}$

is the contact angle of equilibrium point of the three interfaces. Small contact angle indicates high spreading of liquid and good wetting. On the contrary, high contact angle tells that the surface is inert and has poor wetting. [19] [82] [83] Furthermore, the Young-Dupré equation describes the work of adhesion:

$$W = \gamma_{LV}(1 + \cos \theta_{eq}), \quad (8)$$

where  $W$  is the work of adhesion. Universally, surface energies vary because materials have different chemical compositions that affect amount of free energy on surfaces. With the same reason, the surface energy can be split to more refined components that present chemical bonding of surfaces. In the most cases, surface free energy is classified to polar and disperse components, where the polar component includes strong interactions, such as primary bonds. The disperse component contains weaker secondary forces. The polar and disperse components can be combined with Equations 7 and 8, so that Equation 9 can be deduced:

$$\frac{\gamma_{LV}(1 + \cos \theta_{eq})}{2\sqrt{\gamma_{LV}^D}} = \sqrt{\gamma_{SV}^P} \left[ \frac{\sqrt{\gamma_{LV}^P}}{\sqrt{\gamma_{LV}^D}} \right] + \sqrt{\gamma_{SV}^D}, \quad (9)$$

where  $\gamma_{LV}^D$  is the dispersion component of the liquid and vapor interface,  $\gamma_{LV}^P$  is the polar component of the liquid and vapor interface,  $\gamma_{SV}^D$  is the dispersion component of the solid and vapor interface and  $\gamma_{SV}^P$  is the polar component of the solid and vapor interface. The order of Equation 9 represents the equation of straight line:

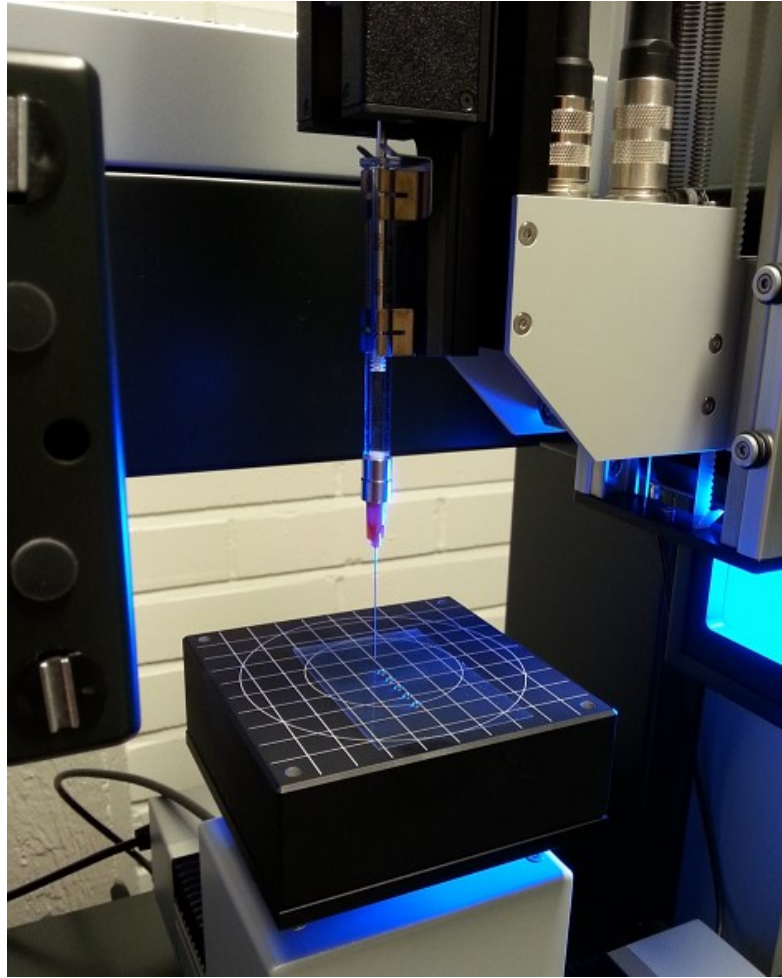
$$y = mx + c, \quad (10)$$

where  $y$  is  $y$  coordinate,  $x$  is  $x$  coordinate,  $m$  is the slope of line and  $c$  is the intersection of the line and  $y$ -axis. Multiple test liquids that differ chemically and have the different proportions of polar and disperse components are used to calculate the surface energy. Combining Equation 9 and 10, the “ $y$ ” and “ $x$ ” components in Equation 9 can be solved. Each test liquid provides one point that are used to form a straight line. From the straight line, the polar and disperse components of the surface energy can be seen and summed to get the total surface energy of the surface. [82] [83] [84] [85]

To calculate the surface energy, there has to be enough test liquids to draw the straight line exactly. With only few test liquids, the straight line is not precise and thus the surface energy value is also inaccurate. In that case, the wetting of the test liquids evaluates better how liquids behave on the surface. [83] [84] [85]

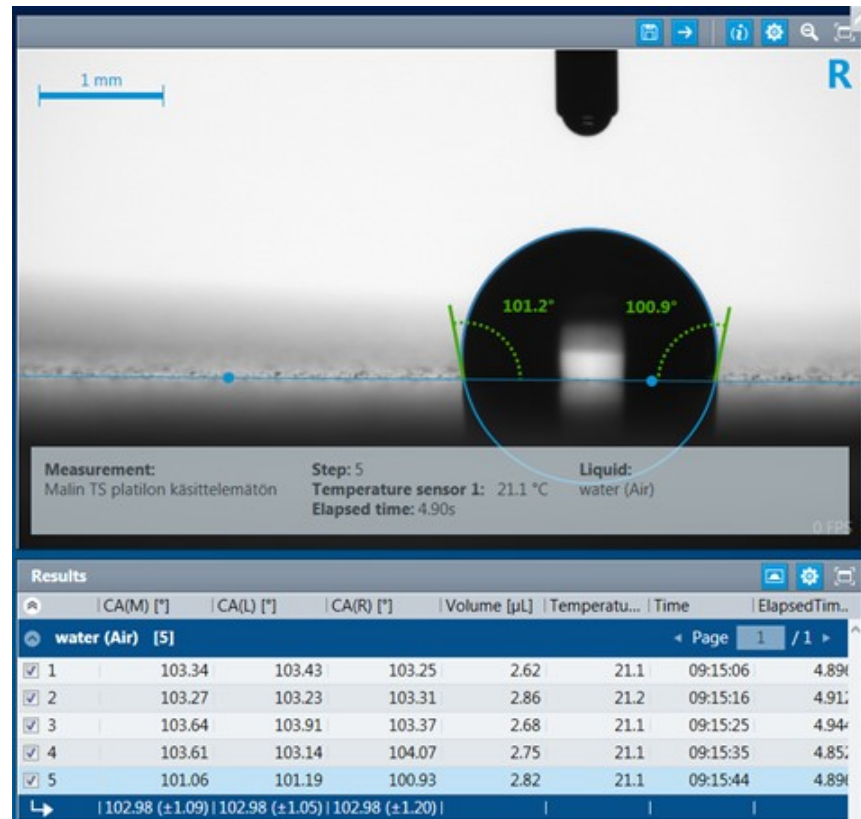
### 5.1.2 Contact angle measurements

The used test equipment Krüss DSA100 drop shape analyzer and the test situation is presented in Figure 19.



*Figure 19. Krüss drop shape analyzer DSA100.*

The Krüss DSA100 places droplets over a sample, takes pictures from the settled droplets after certain time and analyzes the contact angle of the droplets in a software. The software calculates the contact angle of the sessile drops from average of left and right side contact angles, which is seen in Figure 20.



*Figure 20. Contact angle analyzing with the software of the Krüss DSA100.*

In the thesis, the Krüss DSA100 device is set to use 3- $\mu$ l-volume water (grade 1) and ethylene glycol droplets on Platilon U 4201 AU TPU-film samples. Each samples are measured with 5 droplets of both liquids and the droplet shape analyzer pictures the droplets after 2 seconds they are placed on the samples. Before the testing, the samples are conditioned for 24 hours at 23 °C and 50 % air humidity.

### 5.1.3 Roughening

A roughening pre-treatment is used to increase surface area and the adhesion of substrate and is especially effective when the substrate is naturally inert like rubbers. Generally, uniform roughening can be realized with sand blowing but also sandpapering is used for small scale coarsening. [64] [74] In this thesis, the sandpapering is exploited for the TPU-film that is roughened with P400 coarse sandpaper.

A sample is roughened by attaching the TPU-film over metal plate (and cleaning it with IPA). The sandpaper is pressed on the TPU-film with a weight that assures that the surface is sanded with same pressure during the roughening. The TPU-film is sanded by 20 movements vertically, horizontally and circularly to achieve even coarse surface. After the roughening, the excess particles are removed from the film with compressed air and IPA.



### 5.1.4 Plasma pre-treatment

A plasma pre-treatment is used to improve surface energy of substrate by exposing the surface directly to a cloud of ionized gas. The ionized gas change the surface chemically and creates new more active chemical compounds on the surface. The plasma pre-treatment is exploited for example, in package manufacturing to increase adhesion between plastic films and inks. Moreover, there are smaller plasma devices for laboratory scale production. [72] For instance, the plasma tool Plasmatherm 790 is used to increase hydrophilicity of substrate in stretchable electronics [86]. The TPU-film sample in the surface pre-treatment test is exposed with the Piezobrush PZ2 handheld plasma device.

The Piezobrush PZ2 uses piezoelectric direct discharge technology (PDD<sup>®</sup> technology) to make cold atmospheric plasma. The device is meant for small-scale production to improve adhesion or clean surfaces, for example in laboratories and dentistry. The PDD<sup>®</sup> technology does not heat surface over 50 °C, which makes the device well compatible with plastic substrates. [87] The used Piezobrush PZ2 is introduced in Figure 21:



*Figure 21. The handheld plasma device Piezobrush PZ2*

The plasma treatment of the sample by cleaning the TPU-film with IPA and sweeping the Piezobrush PZ2 two times vertically and horizontally over the sample. The device is handheld and distance between the nozzle and the sample is 2 mm – 10 mm. The pre-treatment is done right before the contact angle measurement because the effect of plasma treatment decrease over time on non-bonded substrate [87].

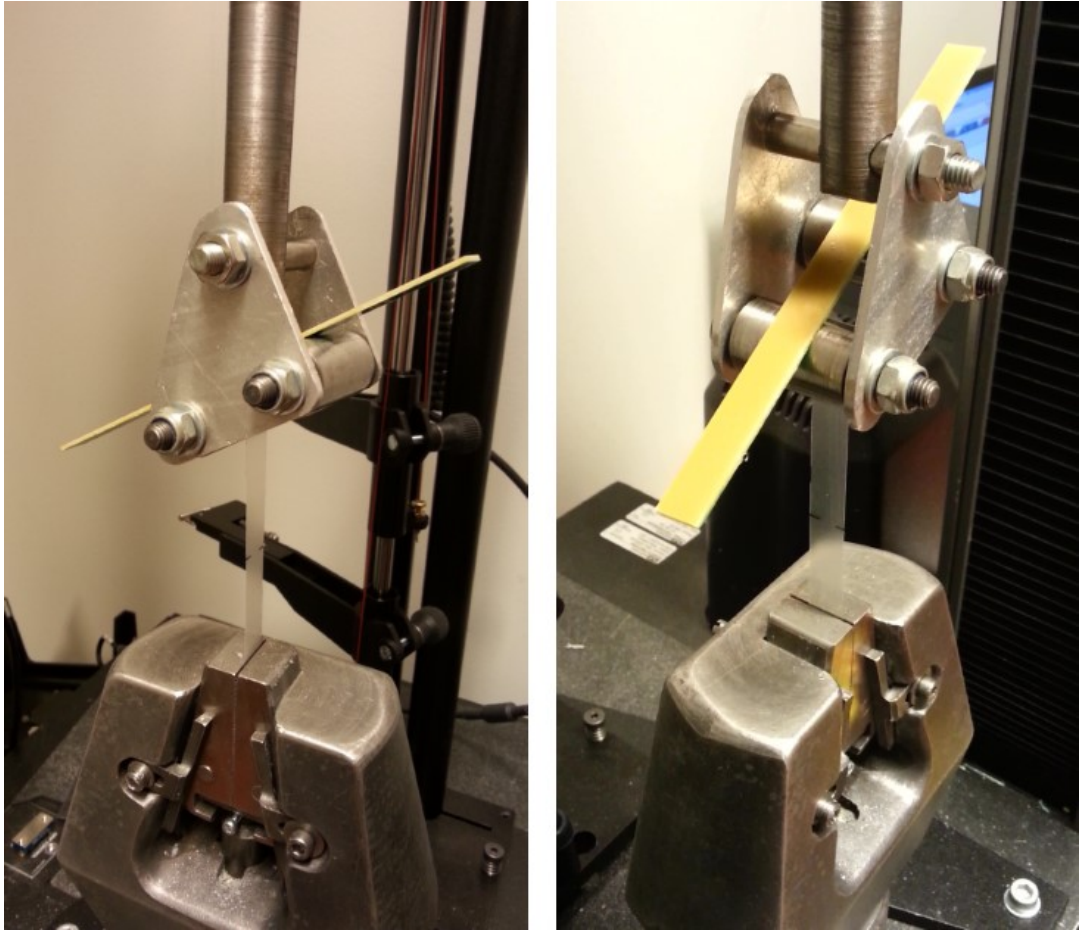
### **5.1.5 Heat treatment**

Products can undergo elevated temperatures during manufacturing processes, which may affect materials and change surface properties. In semicrystalline plastics, high temperatures can induce re-crystallization via cooling. Uncontrolled heating and cooling of the plastics can increase total crystalline content of the surfaces and decrease the surface energy and the wetting. [23]

The TPU-film substrate is attached on a metal plate and cleaned with IPA before heating. The cleaned sample is heated in an oven where the sample is held for 30 minutes at 140 °C. After the heating, the sample is let to cool down in an ambient temperature.

## **5.2 Peel tests**

In stretchable electronics, adhesives need to bond two different surfaces together. The rigid surfaces and PCBs can be joined with elastic substrates with NCA that form non-conductive contacts. At the same time, conductive contacts are maintained via compression. The composition and properties of NCAs vary, which further affect how well they bond the module and stretchable substrate. Adhesion quality of NCAs can be tested with a peel test, which is carried out to investigate which common types of NCAs has high adhesion. After a peel test, also failure mechanisms of the peeled sample are examined to analyse possible methods to increase adhesion of NCAs in future.



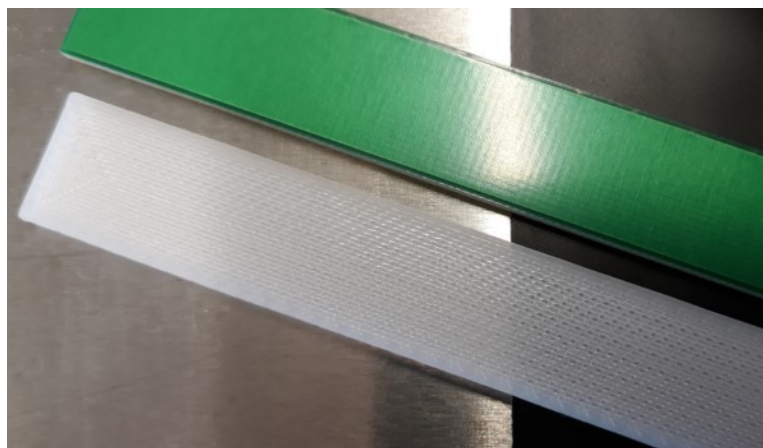
*Figure 22. The floating roller jig with a peel test sample.*

A peel test is done by using a floating roller method that peels the samples in a 45 degrees angle, which is presented in Figure 22. The floating roller jig is fixed in Instron 5967 tensile test machine that is equipped with a 2kN load cell in this study. The samples are loaded at a 50 mm/min speed until failure of the samples or point of maximum movement of the machine. The peel test NCA samples are shown in more detail in Table 9.

**Table 9.** Peel test samples in this study.

Series	Adhesive type	Manufacturer and adhesive name	Handling time of the samples	Sample code
1	Epoxy	Permabond ET515	30 min	ET
2	Epoxy	Permabond MT382	2 h	MT
3	Polyurethane	3M DP610	2 h	DP
4	Pressure-sensitive	3M 8132LE	20 s / 50 °C	LE
5	Cyanoacrylate	Loctite 406	5 min	406
6	Cyanoacrylate with primer	Loctite 406 with Loctite SF 7239	5 min	724

Each NCA type is applied on two different rigid substrates so that there are altogether 12 different samples. The each type of samples have 6 parallel samples. The samples consist of a 12 mm wide and 160 mm long rigid substrate, which is either from solder mask covered FR4 or 3D-printed polylactic acid (PLA). The FR4 substrate is coded as “F” and the PLA substrate is coded as “P” in the sample names. The materials and surface topographies affect adhesion on a rigid substrate; the surface of FR4 is smooth and dense and the surface of a PLA substrate is uneven and permeable. Furthermore, the solder mask is made from hard epoxy and the PLA is biodegradable plastic. The rigid substrates are adhered over a 12 mm wide and 210 mm long TPU-film. The TPU-film is 50 mm longer so that the samples can be fixed to the lower jaw of the tensile test machine. Figure 23 shows the smooth FR4 substrate and the rough 3D-printed PLA substrate.



**Figure 23.** FR4 and 3D-printed PLA substrate.

Before the assembly of the samples, the TPU-film and rigid samples are conditioned for 24 h at 23 °C and 50 % air humidity. The samples are prepared by spreading adhesive over rigid substrates with a brush, and then pressed on the TPU-film. The samples are compressed with a 10,1 kg weight certain times, where the time depends on reported handling strength time of the adhesives. The 6 parallel samples of the two-component adhesives are prepared all at once because of the long handling time. The all parallel samples are compressed under the 10,1 kg weight at the same time.

On the contrary to the two-component adhesives, the very short handling time possessing cyanoacrylate adhesive samples are compressed one at the time so that the compressive strength is same as with the two-component adhesives. The exception from other peel samples are the PSA 8132LE transfer tape samples that are pressed over the TPU-film with the press at 50 °C, 3 bar and 20 s. When all samples have achieved handling strength, they are allowed to dry 7 more days at room temperature.

The prepared peel test samples are conditioned for 24 h at 23 °C and in 50 % relative air humidity before the peeling. Also, peeling of the samples is started 20 mm by hand so that the peeling starts evenly. In other words, initiation of a crack is done by hand and propagation of the crack is measured as the peeling. The peeling is measured with Instron 5967 (load (N) and displacement (mm), where the load is changed to bond strength (N/mm) with equation:

$$G_p = \frac{F}{b} (1 - \cos \theta), \quad (11)$$

where  $G_p$  is the momentary peel strength,  $F$  is measured load,  $b$  is the width of sample and  $\theta$  is the angle of peel. In the test here, the width of the samples is 12 mm and the angle of the peel is 45°. Equation 11 is simplified and it ignores elongation of the peel arm that is highly elastic TPU-film. In addition to the elongation of the peel arm, temperature, strain rate and other variables affect the bond strength of samples. [88] [89] In the tests here, all samples are prepared and tested the same way, which makes them comparable with each other.

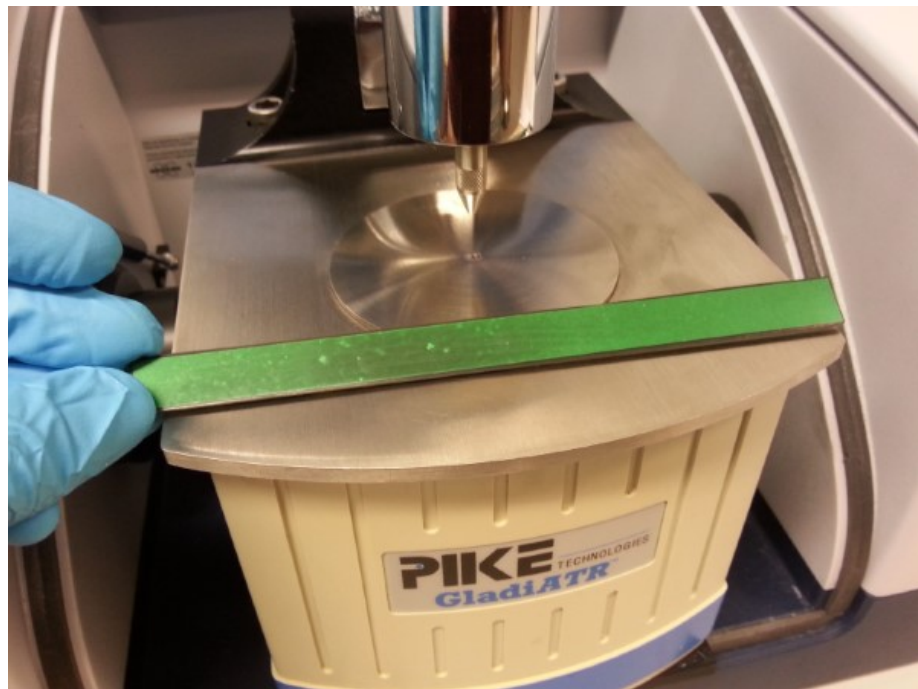
It is notable that the unit of peel strength N/mm “seems” almost same as N/mm<sup>2</sup> (which is equal to MPa), which is also used to define “strength” of interfaces. These are, however, not connected to each other. [36]

### 5.2.1 Examination of failure mechanisms

Failure of the peel test samples depends on how the initiated crack propagates during the peeling. The failure can be cohesive failure that happens solely in adhesive or substrate, or adhesion failure that occurs along the interface between adhesive layer and substrate. The failure can be also both cohesive and adhesion failure. By examining the failure

mechanisms in peel test samples, it is possible to determine how failures evolved and how their durability can be improved. [67]

The peel test samples are analysed with an FTIR device that examines properties of samples by following how infrared radiation (IR) interfere with them. The used FTIR exploits a horizontal attenuated total reflection (ATR) method, which measures the surface composition of the samples. The ATR directs horizontally a broad range IR beam to a crystal that further leads the IR upwards to the surface of the sample. The IR progresses small distance in the sample and reflects back to the crystal. The reflected IR is compared to the original IR-spectrum of the crystal and the IR-spectrum of the sample is recorded. The IR-spectrum of the sample is comparable to the existing specimens and qualitative and quantitative properties of the sample can be recognized. [90] Figure 24 shows the ATR device GladiATR that is used with the FTIR test machine Bruker Optics Tensor 27.



**Figure 24.** *GladiATR test device and a peeled FR4 substrate with a visible adhesive layer.*

The ATR-FTIR uses the diamond as the crystal, which can be seen as small area in the middle of the circular plate in Figure 24. The diamond is compatible with the commonly used mid-region IR-spectrum (where wavenumber varies between  $4000\text{ cm}^{-1}$  –  $400\text{ cm}^{-1}$ ). The mid-region IR-spectrum consist of vibration states of the most molecular functional groups. The IR-spectrum has generally two areas, an area between  $4000\text{ cm}^{-1}$  –  $1500\text{ cm}^{-1}$ , where single chemical bonds are recognizable and an area between  $1500\text{ cm}^{-1}$  –  $400\text{ cm}^{-1}$ , where materials have individual fingerprint vibrations. [90]

Furthermore, each sample is scanned 128 times with a  $4 \text{ cm}^{-1}$  resolution to remove noise from the IR-spectrums.

### 5.3 Tensile testing

While the contact angle test and the peel test study properties of local areas in stretchable electronics, tensile testing investigates the durability of the whole joint. The tensile testing examines the endurance of a sample by following force, displacement and voltage development. The recorded values are later converted to stress, elongation and resistance values. The samples with conventional joints have a module, substrate with printed interconnections and conductive adhesive. The wideness of the interconnections varies, and 2 mm and 1,5 mm wide tracks are tested. Also, alternative joint designs with additional rigid frame around the module is varied and studied in this thesis. The prepared tensile test samples are presented in Table 10:

*Table 10. Tensile test samples in this study.*

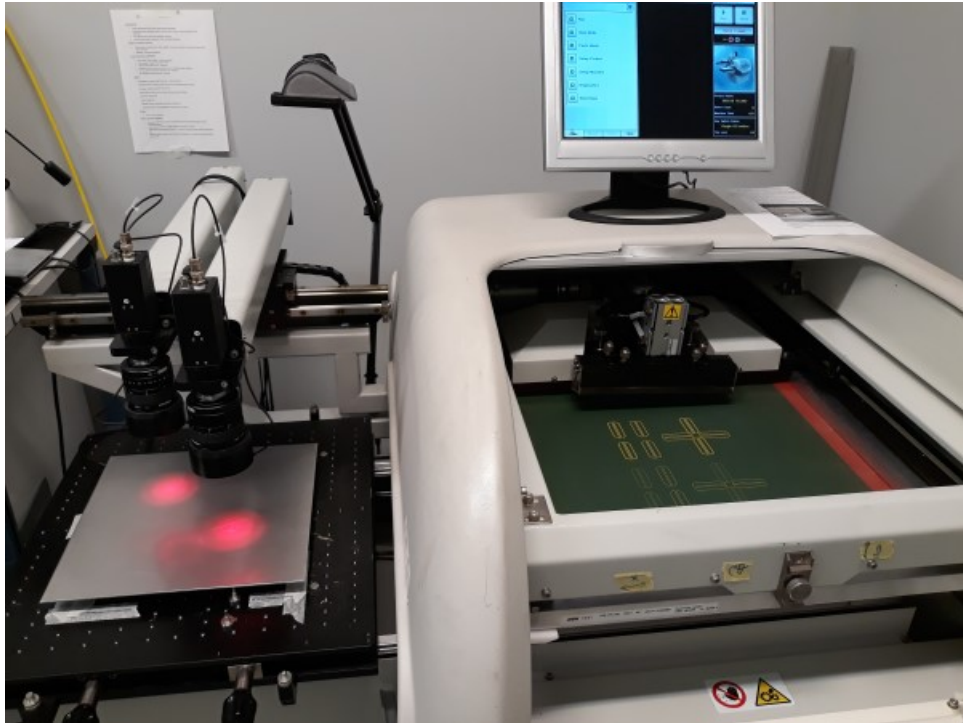
Series	Size of the ACF	Thickness of inter-connection (mm)	Additional component with the module
1	patch	2	-
2	strips	2	-
3	patch	2	Frame
4	strips	2	Frame
5	patch	1,5	-
6	strips	1,5	-
7	patch	1,5	Frame
8	strips	1,5	Frame

The modules are attached on a printed TPU-film with the ACF tape tesa HAF<sup>®</sup> 8412 that is used as strips under the contact pads and also as the module size patch under a module. Both the strips and the patch create electrical contacts in the joint but mechanically support the joint different amount. By varying the amount of the ACF in the joint, durability of the ACF can be studied in more detail. All 8 differing tensile test samples have 3 parallel samples.

#### 5.3.1 Screen-printing of interconnections

The interconnections of the samples are screen-printed with a conductive ink on a substrate. The substrate consists of a TPU-film that is attached on a supportive metal plate.

The used screen-print machine DEK 248 is presented in Figure 25. The DEK 248 machine consist of a black carriage that moves the substrate under the green-colored screen that has printable patterns. Over the screen are two squeezes that sweep on the screen and press the conductive ink through the screen to the substrate.

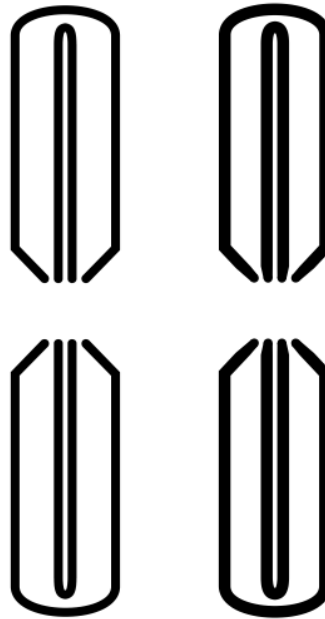


*Figure 25. Screen-printing machine DEK 248.*

Between the screen and the substrate, there is 1 mm gap so that only the area of the screen that is pressed by squeezes is in contact with the substrate. The squeezes provide 12 kg load towards the screen during a printing cycle. The printing cycle includes two passing of the squeezes, where the forward speed of a squeeze is 50 mm/s and backward speed is 70 mm/s.

The screen is made from polyester mesh of which thickness is 79  $\mu\text{m}$ . The mesh count is 195 (77/55) and the screen tension is 23,3 N/cm. The screen has several patterns that consist of nested U-shape interconnections, which are presented in Figure 26. The U-shape interconnections form closed loops when a module is attached in the middle of the pattern. The loop shape makes possible to measure electrical changes in the loops when they are elongated. Wideness of the selected interconnections are 1,5 mm and 2 mm, where the 2 mm wide interconnection has better mechanical and electrical properties (because of its width).



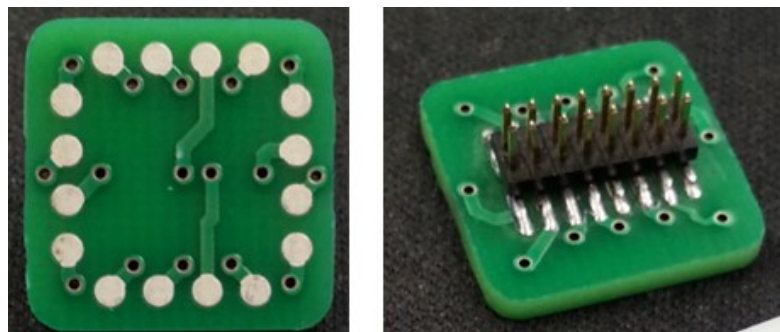


*Figure 26. The interconnection patterns in this study.*

After the screen-printing, the substrates with recently printed interconnections are heat treated for 30 min at 125 °C in the oven. The time of the heat treatment is long compared to the recommended curing time of the conductive ink CI-1036 because of bulky metal plates under substrate which take time to heat and cool. The TPU-film substrates with the prepared interconnections are cut to 29 mm wide slices, where the printed pattern is in the middle of the film.

### 5.3.2 Modules

In a tensile test, the square shape modules are attached on the printed substrate. The modules are two-side PCBs and are 1,6 mm thick. The size of a module is 15 mm x 15 mm with 2 mm rounding in the corners. On downside of the module are contact pads, which have a diameter of 1,5 mm. On topside of the module, there are coupling pads, where is soldered a pin header. Figure 27 presents the downside and topside of a module:

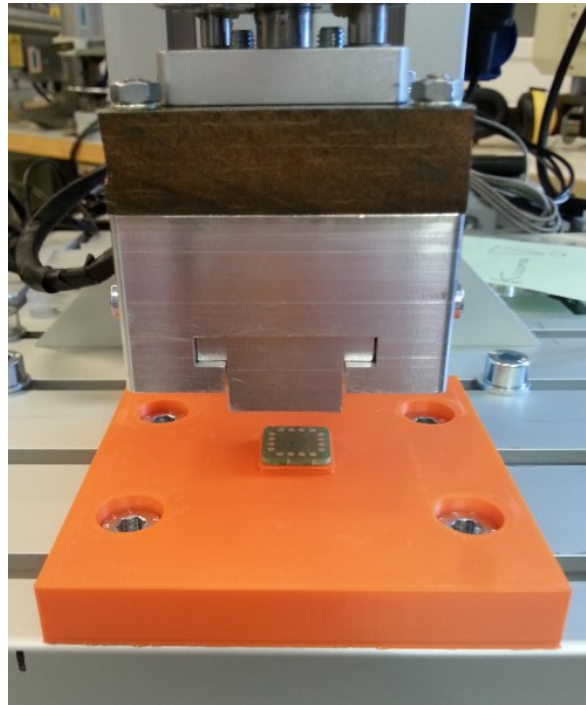


*Figure 27. Bottom and upper side of the module.*

Modules of the tensile tests are provided in boards where they are cut separately. The cut sides of the modules are smoothed with sandpaper and the pin headers are soldered on the modules by hand.

### 5.3.3 Joining of ACF samples

The ACF tape tesa HAF<sup>®</sup> 8412 is used as strips and patches between the module and the TPU-film. The size of a strip is 10 mm x 2 mm and the size of a patch is square with 15 mm sides and 2 mm rounding (which is equal to the size of the module). The ACF strips and patches are cut with a laser cutter to their fixed sizes. The joints are bonded by the ACF with a press, which is shown in Figure 28:



*Figure 28. The ACF press with an module.*

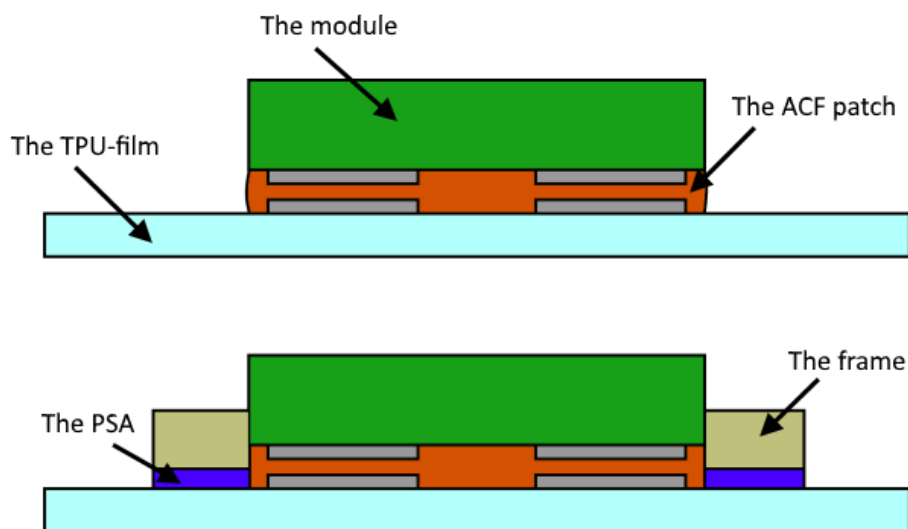
On top of the press is a heated press head and below is a fitting piece that allows pressing a module with soldered pin head to TPU-film. The module is bonded upside down to the printed TPU-film, and the bonding direction is presented in Figure 28. Heat of the press head is conducted through the TPU-film, which is more efficient direction to conduct the heat to the ACF than through the module. In the middle area of the fitting piece is an elevation that has a hole through in it. The elevation ensures that the press head presses only the module and the hole buries the pin head and keeps the module in place. The

fitting piece is 3D-printed with Ultimaker 3 from acrylonitrile butadiene styrene (ABS) plastic.

Temperature, pressure and press time used in the press are controlled and optimized to bond the joints. However, the maximum temperature of the press head is 150 °C, which is lower than the recommended bonding temperature of the ACF (180 °C – 220 °C) [58]. The used parameters for the bonding are 150 °C, 1,5 bar and 7 s, where the lower temperature is compensated with a longer press time. In addition, a teflon film is added between the press head and the sample because the temperature and pressure of the press head are high enough to deform the TPU-film over the module.

### 5.3.4 3D-printed frames

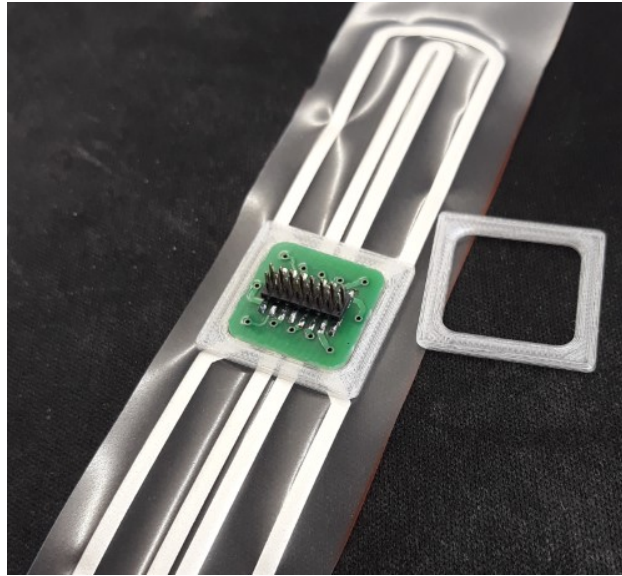
In addition to the conventional stretchable electronics joints, rigid frame components are added on TPU-film around the modules in this study. A frame around the module is an alternative method to strengthen the joint and transfer the stress concentration area further away from electrical contacts. Figure 29 presents differences between a framed module and a bare module:



*Figure 29. The bare module and the framed module.*

In principle, the framed joints have better durability than conventional joints because the frame increases adhered surface area of the joint. The frame makes the joint more rigid and hinder bending of TPU-film close to the module. Also, there is a new boundary between the module and the frame that shields the electrical contacts from direct cracking. If the framed joint starts to crack, the crack first initiate and propagate through the bonded frame before it can initiate and propagate under the module.

The frames are made by 3D-printing with Ultimaker 3. They are printed from transparent PLA plastic with a nozzle which diameter is 0,25 mm. The thickness of the frames is 0,8 mm (half of the thickness of the module) and an inner diameter is 15,2 mm with 2 mm rounding to compensate dimensional errors from the 3D-printing. The width of the frame is 2 mm and rounding at outer sides is 1 mm. Figure 30 shows the 3D-printed frame and the framed tensile test sample:



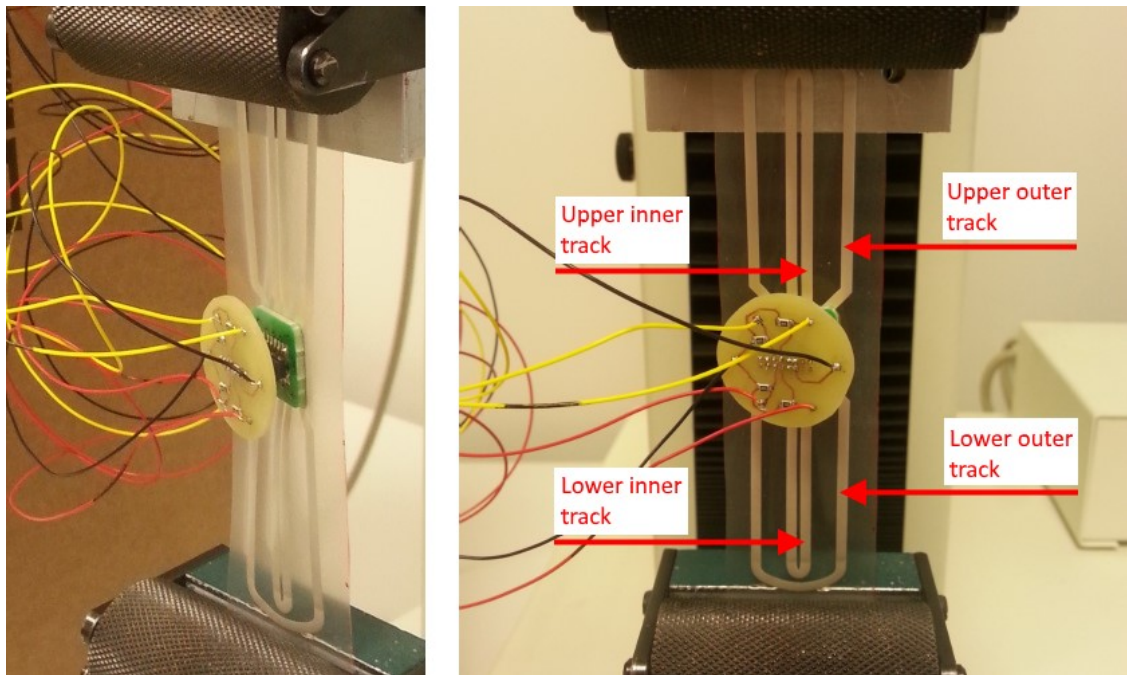
*Figure 30. The 3D-printed frame and a framed tensile test sample.*

The frames are attached on TPU-film with PSA tape 8132LE by 3M that is laser cut to same size pieces as the frames. Frames with PSA tape are aligned over printed TPU-films and are fixed with a press with parameters of 50 °C, 3 bar and hold for 20 s. The press is a top head press and presses the samples on the substrate side (which is covered with a teflon film during the pressing). The frames are bonded on the TPU-films before modules since the frames are thinner than the modules. The frames do not hinder the bonding of the modules. On the contrary, they simplify alignment of the modules over contact pads and make preparation of the joints easier.

### **5.3.5 Measurement of the samples**

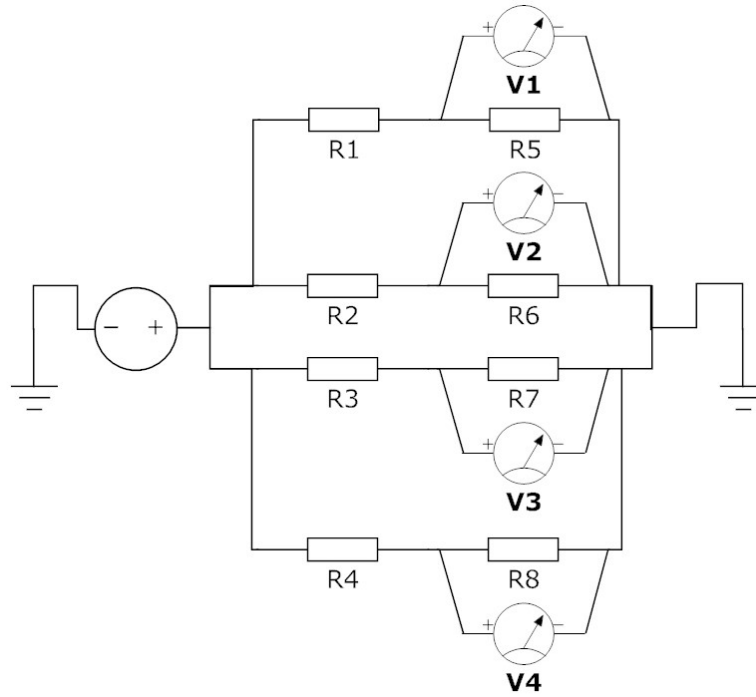
The tensile test samples are loaded with a Tinius Olsen H5KT Benchtop Tester. The tensile test machine measures displacement (mm) and load (N) of a sample. An original length of a sample is 120 mm and the speed of the test is 50 mm/min. By the original length of the sample, the measured displacement is converted to elongation (%). In addition, measured load is converted to stress (MPa) by dividing load with cross-sectional area of the sample, which is thickness of a TPU-film (0,1 mm) times a width of the sample (29 mm). Moreover, the tensile test is implemented 24 h after preparation of the samples.

In addition to displacement and load values, two NI myDAQ measuring equipment units by National Instruments are used to determine resistance changes in the samples. The NI myDAQs measure at the same time four interconnections of a sample and record voltage (V) in relation to time (s), which are recorded with LabVIEW 2017 Robotics program. By knowing the speed of the tensile test and the length of a sample, the time can be computed to elongation (%). Calculated elongation values of the NI myDAQs and the tensile test machine are combinable with each other. Between the NI myDAQs and the module is a connector PCB that is attached on the pin head of module. Figure 31 shows the fabricated connector PCB and the measured interconnections.



**Figure 31.** A tensile test sample with connector PCB.

Both NI myDAQs units have two channels where one channel measures voltage of single interconnection. The channels are measured and recorded separately so that resistance development of each interconnections are traceable. The voltage changes of interconnections are measured from zero to maximum voltage output, which is achieved by using common earth and voltage output in the NI myDAQs. The more detailed circuit diagram of the connector PCB is presented in Figure 32.



**Figure 32.** The circuit diagram of connector PCB in this study.

The output voltage of the PCB is 5 V and it is divided to four channels. The channels have two resistors, where the first resistors R1, R2, R3 and R4 are 5600  $\Omega$  surface mount resistors. The second resistors R5, R6, R7 and R8 are printed loop interconnections of the sample, of which resistance values increase when the interconnections elongate. The increase of resistance also increases voltages over the resistors, which are measured with V1, V2, V3 and V4 (that are in the NI myDAQs and LabVIEW test setup). The resistance is calculated by the Ohm's circuit law:

$$V = RI, \quad (12)$$

where  $V$  is the voltage,  $R$  is the resistance and  $I$  is the current [12]. By the rules of resistors in series or in parallel, the Ohm's law is used to deduce the used Equation 13:

$$R_2 = \frac{R_1}{\left(\frac{V_1}{V_2}\right) - 1}, \quad (13)$$

where  $R_2$  is the resistance of the printed interconnection,  $R_1$  is the resistance of the surface mount resistor,  $V_1$  is the output voltage of the system and  $V_2$  is the voltage over the printed interconnection [12]. In the NI myDAQ units, there are inherent resistances without a sample (without the second resistors). An initial resistance of the NI myDAQ unit one is 8  $\Omega$  and an initial resistance of the NI myDAQ unit two is 16  $\Omega$ , which are taken into account and removed from the reported resistance values of a sample.

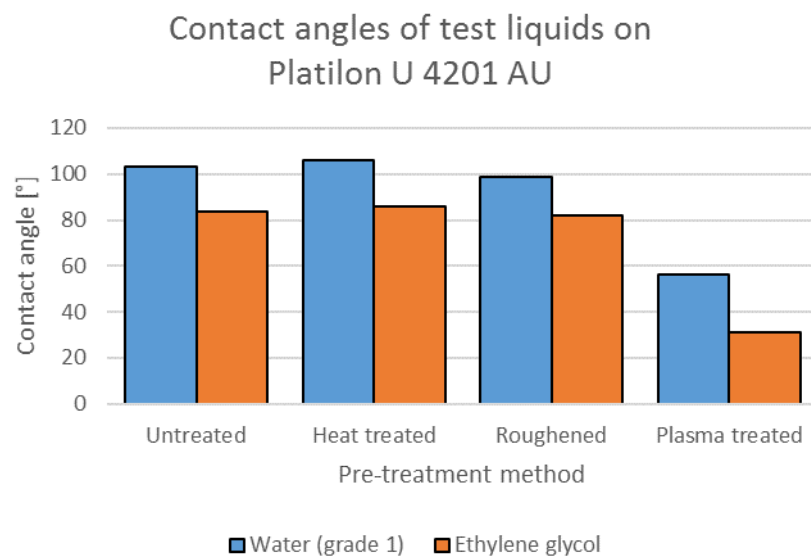
During testing of samples, the resistance of printed interconnections increases because their length increases (as seen in Equation 1) and matrix of the conductive ink deforms. Finally, the resistance enormously increases and the interconnection is defined to be failed. The failure can be caused by breakup of electrical contacts between a module and TPU-film or snapping of the printed interconnection.

## 6. RESULTS

Results from the surface treatment test, the peel test and the tensile test are introduced in this Chapter.

### 6.1 Surface treatments and wetting

The effect of surface treatments on wetting of TPU-film is inspected with the Krüss DSA100 droplet shape analyzer. The results of the testing are presented in Figure 33.



*Figure 33. Contact angles of test liquids on Platilon U 4201 AU.*

Figure 33 shows that grade 1 water and ethylene glycol have high average contact angles on untreated Platilon U 4201 AU TPU-film. Moreover, the heat treated and the roughened samples have almost the same average contact angles as the untreated reference TPU-film. The heat treated samples have slightly higher contact angles and the roughened samples have slightly lower contact angles than the reference samples. In addition to Figure 33, the average contact angles are presented in more detail in Table 11.



**Table 11.** Listed contact angles of the TPU-film.

Surface	CA(M) water [°]	CA(M) etyl. [°]
Untreated	103	84
Heat treated	106	86
Roughened	98	82
Plasma treated	56	31

The Figure 33 and Table 11 state that the plasma pre-treatment is the most efficient method to increase wetting of adhesives. With both test liquids that have different disperse and polar proportions, the contact angles of droplets decrease tens of percent. With the grade 1 water, the average contact angle decreases 45 % and with the ethylene glycol, the average contact angle decreases 63 %.

## 6.2 Peel tests

### 6.2.1 Average maximum values of peel samples

The first peel testing is carried out with six adhesives, two rigid substrates and Plaiton U 4201 AU TPU-film. Load of the samples and displacement of the tensile test machine vary during the peel tests and differently shaped peel curves are formed. At some point, the peel curves have the maximum load (N) that is converted to the maximum bond strength (N/mm). Average maximum bond strength of the peel samples with ranges are shown in Figure 34.

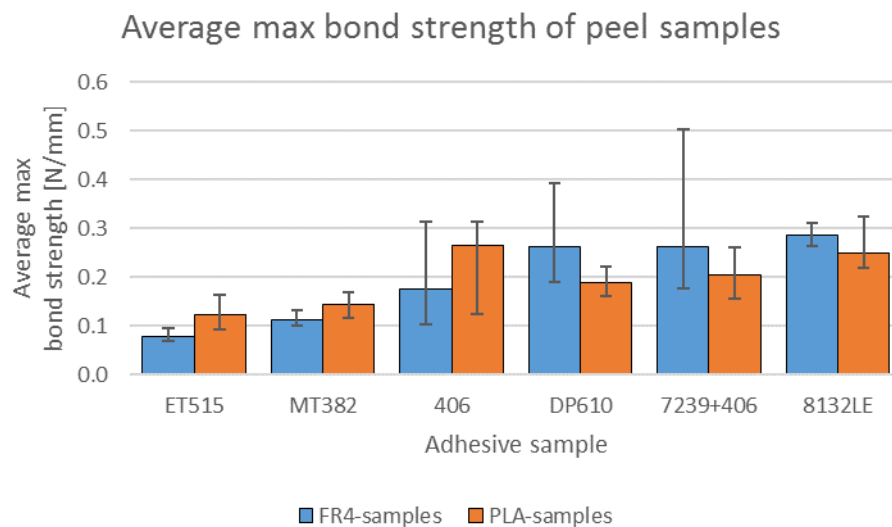
**Figure 34.** Average max bond strengths and ranges of NCA peel test samples.

Figure 34 shows that samples with ET515 and MT382 epoxy adhesives have the lowest average maximum bond strengths in the peel tests. The samples with other adhesives have higher average bond strengths than the epoxy adhesives but their results alternate more. The exception is 8132LE transfer tape samples that have bond strengths between 0,2 – 0,3 N/mm with moderate ranges. Table 12 shows in more detail the average maximum bond strengths and standard deviation (SD) and coefficient of variations (CoV). Moreover, the maximum averages, SD and CoV of the fixed samples are introduced.

**Table 12.** Average maximum bond strength and fixed average maximum bond strength values with SD and CoV of peel samples with the FR4 substrates.

<b>Adhesive</b>	<b>Average max values and SD (N/mm)</b>	<b>CoV (%)</b>	<b>Fixed max average values and SD (N/mm)</b>	<b>Fixed CoV (%)</b>
<b>ET515</b>	0,08 ± 0,01	11	0,08 ± 0,01	11
<b>MT382</b>	0,11 ± 0,01	12	0,11 ± 0,01	12
<b>406</b>	0,18 ± 0,07	39	0,15 ± 0,03	21
<b>DP610</b>	0,26 ± 0,07	28	0,26 ± 0,07	28
<b>SF 7239+406</b>	0,26 ± 0,11	43	0,21 ± 0,03	15
<b>8132LE</b>	0,28 ± 0,02	6	0,28 ± 0,02	6

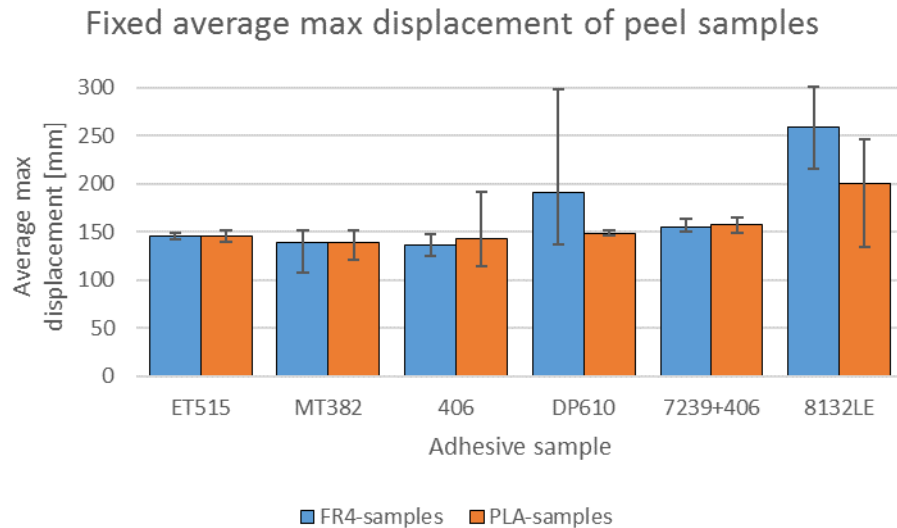
PU adhesive DP610, Loctite 406 cyanoacrylate with the primer Loctite SF 7239 and 8132LE transfer tape have the highest average maximum bond strengths on FR4 substrate in Table 12. However, the CoV between the parallel samples are also high with most sample types. When the average maximum bond strength values are fixed and single differing samples from six parallel samples are removed from the calculations (the samples 406-6F and 724-6F), the maximum average bond strength and CoV of cyanoacrylate samples decrease considerably. In addition to the FR4 substrate samples, Table 13 presents the average maximum bond strengths with SD and CoV of the unedited samples and the fixed samples with the 3D-printed PLA substrates.

**Table 13.** Average maximum bond strength and fixed average maximum bond strength values with SD and CoV of the PLA substrate peel samples:

<b>Adhesive</b>	<b>Average max values and SD (N/mm)</b>	<b>CoV (%)</b>	<b>Fixed max average values and SD (N/mm)</b>	<b>Fixed CoV (%)</b>
<b>ET515</b>	0,12 ± 0,02	18	0,11 ± 0,01	12
<b>MT382</b>	0,14 ± 0,02	14	0,14 ± 0,02	14
<b>406</b>	0,26 ± 0,07	26	0,26 ± 0,07	26
<b>DP610</b>	0,19 ± 0,02	12	0,19 ± 0,02	12
<b>SF 7239+406</b>	0,20 ± 0,04	18	0,19 ± 0,03	15
<b>8132LE</b>	0,25 ± 0,03	14	0,23 ± 0,01	4

The peel test samples Loctite 406 with and without the primer Loctite SF 7239 and the 8132LE transfer tape have 0,20 N/mm or higher average bond strengths. Except the cyanoacrylate samples without the primer, the samples have 18 % or lower CoV. After the single abnormal sample of 6 parallel samples are removed from the calculations (the samples ET3-P, 724-5P and LE-4P), only the Loctite 406 and 8132LE transfer tape samples have the average bond strengths over 0,20 N/mm. Moreover, only the Loctite 406 samples have the high CoV (26 %) and the CoV of the other samples is low (15 % or less).

In addition to the bond strength values of the peel test samples, final displacement values of the tensile test machine in the tests are good to take into account since they tell about the durability of the bond as the peeling continues. The original length of the TPU-film (peel arm) is 160 mm, which is shortened to 140 mm after the peeling is started by hand. The final displacement of the peel tests can be compared to the shortened length of TPU-film to see how much the length of the elastic TPU-film is changed in the peel tests. The maximum displacement and bond strength values describe together behavior of NCAs during the peeling process. Figure 35 presents fixed average maximum (final) displacement of the peel test samples.

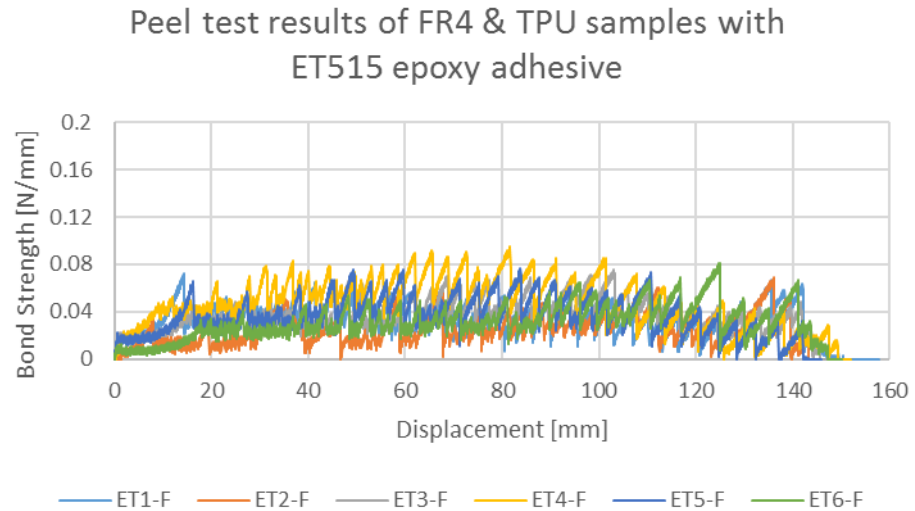


**Figure 35.** Fixed average max displacements of peel test samples.

Figure 35 describes the fixed average maximum displacement of the loading head of the tensile test machine in the peel tests. In the fixed results in Figure 35, the same samples are ignored as in average bond strength values in Table 12 and 13. Figure 35 shows that the TPU-films in the structural adhesive samples hardly elongate, except in the PU adhesive samples with the FR4 substrates. In the elastic pressure-sensitive adhesive 8132LE samples, the TPU-films elongate during the peel tests. With few samples, final displacement in the tests is 300 mm that is the limit of the tensile test machine. In the peel tests of the samples, the displacement of the tests would have been bigger if the tests could have been finished.

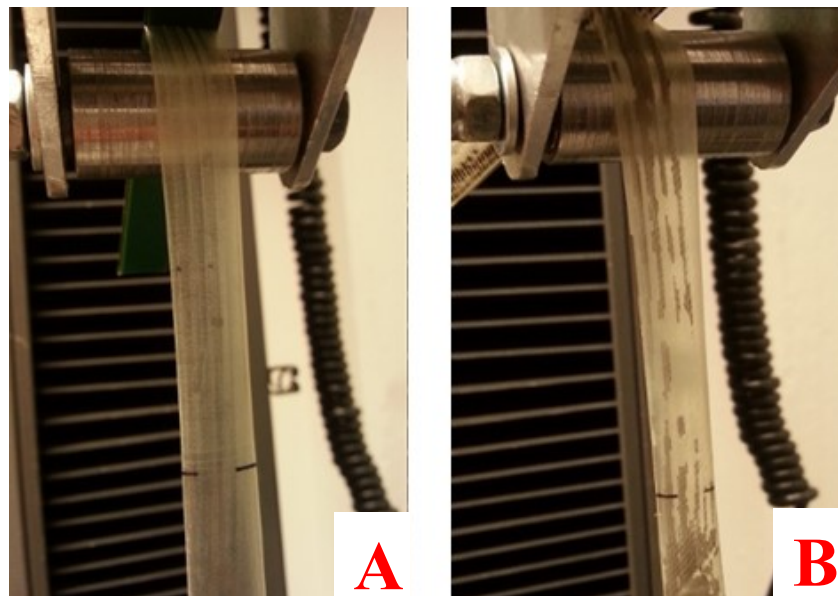
## 6.2.2 Epoxy adhesive samples

The epoxy adhesives ET515 and MT382 by Permabond have same degree adhesion over the rigid substrates and their peeling realizes in same manner. The both adhesives peel different way over the FR4 substrate and the PLA substrate, where the realized peeling curves of samples with ET515 adhesive and the FR4 substrate are shown in Figure 36.



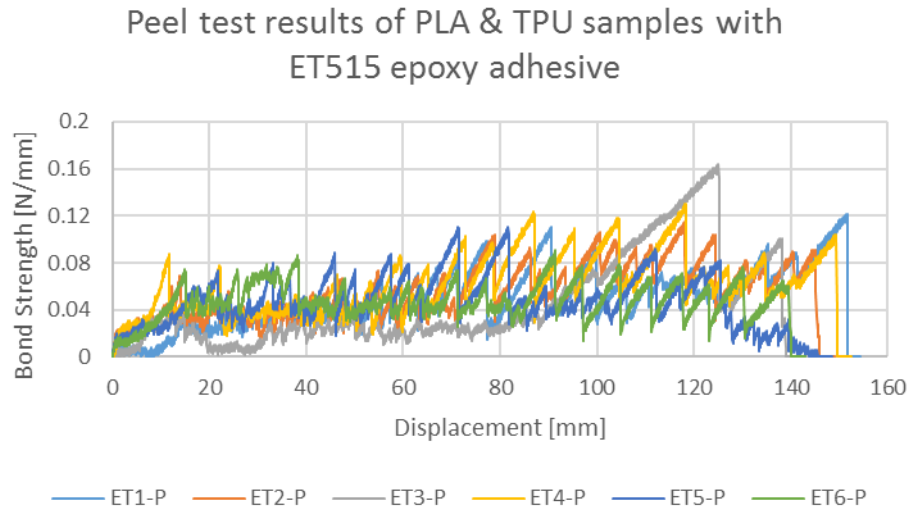
**Figure 36.** Peel test results of epoxy adhesive ET515 with FR4 substrate.

Figure 36 presents that the ET515 epoxy adhesive samples with the FR4 substrate have even zigzag shaped peeling curves. The FR4 substrate have smooth solder masked surface that attracts the epoxy adhesives and the peeling happens visibly in the interface of adhesive and TPU-film. Figure 37 presents a TPU-film from the FR4 substrate sample and a TPU-film from the PLA substrate sample.



**Figure 37.** TPU-films of FR4 (A) and PLA (B) substrates that are adhered with black colored MT382 epoxy adhesive.

As seen in Figure 37A, the epoxy adhesive on the FR4 substrate peels in the adhesive-TPU-film interface leaving no adhesive residues over the TPU-film. On the contrary to the FR4 substrate samples, the PLA substrate samples have varying failure mode upon peeling, which is shown in Figure 37B. The peeling happens on both interfaces of the adhesive, which increases bond strength of samples. The results are displayed in Figure 38.

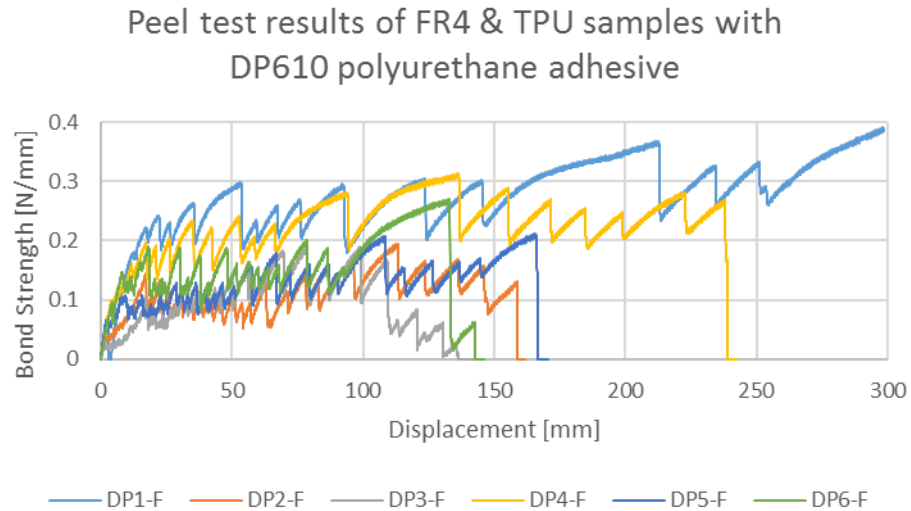


**Figure 38.** Peel test results of epoxy adhesive ET515 with PLA substrate.

The results of the epoxy adhesive samples with PLA substrate are more varying than the results of FR4 substrate samples. The unevenness increases when the peeling advances and bond strength can double during the testing.

### 6.2.3 Polyurethane adhesive samples

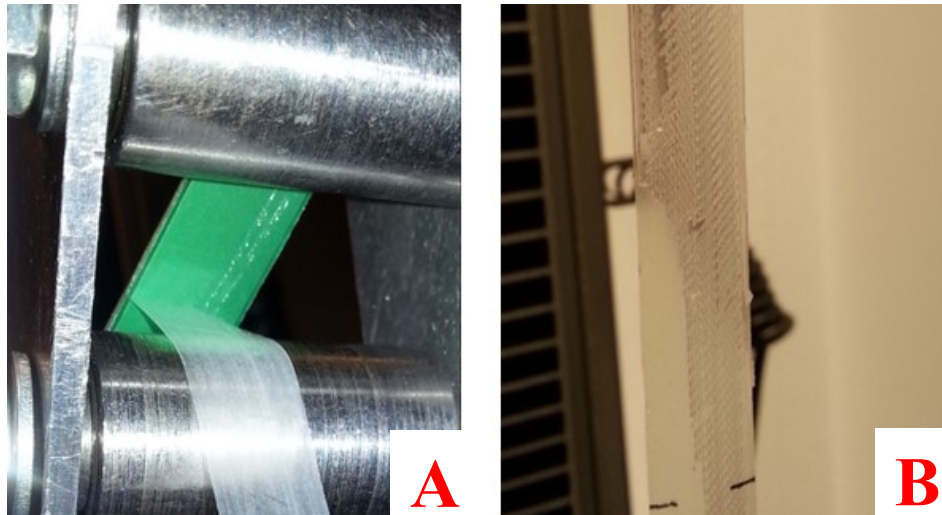
The polyurethane adhesive samples have 0,19 N/mm average bond strength on the PLA substrate while the peel tests have 148 mm average displacement. For the FR4 substrate, the average bond strength is 0,26 N/mm with 190 mm average displacement during the tests. The DP610 adhesive makes distinct adhesion to the FR4 substrate, which is noted during the peeling of 20 mm start of the samples by hand. The peel curves of DP610 adhesive with the FR4 substrate are shown in Figure 39.



**Figure 39.** Peel test results of polyurethane adhesive DP610 with FR4 substrate.

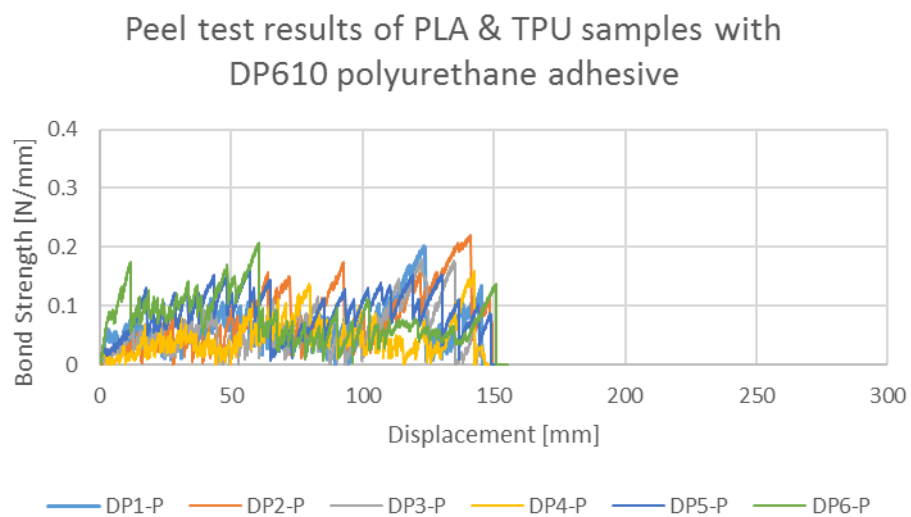
There are two kinds of results in Figure 39. Four of the samples, (DP-F samples 1, 2, 3 and 6) have approximately 0,2 N/mm maximum bond strengths and they form regular zigzag curves. On the contrary, the two samples (DP-F samples 4 and 5) have higher bond strengths and their peel tests have longer displacements (duration). Especially the sample 5 lasts throughout the test machine displacement range.

During the peel tests, it can be observed that the samples have two different types of peeling behavior that comply with the peel curves in Figure 39. The weaker samples peel solely in the adhesive-TPU-film interface and the adhesive layer remains completely on the FR4 substrate. In the more durable samples, the majority of peeling happen in the adhesive-TPU-film interface, but there are also minor amount of peeling in the other interface of the adhesive. The peeling in the substrate-adhesive interface is realized as single or multiple thin longitudinal stripes, which is shown in Figure 40A.



**Figure 40.** Peeled track in FR4 and DP610 adhesive interface (A) and a TPU-film of PLA substrate that is covered partly with DP610 (B).

Figure 40A shows a sample that has major peel in the adhesive-TPU interface and minor stripe-shaped peel in the substrate-adhesive interface. Adjacent Figure 40B presents the peeled TPU-film from a PLA substrate sample, which has the distinct irregular adhesive layer on it. The peel curves of DP610 adhesive samples with the PLA substrate is seen below in Figure 41.



**Figure 41.** Peel test results of polyurethane adhesive DP610 with PLA substrate.

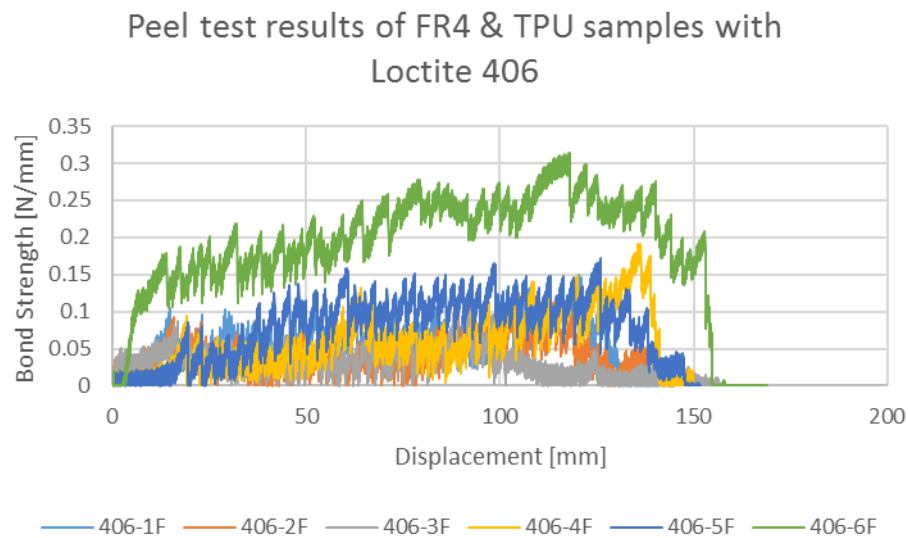
For the comparison, Figure 41 is in the same scale as Figure 39. The samples in Figure 41 have occasional bond strength peaks in 0,2 N/mm while having constant more lower



bond strength values. In addition, the peel tests of the samples have limited displacement, which tells that length of the TPU-films are hardly changed.

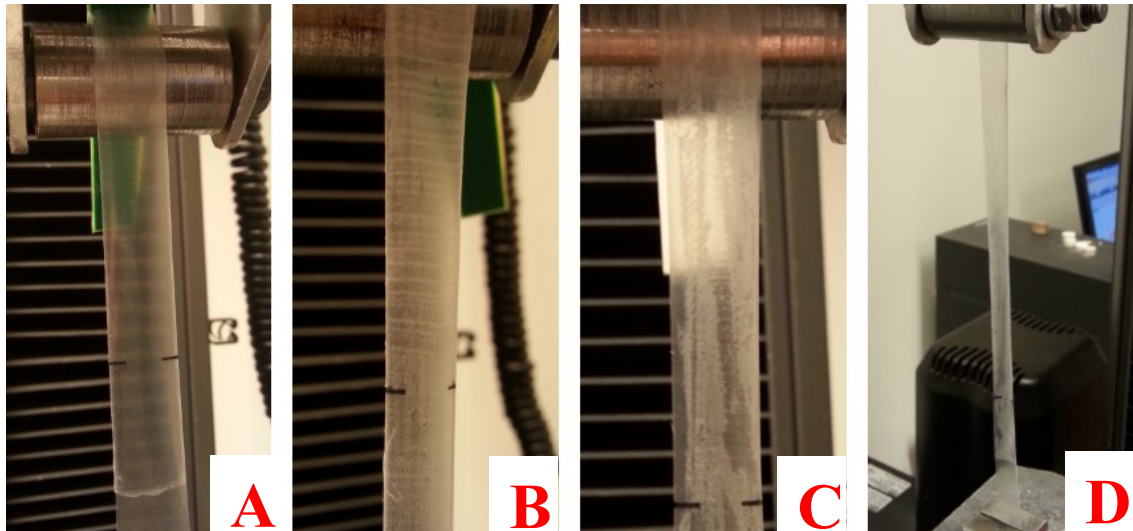
## 6.2.4 Cyanoacrylate adhesive samples

The rigid substrate and usage of the primer affect the peeling of the cyanoacrylate samples. The average maximum bond strength of Loctite 406 samples with the FR4 substrate is 0,18 N/mm and with the PLA substrate 0,26 N/mm, while the both kinds of peel tests have low displacements. On the contrary, the average maximum bond strength of Loctite 406 with the primer SF 7239 with the FR4 substrate increases to 0,26 N/mm and with the PLA substrate decreases to 0,20 N/mm. Moreover, one primed FR4 substrate sample is an exception and has 0,50 N/mm maximum bond strength, which is the highest bond strength value in the peel tests. Figure 42 presents the results of Loctite 406 on the FR4 substrate.



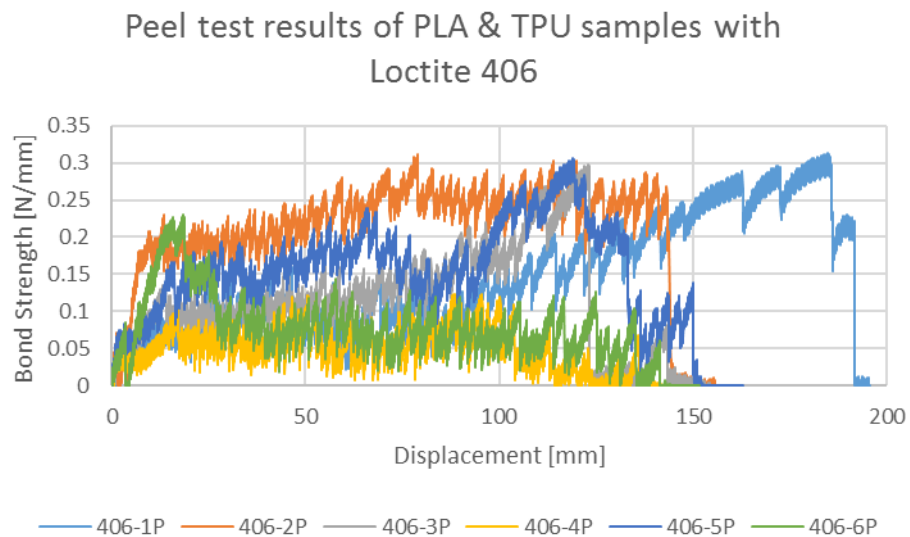
**Figure 42.** Loctite 406 cyanoacrylate adhesive in FR4 substrate.

The bond strength of the samples varies, which can be seen in the peeling curves in Figure 42 and in the observations in Figures 43A and 43B. Figure 43A shows the peeled TPU-film of a sample that had low bond strength values. Figure 43B presents the TPU-film of the sample 406-6F that had high bond strength values. The both films have distinct adhesive layers on them. The weak peeling has not left traces to the adhesive layer unlike the stronger peeling. The perpendicular stripes in Figure 43B shows that the peeling propagates in stages.



**Figure 43.** Observations of peeled TPU-films of cyanoacrylate adhered samples.

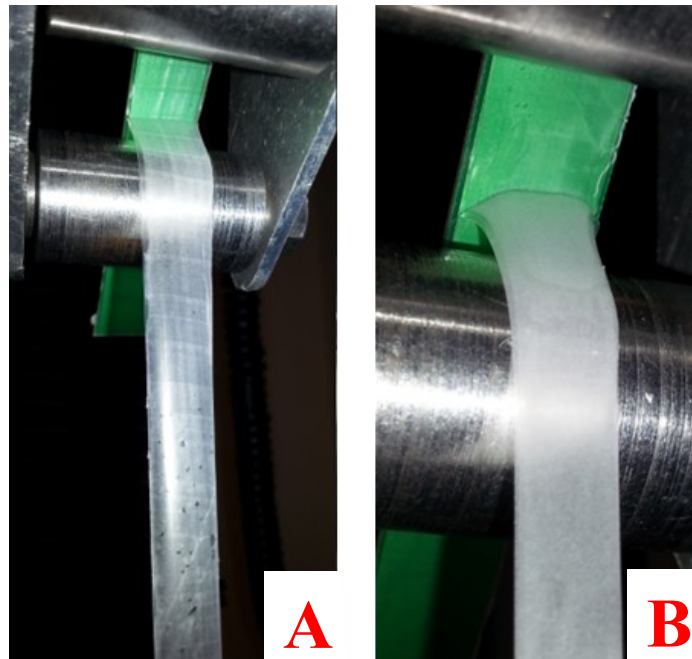
The peeled TPU-film in Figure 43C has uneven surface, which is typical for the samples with the PLA substrate. Figure 43D presents a TPU-film during the peel test, which is curved broadly under tension rather longitudinal elongation and necking. The peel curves of Loctite 406 samples on the PLA substrate are shown in Figure 44.



**Figure 44.** Peel test results of PLA substrate peel samples with Loctite 406.

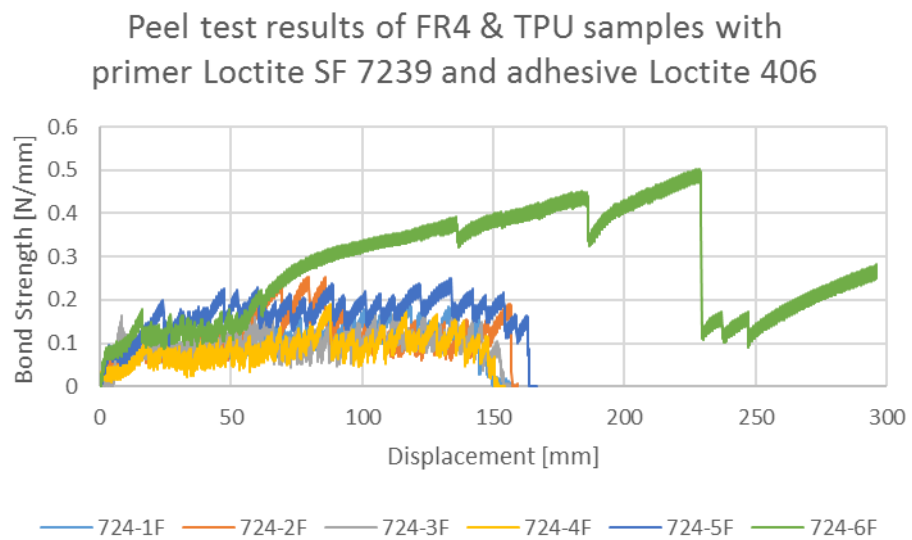
The bond strengths of Loctite 406 adhesive in the PLA substrate samples vary and could reach to 0,3 N/mm. Compared to the FR4 substrate samples, the PLA substrate samples are more unstable yet can momentarily reach a high level of peel force. Furthermore, priming the samples with Loctite SF 7239 before applying the adhesive seems to increase

unevenness of the adhesive layer. In Figure 45A, the primed Loctite 406 sample with the FR4 substrate has additional small dots in the adhesive layer.



**Figure 45.** Loctite 406 with Loctite SF 7239 primer.

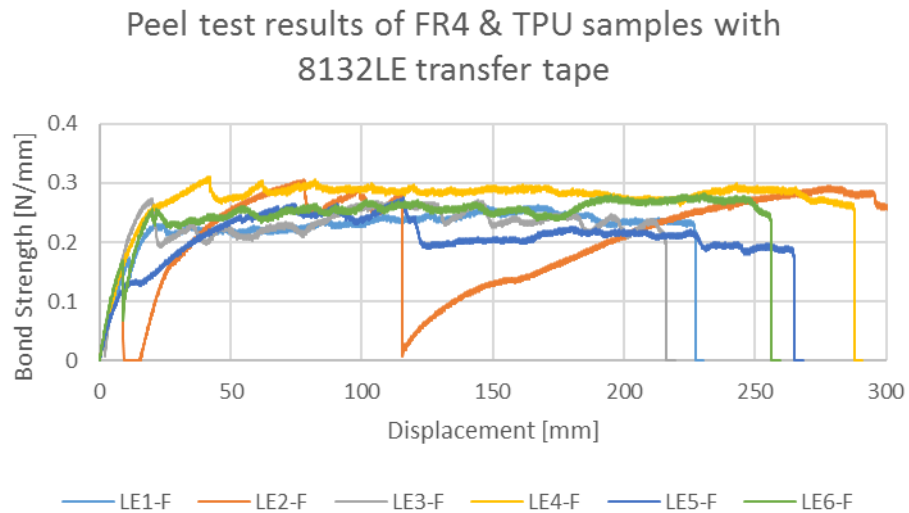
Figure 45B displays the close up from the peeling of the sample 724-6F that has abnormal bond strength results. The peeling of the sample stopped completely to the displayed spot and the film started to elongate plastically. The high bond strength of the sample 724-6F is also seen in the peel curve in Figure 46.



**Figure 46.** Peel test results of FR4 substrate samples with Loctite 406 and Loctite SF 7239 primer.

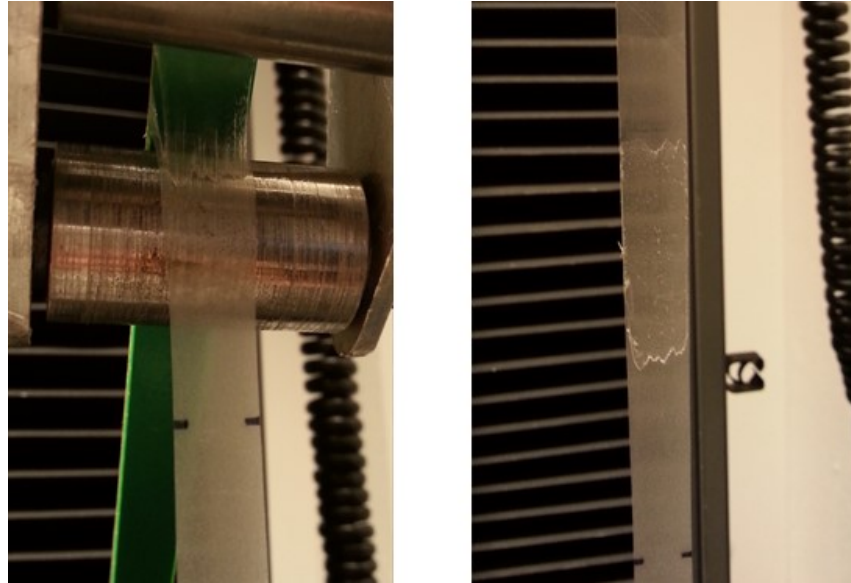
### 6.2.5 Pressure sensitive adhesive samples

The peel curves of the 8132LE tape samples with the FR4 substrate are below in Figure 47. The results present that the 8132LE tape samples have relative high average bond strengths and their peel tests have longer displacements than the original length of the peel arms (140 mm).



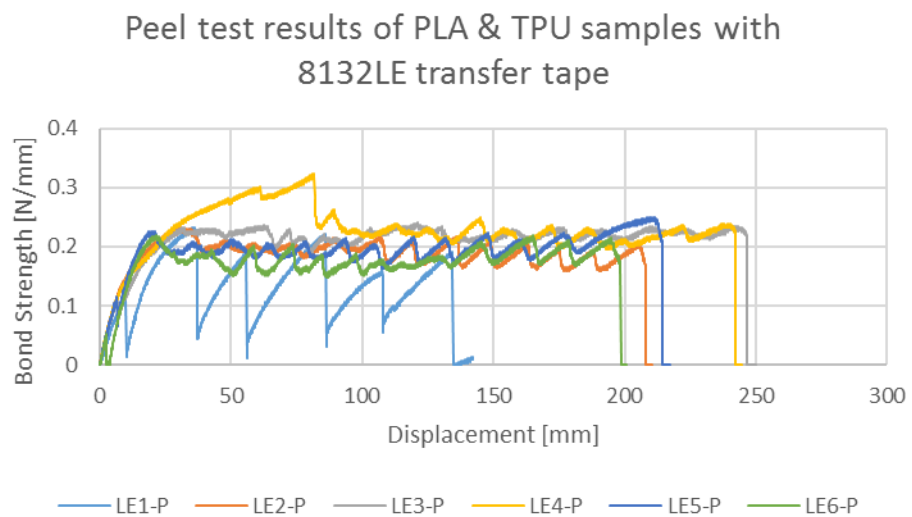
**Figure 47.** Peel test results of FR4 substrate samples with 8132LE.

Figure 47 shows that the peel behavior of the PSA tape differs from that of structural adhesives. After the start of the test, the peeling force remains constant (value between 0,2 – 0,3 N/mm bond strengths) until the failure of the sample. As the exception in Figure 47, the bond strength of sample LE2-F decreases almost zero at the middle of test. Figure 48 shows how the sample LE2-F is peeled.



**Figure 48.** Uneven peeling of the 8132LE sample LE2-F.

In the peel test of the 8132LE samples with the FR4 substrate, it is noticeable that the peeling that happens in the substrate-adhesive interface is constant (LE-F samples 1, 3, 4 and 6). In some cases, the peeling varies between the interfaces, which causes the lower and more unstable peel curves (LE-F samples 2 and 5). Figure 48 presents the unstable peeling of the sample LE2-F where the interface of the PSA tape change temporary. Before the interface change, the PSA tape elongates between the both interfaces and after some elongation snaps instantly, which is seen as the collapse of bond strength in Figure 47. The PSA tape samples with the PLA substrate are presented in Figure 49.

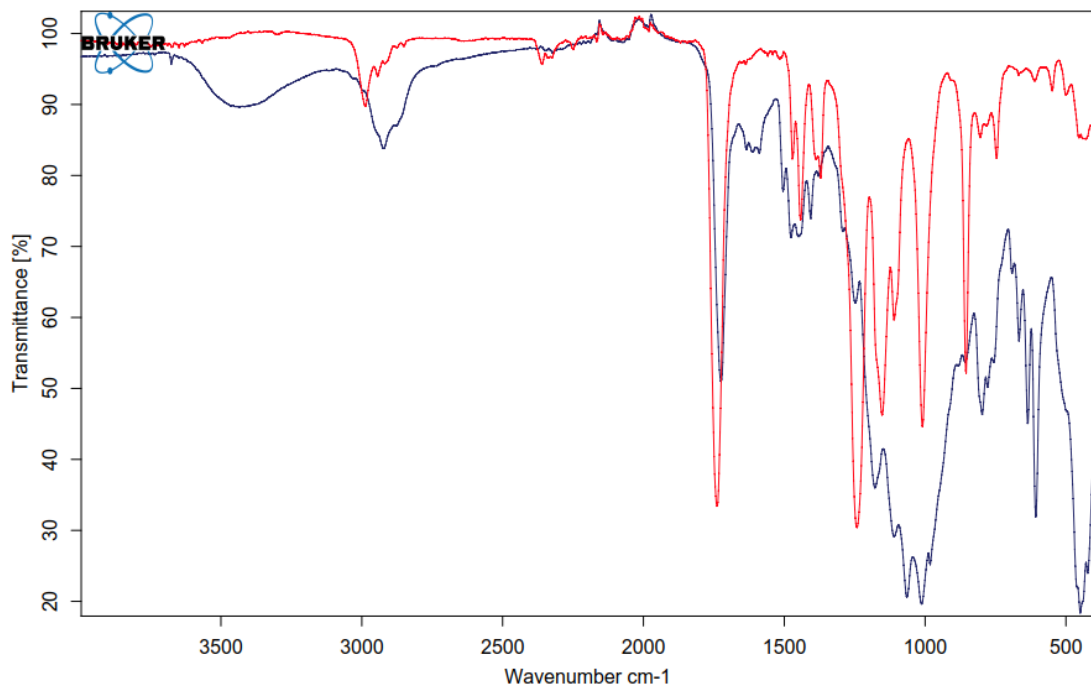


**Figure 49.** Peel test results of PLA and TPU samples with 8132LE.

The peeling behavior in the 8132LE samples with the PLA substrate is wavy and stays around 0,2 N/mm when the adhesive remains on the TPU-film (LE-P samples 2, 3, 5 and 6). In the sample LE1-P, the peeling happens in the adhesive-TPU interface and the PSA tape remains on the PLA substrate. The TPU-film is peeled in jerks and between the intervals starts to elongate from zero to the critical peeling point. Furthermore to the simple peeling on an interface, the peeling of the sample LE4-P begins exceptionally in multiple interfaces, which increases the maximum bond strength of the sample over 0,3 N/mm.

## 6.2.6 Failure modes of peel test samples

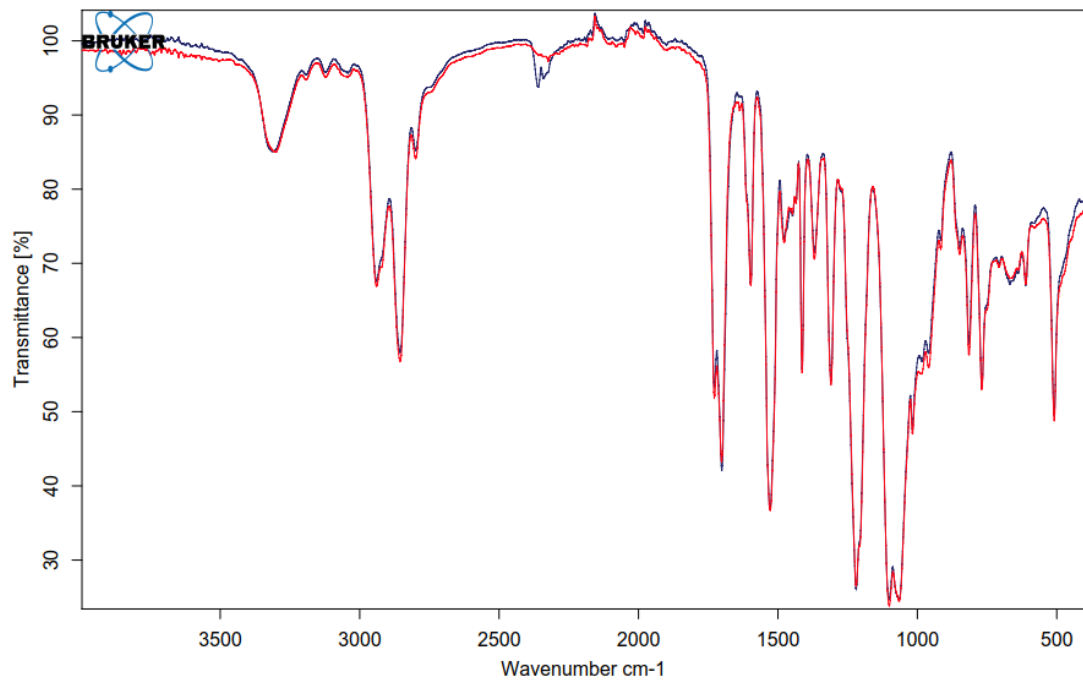
The peeled peel samples are analyzed visually and with the ATR-FTIR that tells chemical composition of peeled surfaces. The results of the ATR-FTIR inspection from the peeled samples are compared with each other and with unused reference samples; this gives a procedure that can tell where the failure locus is on a microscale. Existence or absence of adhesive residues can be used to deduce failure mechanisms of the samples. In some cases, the adhesive residues are visible but in case of transparent or non-obvious adhesives the ATR-FTIR analysis is clarifying method. The example about the ATR-FTIR results are shown in Figure 50.



**Figure 50.** ATR-FTIR analysis of reference FR4 substrate (blue) and FR4 substrate from the sample 1 of 406 cyanoacrylate adhesive (red).

The results of ATR-FTIR analysis can be easy to interpret that surfaces either consist of same or different chemical compositions. In Figure 50, the surface of FR4 substrate from a 406 cyanoacrylate sample has clearly different IR-spectrum compared to the unglued

reference sample and thus has different chemical composition. As the comparison for Figure 50, different kind of ATR-FTIR result is presented in Figure 51.



**Figure 51.** ATR-FTIR analysis of reference TPU-film (red) and TPU-film from the sample 1 of DP610 PU adhesive (blue).

The peeled TPU-film from PU adhesive DP610 sample has same IR-spectrum as the unglued reference TPU-film sample. The result indicates that surface of the TPU-film in the sample is unchanged and the peeling happened cleanly in the adhesive-TPU interface. The small difference in the middle of Figure 51 is the error that is caused by the diamond in the ATR machine. The most common failure types of the peel samples that are solved by visual estimation and the ATR-FTIR analyses are presented in Table 14:

**Table 14.** Failure mechanisms of peel samples.

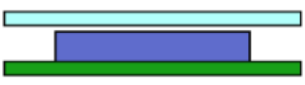
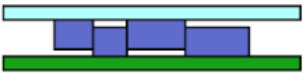




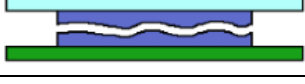
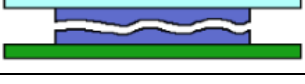

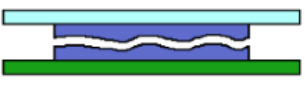


Sample	Rigid substrate	Failure type	Failure mechanism
ET515 epoxy adhesive	FR4	Adhesion failure	
ET515 epoxy adhesive	PLA	Adhesion failure	
MT382 epoxy adhesive	FR4	Adhesion failure	
MT382 epoxy adhesive	PLA	Adhesion failure	
DP610 polyurethane adhesive	FR4	Adhesion failure	
DP610 polyurethane adhesive	PLA	Adhesion failure	
406 cyanoacrylate adhesive	FR4	Cohesive failure	
406 cyanoacrylate adhesive	PLA	Cohesive failure	
406 cyanoacrylate adhesive with SF 7239 primer	FR4	Cohesive failure	
406 cyanoacrylate adhesive with SF 7239 primer	PLA	Cohesive failure	
8132LE transfer tape	FR4	Adhesion failure	
8132LE transfer tape	PLA	Adhesion failure	

Table 14 shows the failure type of peel samples either as adhesion failure or as cohesive failure. Furthermore, the failure mechanisms are illustrated in more detail, where the rigid substrate is colored in green, the TPU-film in light blue and the NCA in blue. The failure mechanisms of the samples are taken into account when the results are considered.



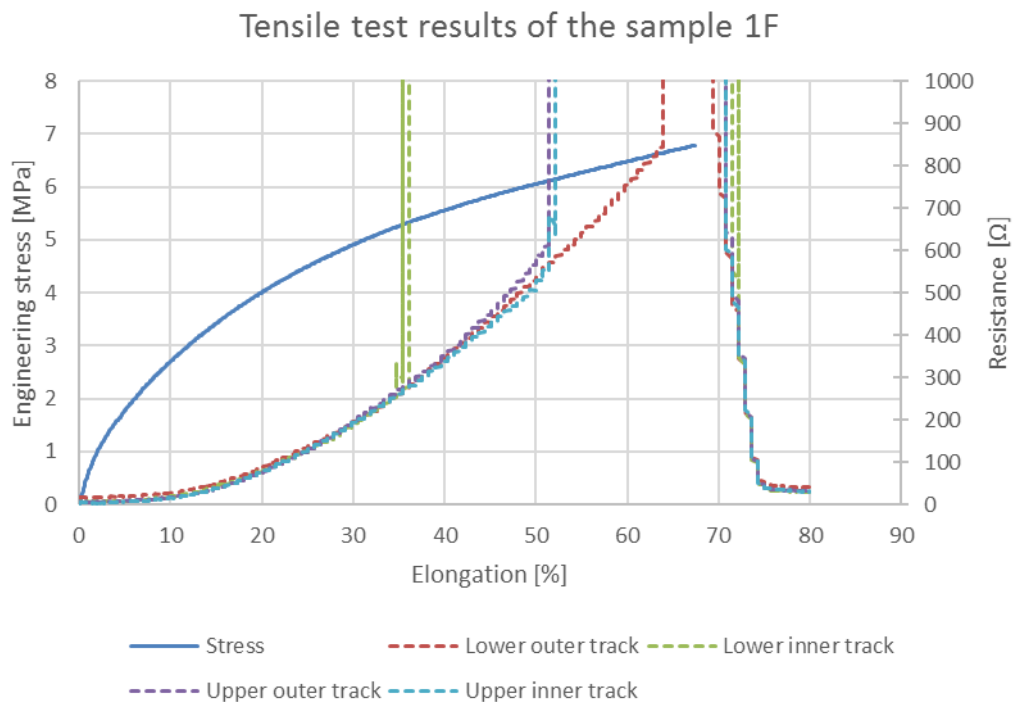
## 6.3 Tensile testing with modules

### 6.3.1 Reading of module test graphs

The tensile test is implemented with samples that have three variables:

1. Supportive frame structure can be added around the module.
2. The ACF is used as module size patch or as small strips just under the contacts.
3. The wideness of the interconnections (tracks) is either 2 mm or 1,5 mm.

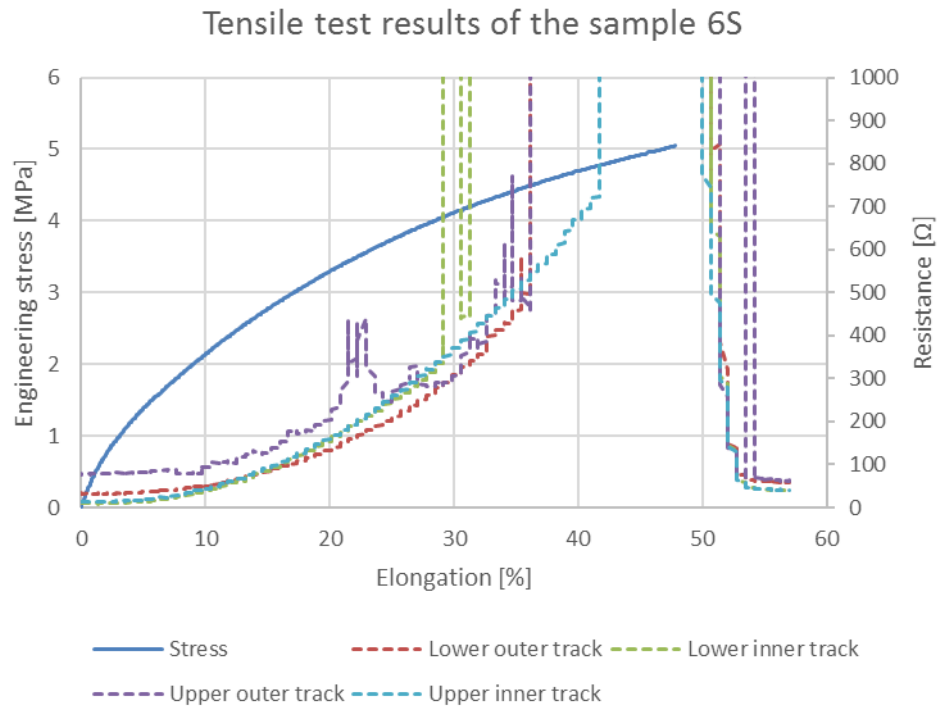
Altogether, there are eight differing samples that each have three parallel samples. The samples consist of four measurable tracks that are presented in Figure 31. The results of the samples form the figures where the resistance of the tracks increase evenly before sudden increase that is read as the failure. Figure 52 presents an example graph about the results:



**Figure 52.** The tensile test results of the sample 1F.

In Figure 52, the final stress, elongation and resistance values of the sample before failure are seen. For example, from Figure 52 can be read that the lower inner track of the sample 1F is broken first at 35 % elongation. The failure required 2 MPa stress and the last resistance value before the failure was approximately 300 Ω. Moreover, the results are not

always as smooth as in Figure 52 and they can have irregularities. Figure 53 presents the more varying results.



**Figure 53.** The tensile test results of the sample 6S with the 1,5 mm tracks and the ACF strips.

Figure 53 displays results of the sample 6S from series 6 that have thin 1,5 mm interconnections and ACF strips. The inner tracks have more steep resistance increase than the outer tracks. Also, the upper inner track has a high initial resistance and unstable resistance increase. In the results of the tensile test samples, the final elongation of tracks before the failure are the most interesting results.

The decreasing resistance values in the end of Figures 52 and 53 are the resistance values after the tensile test and the stress-strain curve (recording) ends before them. After the tensile test, the test machine returns quickly to the starting position, which decreases rapidly the elongation of the sample. The decreasing resistance values mainly tells that the failures of the tracks are not permanent and the conductivity can restore after the elongation.

### 6.3.2 Results of tensile tests with modules

Table 15 shows average values of elongation defined by the level that was required to break the tracks.

*Table 15. Average elongation of tensile test samples.*

Series	Size of the ACF	Width of the tracks (mm)	Support structure	Lower outer track (%)	Lower inner track (%)	Upper inner track (%)	Upper outer track (%)
1	patch	2	-	56.7	58.8	63.4	48.6
2	strips	2	-	46.3	47.2	41.0	34.0
3	patch	2	frame	51.6	49.3	58.8	49.8
4	strips	2	frame	68.5	71.3	52.8	56.9
5	patch	1.5	-	39.4	40.0	36.6	33.1
6	strips	1.5	-	38.4	25.0	34.5	35.4
7	patch	1.5	frame	37.5	34.0	38.9	34.3
8	strips	1.5	frame	38.9	33.8	33.3	39.1

By comparing the results, various observations can be made. The width of the tracks affects clearly the elongation and the thicker tracks of series 1-4 stand higher elongations than thinner tracks of series 5-8.

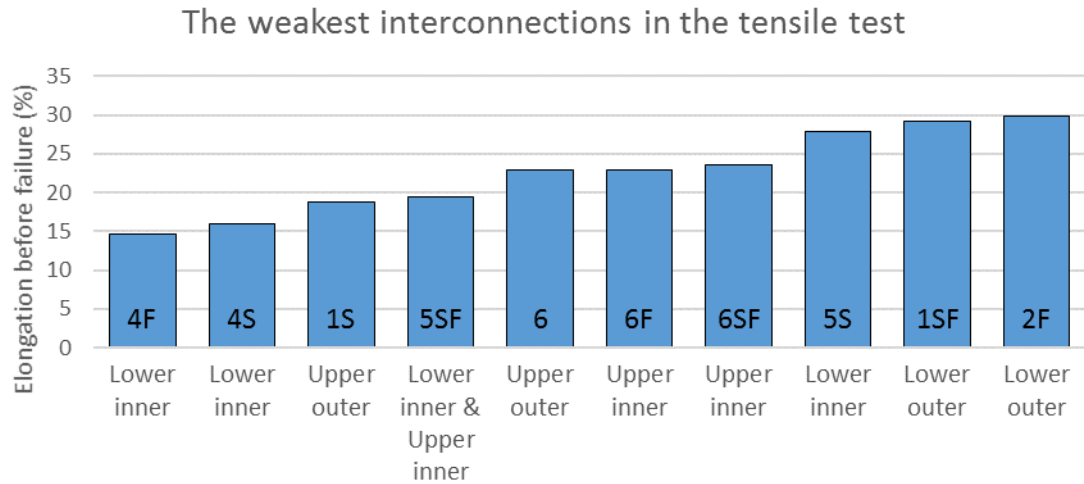
In case of the samples with 2 mm wide tracks, the inner tracks of series 1 endure slightly higher elongations than the outer tracks. Furthermore, series 1 has higher average elongations than series 2 and 3. Series 4 has the highest average elongation except the elongation of the upper inner tracks.

Series 5-8 endure approximately same amount of elongation before failures. However, it is noticeable that the inner tracks of the series 6 and 8 last less elongation than the outer tracks. In series 5 and 7, the average elongation is divided more evenly between the interconnections than in series 6 and 8. Table 16 shows more detailed results about the weakest track of each tensile test sample:

**Table 16.** *The weakest interconnection of each tensile test sample.*

<b>Se-ries</b>	<b>Sample name</b>	<b>Size of the ACF</b>	<b>Width of the tracks (mm)</b>	<b>Support structure</b>	<b>The lowest elongation before failure of a track (%)</b>	<b>Failuring track</b>
1	sample 1	patch	2	-	45,8	Upper outer
	sample 2	patch	2	-	48,6	Upper outer
	sample 3	patch	2	-	48,6	Lower outer
2	sample 1S	strips	2	-	18,7	Upper outer
	sample 2S	strips	2	-	45,8	Lower outer
	sample 3S	strips	2	-	35,4	Upper outer
3	sample 1F	patch	2	frame	35,4	Lower inner
	sample 2F	patch	2	frame	29,9	Lower outer
	sample 3F	patch	2	frame	41,0	Upper outer
4	sample 1SF	strips	2	frame	29,2	Lower outer
	sample 2SF	strips	2	frame	47,2	Upper inner
	sample 3SF	strips	2	frame	48,6	Upper inner
5	sample 4	patch	1,5	-	36,1	Upper outer
	sample 5	patch	1,5	-	30,6	Lower outer
	sample 6	patch	1,5	-	22,9	Upper outer
6	sample 4S	strips	1,5	-	16,0	Lower inner
	sample 5S	strips	1,5	-	27,8	Lower inner
	sample 6S	strips	1,5	-	31,3	Lower inner
7	sample 4F	patch	1,5	frame	14,6	Lower inner
	sample 5F	patch	1,5	frame	39,6	Upper outer
	sample 6F	patch	1,5	frame	22,9	Upper inner
8	sample 4SF	strips	1,5	frame	41,0	Lower inner
	sample 5SF	strips	1,5	frame	19,4	Lower inner & Upper inner
	sample 6SF	strips	1,5	frame	23,6	Upper inner

Table 16 is arranged so that three parallel samples of series are in same columns. Table 16 displays that series 1 has the most even lowest elongation values required to cause failure in outer tracks. In addition, it seems that the samples do not necessarily get weaker when the amount of ACF under the module is decreased to the ACF strip size. However, the lowest elongation of the other series (except series 1) is commonly lower and has higher variation. Figure 54 names the ten weakest tracks in the tensile testing.



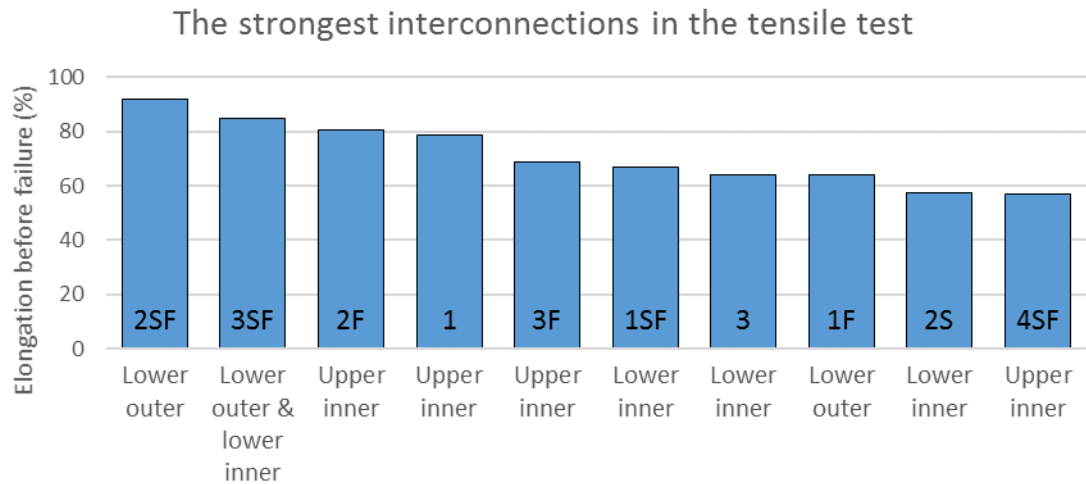
**Figure 54.** *The weakest 10 interconnections in the tensile test.*

Out of the ten weakest samples and tracks, the six samples are framed and the six samples have the ACF strips. Moreover, seven samples out from the ten have thinner 1,5 mm wide tracks. The weakest track in the tensile testing is the lower track of the sample 4F from series 7, which fails after 14,6 % elongation. As Table 15 and 16 list the weakest interconnections of the tensile test samples, Table 17 presents the highest elongating interconnections of the samples.

*Table 17. The strongest interconnection of each tensile test sample.*

<b>Series</b>	<b>Sample name</b>	<b>Size of the ACF</b>	<b>Width of the tracks (mm)</b>	<b>Support structure</b>	<b>The highest elongation before failure of a track (%)</b>	<b>Failing track</b>
1	sample 1	patch	2	-	78,5	Upper inner
	sample 2	patch	2	-	54,9	Upper inner
	sample 3	patch	2	-	63,9	Lower inner
2	sample 1S	strips	2	-	47,9	Lower outer
	sample 2S	strips	2	-	57,6	Lower inner
	sample 3S	strips	2	-	46,5	Lower inner
3	sample 1F	patch	2	frame	63,9	Lower outer
	sample 2F	patch	2	frame	80,6	Upper inner
	sample 3F	patch	2	frame	68,7	Upper inner
4	sample 1SF	strips	2	frame	66,7	Lower inner
	sample 2SF	strips	2	frame	91,7	Lower outer
	sample 3SF	strips	2	frame	84,7	Lower outer & Lower inner
5	sample 4	patch	1,5	-	49,3	Lower outer
	sample 5	patch	1,5	-	40,3	Upper outer
	sample 6	patch	1,5	-	42,4	Lower inner
6	sample 4S	strips	1,5	-	32,6	Lower outer
	sample 5S	strips	1,5	-	46,5	Lower outer
	sample 6S	strips	1,5	-	41,7	Upper inner
7	sample 4F	patch	1,5	frame	43,1	Upper inner
	sample 5F	patch	1,5	frame	52,8	Lower inner
	sample 6F	patch	1,5	frame	34,7	Lower inner
8	sample 4SF	strips	1,5	frame	56,9	Upper inner
	sample 5SF	strips	1,5	frame	27,1	Upper outer
	sample 6SF	strips	1,5	frame	53,5	Lower outer

Table 17 accompany the other tensile testing results that series 1-4 with wider tracks last longer than series 5-8 with thinner tracks. Also, adding of the frame does not lead any lower highest elongation values. The framed samples have either similar level of highest elongation or somewhat higher values. Figure 55 shows the ten strongest tracks of the tensile test.

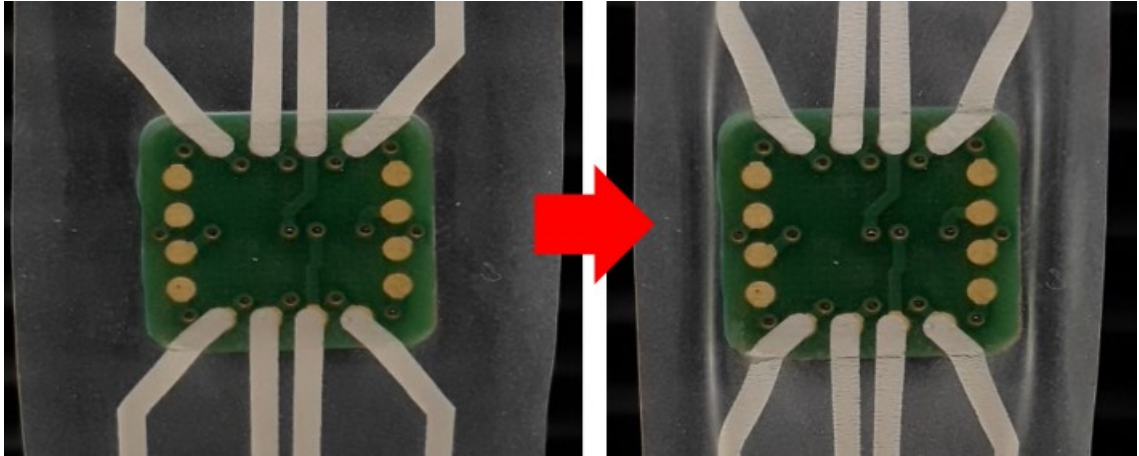


**Figure 55.** *The strongest 10 interconnections in the tensile test.*

Figure 55 presents clearly that from the ten most durable tracks, nine of them are 2 mm wide and only one is 1,5 mm wide. In addition, seven samples out from the ten have the frame, where series 4 is altogether presented. Based on Table 17 and Figure 55, the frame can increase maximum elongation of the samples, especially when only small amount of ACF tape is used.

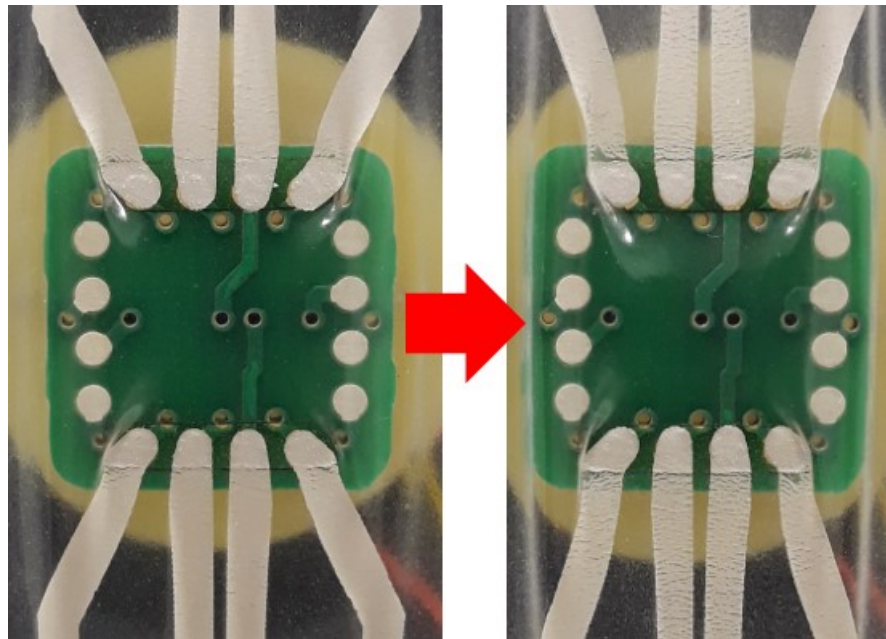
### 6.3.3 Deformations of tensile test samples

During the tensile testing, the samples undergo deformations when they elongate. The thickness of interconnections and the amount of ACF affects the occurring deformations. Furthermore, the frame around the module change the situation. Figure 56 displays, how a sample with ACF patch deforms during tensile testing.



**Figure 56.** Deformation of the sample with 1,5 mm wide tracks and the ACF patch.

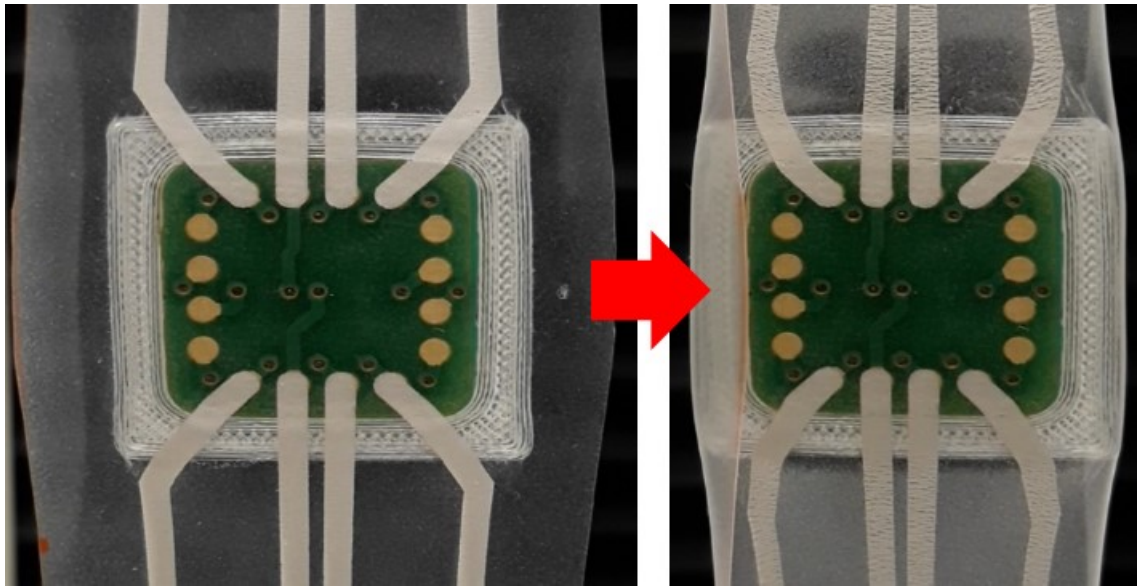
When the test advances, damage near edge of the module onsets in the interconnections. Especially, the outer interconnections seems have higher damage than the inner interconnections. The same phenomenon can be seen in Figure 57.



**Figure 57.** Deformation of the sample with 2 mm wide tracks and the ACF strips.

Figure 57 presents a samples with the ACF strips. Like in Figure 56, the outer interconnections have higher damage than the inner interconnections. In addition, only the area of contacts hold the module in place on the TPU-film. The film can elongate under the module, which can be seen as folding of the film. The deformation of the film is different when the frame is still attached in the sample, as shown in Figure 58.





**Figure 58.** Failure pattern of the sample with 1,5 mm wide tracks, the ACF patch and the frame.

As Figure 58 displays, the framed module has significantly bigger adhered area than the non-framed module. The frame affect the deformation of the interconnections and the outer and inner interconnections tend to elongate quite evenly.

## 7. DISCUSSION

In this Chapter, the presented results from the wetting tests, the peel tests and the tensile tests are discussed in more detail.

### 7.1 Surface treatments and wetting

As in Figure 33 and Table 11 have shown, the heat treating and the coarsening affect slightly to the contact angles of the test liquids. The heat treated samples have slightly higher contact angles, which can be caused by structural changes of the surface. The heat treatment can have triggered additional deformation of polymer structure in the TPU-film, which leads to higher crystallization on the surface. The more crystallized surface is more passive and have lower surface energy than the untreated TPU-film. Moreover, additives of the film are also considered. If a film consist of additives, also migration of the additives can be initiated during the heat treatment. The additives migrate and accumulate to the surfaces of the film and can make the surface more inactive. [23]

Correspondingly, the roughened samples have slightly lower contact angles, which are results from more uneven surface. Theoretically, higher amount of surface area increases surface activity and thus decreases contact angles of droplets. The roughing also makes the surface topography more irregular, which affects spreading of liquid and setting of the droplets, which becomes more irregular as well. Furthermore, the roughening always produces excess debris that is removed after the surface treatment. Despite the cleaning of the surface, some debris can remain in the grooves and affect to wetting and the contact angles.

The plasma pre-treatment is effective surface treatment method to increase activity of the surface, which realizes as lower contact angles of the droplets. For example, the contact angle of grade 1 water decrease 45 % and the contact angle of ethylene glycol decrease 63 %. The method how the plasma treatment is done affect greatly to the results. More intense plasma treatment improves the efficiency of the treatment. More powerful plasma treatment can be done by increasing exposure time or setting optimal distance between the plasma beam and the surface. Moreover, the effectiveness of the plasma treatment decreases over time because the treated surface reacts with environment. The impermanent nature of the treatment means that the treatment should be done right before applying adhesive or ink.

### 7.2 Peel tests

The peel tests provide numerical results about bond strength, visual observations considering peel behavior and comparison of chemical composition of the samples. The results

are combined and general conclusion about the realized peeling are made. Moreover, the samples show the optimal peeling conditions that should be pursued to maximize bond strength of NCAs.

### 7.2.1 Epoxy and polyurethane adhesive samples

Peeling of the epoxy adhesives ET515 and MT382 and the polyurethane adhesive DP610 resemble each other and they follow the same pattern. With the FR4 substrate, the peeling happens solely or mostly in one interface. In the PLA substrate samples, the peeling realizes in both interface and the adhesive layer tears randomly and leaves adhesive residues on both surfaces (on PLA substrate and on TPU-film). The roughness of the rigid substrate affect the peeling of the sample, where the rough substrate encourage multi-interface peeling of NCAs.

The bond strength of the samples varies and it can be interpret that the degree of the multi-interface peeling affects the bond strength of the samples. When the samples peel in one interface of adhesive (the amount of multi-interface peeling is zero or low), adhesion of the interface govern the peeling and define bond strength of the sample. On the contrary, when the samples clearly peel from both interfaces, properties of adhesive layer increase bond strength of the samples. In multi-interface peeling, there are adhesion failures in both interfaces and tearing of adhesive layer when the crack change the interface. The tearing of adhesive layer consume additional load that increase bond strength of the sample. However, the peeling in multiple interfaces increase the bond strength only limited amount and it cannot replace originally weak adhesion of NCA (like in the epoxy adhesive samples).

The polyurethane adhesive DP610 samples with FR4 substrate present that it is useful to increase amount of the multi-interface peeling when the original adhesion is the NCA is at sufficient level. Furthermore, tearing resistance of adhesive layers vary and it can be affected, for example, by thickness and chemical composition of adhesive layer. For instance, bond strength of the epoxy adhesive samples with PLA substrate (which have high amount of multi-interface peeling) increase 0,04 N/mm that is 50 % of the original bond strength of the samples. In addition, in polyurethane adhesive samples with FR4 substrate, the minor amount of multi-interface peeling can also increase the bond strength by 50 %, which is 0,1 N/mm. Compared to the FR4 substrate samples, the PLA substrate samples of the polyurethane adhesive have lower bond strength values. The lower bond strength can be explained by possible poor compatibility of PLA and PU, thickness variation of adhesive layer or stiffened TPU-film.

The PLA substrate has rough surface that increases unevenness and thickness variation of the adhesive layer. The varying thickness can allow forming of weak “easy paths” in the adhesive layer that guide propagation of the crack. The effect of “easy paths” depends

on the peel speed of sample, where at the low peel speed the crack has more time to develop along the weak route.

Moreover, TPU-films of the PLA substrate samples have adhesive residues that stiffen the film and hinder elongation of the film. The elongation is “an additional deformation” in the peeling that needs load to happen. When the film elongates in the tests, some load is consumed to the elongation, which decreases load in the crack tip.

Despite the good results of the polyurethane adhesive samples with the FR4 substrate, two disadvantages are discovered during preparation of the samples. The curing time of the DP610 adhesive is seven days, which is long compared to other available adhesives and do not support fast manufacturing. Secondly, the adhesive is highly sensitive to moisture. The used sample materials are conditioned before the assembly and the remained moisture in the materials reacted with the adhesive. The adhesive formed few gas bubbles with moisture, which stayed inside the adhesive layer while the adhesive hardened.

## 7.2.2 Cyanoacrylate adhesive samples

The color of the cyanoacrylate adhesive is more or less transparent and its fracture mechanism is not as simply to define as other adhesives. Still, by the FTIR-ATR inspection, the cyanoacrylate adhesive samples with or without primer have the same failure patterns. The chemical composition of peeled FR4 and PLA substrates are same although they are different materials. Also, the peeled TPU-films have chemically same surface with each other. Based on the results, the cyanoacrylate samples fail cohesively, which means their adhesive layer break.

The cyanoacrylate samples can fail cleanly or unevenly, which leave tracks in the peeled adhesive layer on the TPU-films. The weak samples peel easily and leave clear TPU-film without marks (Figure 43A). Some samples require higher bond strength and the peeling leaves light stripes in the peeled adhesive layer, which can indicate periodic high deformations in the sample (Figure 43B). Moreover, the adhesive layer change properties of the TPU-film and blocks its elongation. In Figure 43D, the film curves transversely rather than elongates longitudinally. The stiff TPU-film affects the bond strength values of the samples different way than the elongating TPU-film.

Especially the cyanoacrylate samples with the PLA substrate have irregular looking adhesive layers. The samples are thoroughly covered with the adhesive, which means that the adhesive thickness varies in the PLA substrate samples. Varying adhesive thickness indicates that the cohesive peeling inside the samples happen more irregularly. Generally, clean peeling happen easier than the uneven peel, which can partially explain the higher bond strength values of the PLA substrate samples.

Because of permeable and rough nature of the PLA substrate, the thickness of the adhesive layer varies spontaneously. The cyanoacrylate adhesive layer has thicker and thinner areas, where the thinner areas create the high bond strength of the samples [19] [38] [91]. However, presence of the thicker areas make the PLA substrate samples unstable. The unstableness is also increased when Loctite SF 7239 primer is applied on substrate and TPU-film before Loctite 406 cyanoacrylate adhesive. Theoretically, the primer increase bond strength and shortens the curing time of the adhesive. [38] [45].

Adding the primer to the samples increase unevenness of adhesive layers. For example, there are small dots in the TPU-film in Figure 45A that shows that the adhesive layer has cured unevenly. The primer can also increase bond strength of the samples. From Figure 45B that displays the strongest sample in the peel test (724-6F), the FR4 substrate and the TPU-film have irregularities on their surfaces, which indicates changes in thickness of the adhesive layer. Likely, the sample has optimally thin adhesive layer in the spot and it achieved 0,5 N/mm bond strength. The behavior of TPU-film in the sample 724-6F presents that the optimal bond strength of NCAs is 0,5 N/mm or little less. The high bond strength makes the TPU-film elongate plastically, which deform and damage the film.

Consequently, the primer did not leave chemical traces on the surfaces, which means the primer did not change the surface chemistry of materials. The primer reacted only with the adhesive. The main variable in the samples is the thickness of the adhesive layer, which varies because of the very short curing time of the adhesive and the used applying method. After thin and even cyanoacrylate adhesive layer is achieved, it can form samples that have very high bond strengths.

### **7.2.3 Pressure-sensitive adhesive tape samples**

The pressure sensitive adhesive tape 8132LE differs from other NCAs and can elongate elastically like the TPU-film (Figure 48). Even the PSA tape remains on the TPU-film after peeling, the PSA tape does not hinder the elongation of the film (and allows high displacement in the tests). Peeling of the samples can vary or stay stagnant, which depends on failure mechanism and surface roughness of the samples.

The results of PSA tape in Chapter 6.2.4 can be interpret straightforwardly. Generally, the PSA tape tends to peel in single interface at time. The stabile peeling realizes when the PSA tape remains on the TPU-film (peeling in substrate-adhesive interface), which stableness is governed by the roughness of the surface from where the PSA tape is peeled off. Even surface of the FR4 substrate has smooth peeling and rough surface of PLA substrate has wavy peeling. If the peeling happens in the other interface, in adhesive-TPU-film interface, the peeling realizes in jerks. [92]

Compared to the structural adhesives, the PSA tape can be laser cut and pressed on substrates, which makes it easy to apply. Moreover, thickness of the PSA tape does not alternate like the other adhesives that are spread over substrate in liquid form. Because the tackiness and viscoelastic behavior of the tape, it can somewhat re-attach on surfaces after peel off.

The PSA tape is easy to apply and re-attachable after peel off, which makes the long-term durability of the adhesive questionable. Altogether, there are permanent and detachable PSAs [93]. The tested PSA tape 8132LE by 3M can be used in applications such as in membrane switches and in attachment of graphics [51], which makes the PSA tape possibly usable in stretchable electronics applications. Furthermore, to attach PSA permanently and durably, the plasma pre-treatment should be used to maximize adhesion in joints.

### 7.3 Tensile testing

The tensile testing is used to measure resistance, stress and elongation of the tensile test samples. The stress and elongation are tested with the tensile test machine and the test setup for the resistance measurement of the interconnections have been presented in Figure 31. The numerical results can be compared with visual findings and effects of the varied properties of the samples can be analyzed. The behavior of the interconnections, the ACF pieces and the frame are studied.

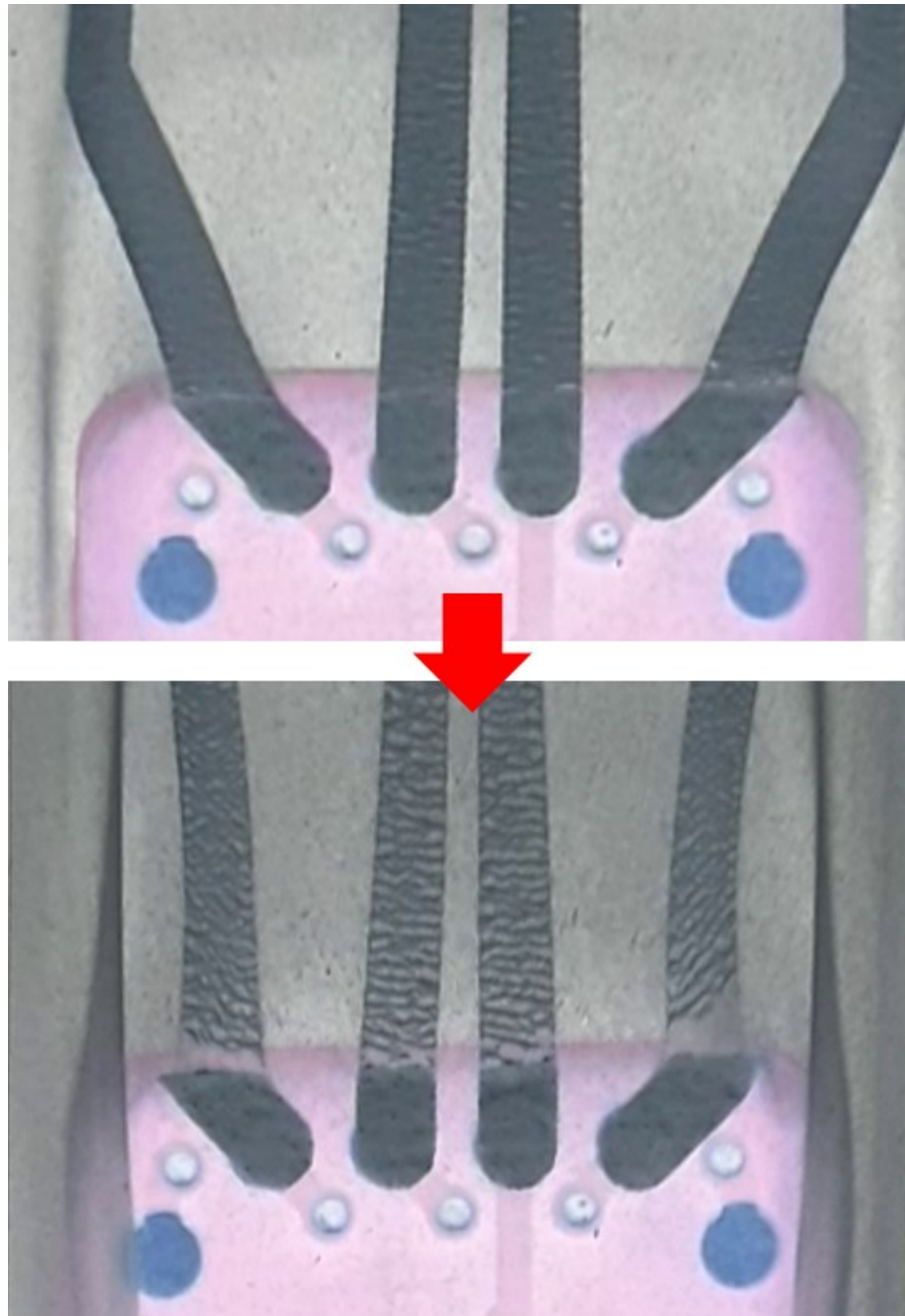
#### 7.3.1 Effect of the interconnections to failure of the samples

The sample in the tensile testing deforms and it affects the interconnections. Because the sample includes the highly elastic TPU-film and the rather stiff module, the elongation is not simple to interpret. In Figure 56, the attached module on the TPU-film obstructs uniform longitudinal elongation of the film. Next to the module, in the lengthwise of the sample, elongation of the film is high just before the edge of the module, which can be seen as folding of the film. To the longitudinal direction, the module hinders elongation that gradually decrease to zero against the module. The elongation differences show up as stress concentrations around the module.

The stress concentration around the module makes the inner and outer interconnections elongate different way. The inner tracks are completely under the stress concentration effect and they elongate uniformly at longitudinal direction. The outer tracks have 45° turns that go under the module to the contact pads (Figure 26). The stress concentration affects to the tilted part of the outer tracks, and the effect decrease when the outer tracks spread away from the module. The outer tracks spread over wider width than the module, which induces the higher longitudinal elongation of the sample sides also to the outer tracks. Consequently, starts of the outer tracks that are tilted in 45° are affected by the stress concentration effect and the straight lines of the tracks elongate more freely.

Elongation affect to the interconnections and can damage them unevenly, which can be seen in Figures 56 and 57. Typically, the highest deformation related to the elongation realizes in the edges of module. The inner tracks have simple longitudinal elongation, which form first small pre-cracks that do not go through the tracks. Later, with higher elongation, microscopic cracks onset and grow into the distinctive cracks that go through the tracks and can cause the failure. The pre-cracks and cracks are formed in the perpendicular direction to the strain. With the outer tracks, the elongation and damaging are more complex in their nature.

Like in the inner tracks, low elongation form small perpendicular pre-cracks to the outer tracks. However, when the elongation increase, the 45° tilted outer tracks (with the perpendicular pre-cracks) tend to straighten longitudinally to the strain direction. The straightening also moves the pre-cracks in the interconnections. The pre-cracks deform from the perpendicular direction to 45° angle toward the module. The pre-cracks guide formation of the distinctive cracks that are tilted according, how much the outer tracks are straightened. Figure 59 inspects the damage in the tracks in more detail and presents the observations in inverted colors.



**Figure 59.** Deformation of the interconnections under high elongation in inverted colors.

The sample in Figure 59 has 1,5 mm wide interconnections and the ACF patch. At lower elongation, there are small pre-cracks that twist and grow through the interconnections. The twisting phenomenon makes the outer tracks tear from the edge of the module unevenly. The tearing develops from outside to inside of the sample. The tearing can break the outer tracks earlier than the inner tracks, which is also presented in Figure 57.



The thickness of the interconnections affect the cracking, where the thicker 2 mm wide tracks are more durable. Generally, when the width of the track increase, the durability of the tracks increase. In the wider tracks, the cracks (damage) have to propagate longer distances to cause electrical failure. Furthermore, even the shape of the interconnections is not originally perpendicular to the elongation, the cracks are still formed perpendicularly. The tilted tracks can be locally wider than the straight tracks in the perpendicular direction, which makes the tilted tracks more durable. However, if the tilted tracks are close to the module (in the stress concentration area), they can twist and fail prematurely.

The twisting behavior is affected by the elongation of the film, which is further affected by width of the film. The width of the TPU-film in the tensile test samples is 29 mm and the results can be different if the wider film is used. With the wider film, the distance of measured interconnections to the sides of the film would be longer and the elongation distribution in the sides (and in the interconnections) would be different.

In addition to the width of the interconnections, also their length affect the results. The outer tracks are longer and they tend to straighten during the elongation, which increase potential elongation of the outer tracks. On the contrary, the inner tracks are shorter and they are already formed like the straight line, which decrease their potential elongation. The stresses induced by the elongation affect faster to the inner tracks, which can be seen as higher amount of cracks (in the stress concentration area). The higher cracking is also observed as the faster resistance increase of the inner tracks. The phenomenon is detected especially in the inner interconnections of the sample 6S in Figure 53. Furthermore, the irregularities of the upper inner track in Figure 53 are caused by poor electrical contacts of ACF strips.

### **7.3.2 Effect of the frame to failure of the samples**

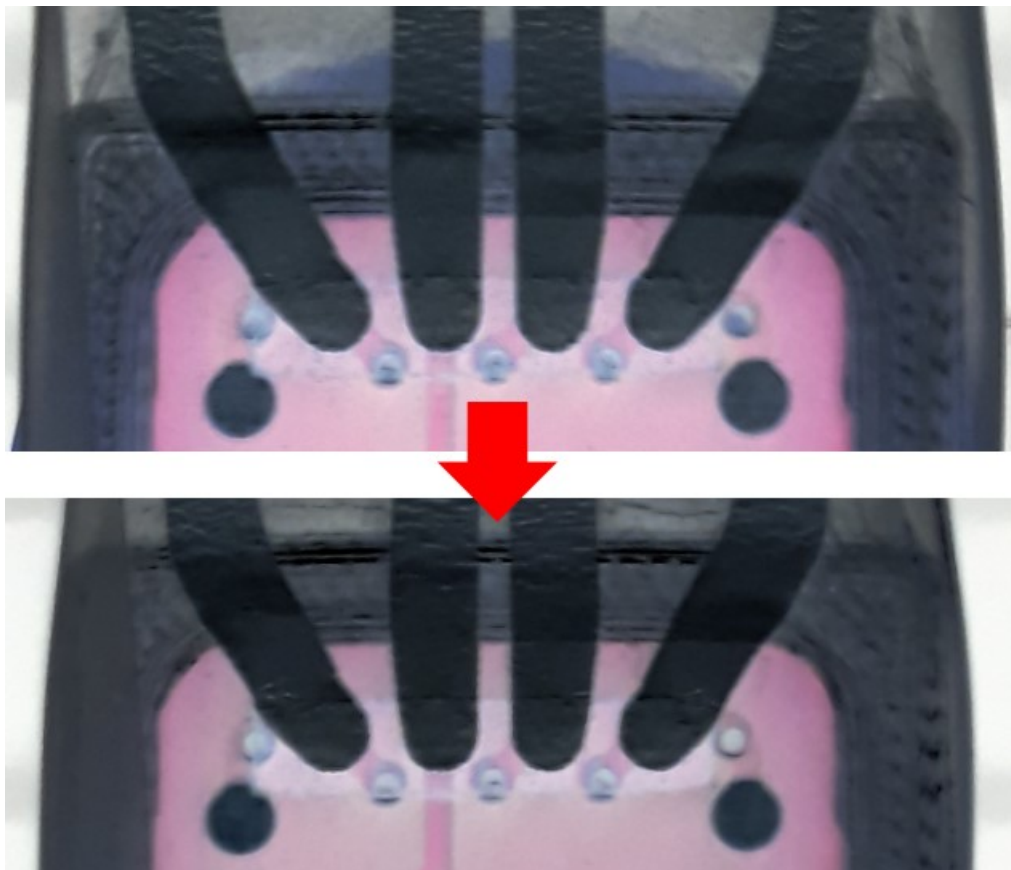
The frame is attached on the TPU-film with the PSA tape 8132LE that can deform and elongate with the TPU-film. The used PSA tape is the main component of the frame that affects to the sample. In other words, the frame is the holder of the PSA tape that restricts the elongation of the film. The PSA tape is flexible adhesive by nature and it is more compliant than the used ACF. The PSA tape elongates along the TPU-film while maintaining the stiff contact to the frame. Figure 58 presents that the PSA tape can move easily with the film and slips beyond the frame. At first, the PSA tape slips from the corners of the frame, which later expands over whole width of the frame. From the movement of the PSA, it can be concluded that the sides of the sample must have higher elongation than the middle of the sample.

The frame covers bigger area than bare module and restricts elongation of the film close to the module. As lengthwise, the frame shields inner and outer interconnections and there are no same kind of folding like in Figures 56 and 57. As longitudinal, starts of the interconnections remain under the frame and their deformation is hindered by PSA tape. The

part of tracks under the module elongate and straighten slower and initiation and propagation of the cracks is obstructed.

The purpose of the frame around of the module is to decrease the stress concentration effect and prevent detachment of the ACF. As a component the frame is simple, but still affect distinctly to the elongation values of the samples. The both minimum and maximum elongating interconnections of the tensile tests are in the framed samples, which express that the frame can change the samples either positively or negatively.

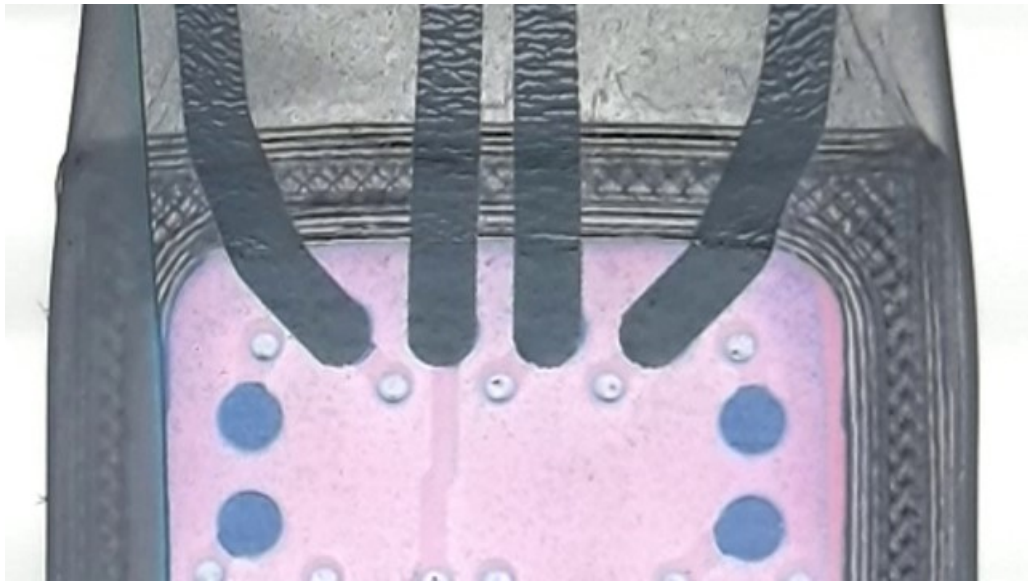
In the framed samples, cracks in the interconnections develop in the same way than in the unframed tensile test samples. However, the outer tracks have less unhindered 45° tilted part to straighten, which decreases the straightening of the outer tracks and makes them crack more perpendicularly (like the inner tracks). Figure 60 displays cracking of the sample with 2 mm wide interconnections, the ACF strips and the frame (series 4) in inverted colors.



**Figure 60.** Deformation of the tracks of the sample with 2 mm tracks, the ACF strips and the frame in inverted colors.

In Figure 60, the cracks grow from the outside of the frame to under the frame. In addition, also flaws close to the ACF strip develop. The PSA tape do not block the advance of cracks like the ACF. The PSA tape hinders the cracking and smoothens the stress concentration area as a “stress concentration reducing component” around the module.

Still, there are the stress concentrations in the framed samples and, especially, the ACF patch samples (series 3 and 7) tend to fail prematurely. The failure of the samples can be caused either by the elongation of the interconnections or pre-cracks between the frame and the ACF patch. The pre-cracks between the module and the frame in the ACF patch sample is shown in Figure 61 in inverted colors.

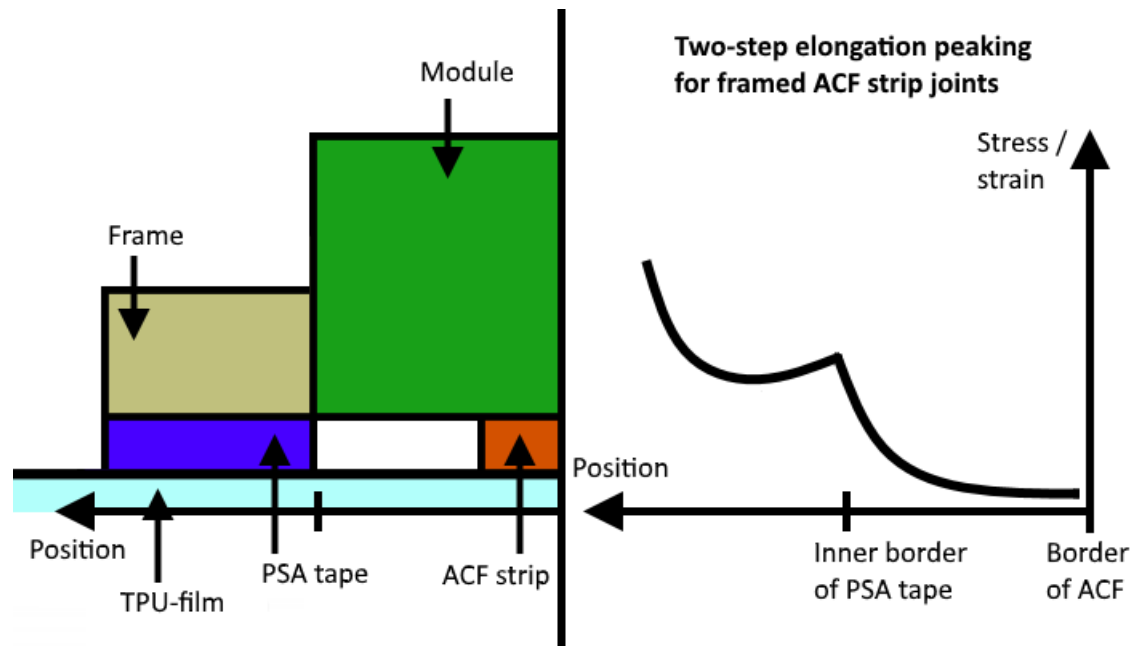


**Figure 61.** *Elongated interconnections that have damage between the module and the frame.*

In Figure 61, the elongation of the interconnections is not propagated enough to cause the perpendicular cracks between the module and the frame, which means that the cracks are not done by the elongation of the sample. The pre-cracks are formed during the preparation of the samples, when the module with the ACF patch is pressed over the sample (that has already the frame attached). The attachment of the module in the frame stresses the interconnections because the pre-attached frame hinders their elongation during the pressing. The pre-damage between the module and the frame explains the weakest interconnection of the tensile testing, which elongates 14,6 % and belongs to the sample from series 7.

In case of the frame with the ACF strips, Figures 60 and 61 display that there are not pre-damages between the frame and ACF strips. Actually, the referred sample type (from series 4) has the most elongating interconnections that can elongate even 91,7 % before failure. In the samples, the ACF strips do not cover the whole area under the frame and

the interconnections can elongate (during the preparation and testing), which prevents the cracking inside the frame. Furthermore, it can be thought that in the framed ACF strips joint elongates differently than the unframed samples, which is sketched in Figure 62.



**Figure 62.** Two-step elongation peaking for framed ACF strips joint.

There are an area of non-bonded TPU-film between the PSA tape and the ACF strip adhesives. The adhesives are attached on the TPU-film and hinder elongation of the film. At the same time, the area between the adhesives is not anyhow fixed in place. The interspace can elongate more than the adhered TPU-film under the adhesives, which changes elongation behavior of the joint. Still, the elongation of the interspace is affected by stiffness of the adhesives and elasticity of the TPU-film.

Moreover, the framed ACF strips sample have less amount of ACF (and mechanical support) under the module than the ACF patch sample and thus has smaller rigid area under the module. Therefore, in the ACF strips samples, the stress concentration affects over smaller area than in the ACF patch samples.

Despite the high elongation, there are still some flaws in the ACF strips samples, which are located close to the ACF. The flaws indicate that the pressing of the ACF stresses the interconnections at any rate and forms the flaws that may in some point advance to the failures of tracks. However, the results show that the framed samples increase the elongation of the samples when the ACF is not fitted too tightly inside the frame.

### 7.3.3 Effect of the ACF to failure of the samples

Compared to the interconnection failure, the failure of the electrical contacts is difficult to assess from visual data. The failure of the contacts can happen if the contacts are prematurely poor or are damaged during elongation of the sample. From the results, exceptional resistance increases indicate the contact failure.

The amount of the ACF affects to durability of the sample, where higher amount of ACF supports the sample mechanically better and forms more stable contacts. The ACF patch adheres completely the module on the TPU-film and has some adhered area between the contacts and the edges of module. The excess ACF between the contacts and the edges protects the contacts from deformations. Moreover, the ACF patch binds the TPU-film under the module and restricts its movement.

Unlike the large ACF patch, the ACF strips are small ACF pieces that cover only the electrical contacts. With the ACF strips, stresses are directly induced to the contacts, which make the contacts more vulnerable to the damages. For example, in Figure 57, the ACF strips are moved. That indicates that the ACF strips have deformed and the contacts may have damaged. Moreover, TPU-film under the module is not anyhow supported and it deforms. The elongation stresses the outer contacts and forms curved folding next to the contacts, which can be also seen in Figure 57.

Adding the frame around the module change stress concentration away from the ACF. In principle, in the framed ACF patch samples, the frame is additional protection of the contacts and increases the durability of the joint. However, the preparation process of the framed ACF patch samples can damage the interconnections and cancel the benefits of the frame.

The benefits of the frame are introduced best in the ACF strips samples, for which contacts normally do not last. The frame shields the contacts and decrease the stress concentration effect toward them. In addition, the framed ACF strips last better than the framed ACF patch samples because the strips are not packed too tightly inside the frame and there remain some non-bonded TPU-film that can comply the elongation.

In addition to the amount of the adhesive, the surface properties of the contacts and the solder masked PCB is different. The contacts are composed of thin layer of copper, which can have different adhesion to the ACF than the green colored solder mask. For instance, during the lamination of the ACF, the copper contacts conduct heat much better than the solder masked area. Good heat conductivity of the contacts can increase adherence of the ACF to the contacts. High adhesion between the contacts and ACF could explain the surprisingly good results of the ACF strips.

Furthermore, the preparation process affects to the quality of the contacts. The ACF patch samples are easier to prepare than the ACF strips samples, which can make the

contacts of the ACF patch samples more durable and behave in a more stable way. If the preparation of the ACF strips samples is improved, some random irregularities of the samples can be removed.

## 8. CONCLUSIONS AND FOLLOW-UP WORK

### 8.1 Conclusions

This thesis investigated properties of stretchable electronics in multiple levels. The wettability of the elastic substrate and effect of the pre-treatments to the substrate were examined. The wettability improves the most with the plasma pre-treatment that increases the wettability tens of percent. The droplets of grade 1 water spread 45 % and ethylene glycol spread 63 % more on the plasma treated surface compared to the untreated surface.

Adhesion and peel behaviour of six NCAs between the elastic substrate and rigid substrates were studied in the peel tests. The failure of the epoxy adhesives and the polyurethane adhesive samples were affected by surface roughness of rigid substrates. The complex adhesion failure increased bond strength of the samples. The other structural adhesive samples, the cyanoacrylate samples, had cohesive failure. The cohesive failure was primarily affected by thickness of the adhesive layer. The short curing time of the adhesive accomplice thickness variations of the adhesive layer, which also caused the variations to the results. The adding of primer shortened the curing time of the cyanoacrylate adhesive. When the adhesive layer thickness was optimal, the cyanoacrylate sample achieved high bond strength (0,5 N/mm). The PSA tape had the most constant peel force (between 0,2 – 0,3 N/mm) when the peeling realized as adhesion failure in the substrate-adhesive interface. In the PSA samples, the TPU-film elongated during the peel tests, which can affect the results.

The tensile testing of the stretchable electronics samples presented that wider interconnections lasted better than thinner interconnections. In addition, the shape of the interconnections affected the deformation of interconnections. Without the frame, the samples with the larger amount of ACF were more durable than the samples with the low amount of ACF. However, the maximum elongating interconnection of the ACF strips samples regularly elongated over 40 % before failure, what were significant results for the samples.

The frame in the tensile test samples increased or decreased the elongation of interconnections. The frame decreased the elongation because the preparation of framed samples created damages in the interconnections. According to the stress peaking concept, the frame increased the elongation because it smoothed the stress concentration near the module and protected the contacts. The framed ACF strips samples had high maximum elongations (up to 91,7 %) because the small amount of ACF bound small amount of TPU-film in place inside the frame (and thus had the smaller stress concentration. Minimizing and spreading the stress concentration in the stretchable electronics increase elongation of the interconnections.

## 8.2 Follow-up work

The object was to introduce different kinds of testing methods to the field of stretchable electronics, which can be used to examine applicability of materials and design of stretchable structures. The results of the implemented tests point out improvable matters that can be taken into account as alone or as whole.

In future, the plasma pre-treatment can be used to increase wettability of the TPU-film, which makes easier to evenly apply liquid adhesive on the substrate. The plasma pre-treatment could be used to control adhesive layer thickness of the cyanoacrylate adhesive samples or to ensure more durable substrate-adhesive interface adhesion failure in the PSA tape samples. Furthermore, the plasma pre-treatment can increase adherence of the conductive ink and make the interconnections more durable.

In addition to the usage of plasma pre-treatment, benefits of the frame structure around the rigid islands (or modules) need more study. The NCA under the frame hinders deformation of elastic substrate. By developing fabrication processes and choosing the best NCA under the frame (via peel tests), the effect of the frame can be optimized. The frame makes deformations of the stretchable electronics structure more complex, which should be examined in more detail, especially when there are unbounded highly elastic substrate between the frame and conductive adhesive. Moreover, the shape of the frame can be varied, for example, to the clover shape [30]. The shape can be used to control elongation of elastic substrate outside the frame.



## REFERENCES

- [1] H. Mattila, Wearable technology for snow clothing, in: X. Tao (ed.), *Smart fibres, fabrics and clothing*, The Textile Institute, Woodhead Publishing, 2001, pp. 246-253.
- [2] L.V. Langenhove, Smart Textiles: Past, Present, and Future, in: X. Tao (ed.), *Handbook of Smart Textiles*, Springer Singapore, 2015, pp. 1035-1058.
- [3] D.J. Lipomi, Stretchable Figures of Merit in Deformable Electronics, *Advanced Materials*, Vol. 28, Iss. 22, 2016, pp. 4180-4183.
- [4] J. Vanfleteren, M. Gonzalez, F. Bossuyt, Y.-Y. Hsu, T. Vervust, I. De Wolf, M. Jablonski, Printed circuit board technology inspired stretchable circuits, *MRS Bulletin*, Vol. 37, Iss. 3, 2012, pp. 254-260.
- [5] R. Viero, T. Loher, M. Seckel, C. Dils, C. Kallmayer, A. Ostmann, H. Reichl, Stretchable Circuit Board Technology and Application, 2009 International Symposium on Wearable Computers Linz, Austria, September 4-7, 2009, IEEE, pp. 33-36.
- [6] K. Kim, K. Jung, S. Jung, Design and fabrication of screen-printed silver circuits for stretchable electronics, *Microelectronic Engineering*, Vol. 120, 2014, pp. 216-220.
- [7] O. Atalay, W.R. Kennon, E. Demirok, Weft-Knitted Strain Sensor for Monitoring Respiratory Rate and Its Electro-Mechanical Modeling, *IEEE Sensors Journal*, Vol. 15, Iss. 1, 2015, pp. 110-122.
- [8] S. Merilampi, T. Laine-Ma, P. Ruuskanen, The characterization of electrically conductive silver ink patterns on flexible substrates, *Microelectronics Reliability*, Vol. 49, Iss. 7, 2009, pp. 782-790.
- [9] T. Houghton, J. Vanjaria, H. Yu, Conductive and Stretchable Silver-Polymer Blend for Electronic Applications, 2016 IEEE 66th Electronic Components and Technology Conference (ECTC), IEEE, 2016, pp. 812-816.
- [10] M. Inoue, Y. Amano, Y. Tada, Design of printed E-textile probes to suppress electrocardiography noise, 2017 International Conference on Electronics Packaging (ICEP), IEEE, 2017, pp. 464-465.

- [11] M. Inoue, Y. Itabashi, Y. Tada, Development of bimodal electrically conductive pastes with Ag micro- and nano-fillers for printing stretchable E-textile systems, 2015 European Microelectronics Packaging Conference (EMPC), IEEE, pp. 1-5.
- [12] I. Sinclair, J. Dunton, Resistors, in: Practical Electronics Handbook, 6th ed. Elsevier Science & Technology, Jordan Hill, 2007, pp. 1-28.
- [13] R. Paradiso, L. Caldani, M. Pacelli, Knitted Electronic Textiles, in: E. Sazonov (ed.), M.R. Neuman (ed.), Wearable Sensors : Fundamentals, Implementation and Applications, Elsevier Science, San Diego, 2014, pp. 153-174.
- [14] S. Merilampi, T. Björninen, V. Haukka, P. Ruuskanen, L. Ukkonen, L. Sydänheimo, Analysis of electrically conductive silver ink on stretchable substrates under tensile load, Microelectronics Reliability, Vol. 50, Iss. 12, 2010, pp. 2001-2011.
- [15] K.R.R. Venkata, A.K. Venkata, P.S. Karthik, P.S. Surya, Conductive silver inks and their applications in printed and flexible electronics, RSC Adv, Vol. 5, Iss. 95, 2015, pp. 77760-77790.
- [16] S. Zhang, H. Zhang, G. Yao, F. Liao, M. Gao, Z. Huang, K. Li, Y. Lin, Highly stretchable, sensitive, and flexible strain sensors based on silver nanoparticles/carbon nanotubes composites, Journal of Alloys and Compounds, Vol. 652, 2015, pp. 48-54.
- [17] Membrane Switches, Engineered Conductive Materials, web page. Available (accessed on 05.01.2018): [http://www.conductives.com/membrane\\_switches.php](http://www.conductives.com/membrane_switches.php).
- [18] CI-1036 Technical Data Sheet, Engineered Conductive Materials, 2010.
- [19] B. Goss, Practical Guide to Adhesive Bonding of Small Engineering Plastic and Rubber Parts, Smithers Rapra Technology, 2010, 194 p.
- [20] T. Vuorinen, A. Vehkaoja, V. Jeyhani, K. Noponen, A. Onubeze, T. Kankkunen, A. Puuronen, S. Nurmentaus, S.P. Preejith, J. Joseph, T. Seppänen, M. Sivaprakasam, M. Mäntysalo, Printed, skin-mounted hybrid system for ECG measurements, 2016, 6 p.
- [21] J.R. Greer, R.A. Street, Thermal cure effects on electrical performance of nanoparticle silver inks, Acta Materialia, Vol. 55, Iss. 18, 2007, pp. 6345-6349.
- [22] SFS-EN ISO 527-1, Plastics. Determination of Tensile Properties. Part 1: General Principles, Finnish Standards Association, Helsinki, 2012, 27 p.

- [23] L.W. McKeen, Introduction to Plastics, Polymers, and Their Properties, in: L.W. McKeen, Effect of Temperature and Other Factors on Plastics and Elastomers, 3rd ed. Elsevier, Pennsylvania, USA, 2014, pp. 1-45.
- [24] D.A. Dillard, Stress distribution: Poisson's ratio, in: D.E. Packham (ed.), Handbook of Adhesion, 2nd ed. John Wiley & Sons, Bath, UK, 2005, pp. 499-501.
- [25] G.H. Michler, Atlas of Polymer Structures - Morphology, Deformation and Fracture Structures, Hanser Publishers, Munich, Germany, 2016, 602 p.
- [26] I. Yilgör, E. Yilgör, G.L. Wilkes, Critical parameters in designing segmented polyurethanes and their effect on morphology and properties: A comprehensive review, Polymer, Vol. 58, 2015, pp. 1-36.
- [27] M.A. Hood, B. Wang, J.M. Sands, J.J. La Scala, F.L. Beyer, C.Y. Li, Morphology control of segmented polyurethanes by crystallization of hard and soft segments, Polymer, Vol. 51, Iss. 10, 2010, pp. 2191-2198.
- [28] Product Information Platilon U, Covestro, 2016.
- [29] M. Schwartz, Soldering - Understanding the Basics, ASM International, Ohio, USA, 2014, 198 p.
- [30] P. Iso-Ketola, J. Vanhala, M. Mäntysalo, The stretching structure for the preparation of a conductive path comprising the structure and the method, Pat. FI 127173 B, Hak.nro. 20165724, 27.09.2016, (29.12.2017), 36 p.
- [31] S.B. Jung, J.W. Kim, Electrical Industry, in: L.F.M. da Silva (ed.), A. Öchsner (ed.), R.D. Adams (ed.), Handbook of Adhesion Technology, Springer, Berlin, Heidelberg, 2011, pp. 1289-1313.
- [32] C. Goth, Interconnection Technology, in: J. Franke (ed.), Three-Dimensional Molded Interconnect Devices (3D-MID) - Materials, Manufacturing, Assembly, and Applications for Injection Molded Circuit Carriers, Hanser Publishers, Munich, Germany, 2014, pp. 139-171.
- [33] I. Singh, K. Debnath, A. Dvivedi, Mechanical Joining, in: V.K. Thakur, A.S. Singha (ed.), Biomass-based Biocomposites, Smithers Rapra Technology, UK, 2013, pp. 154-160.
- [34] T. Loher, M. Seckel, R. Viero, C. Dils, C. Kallmayer, A. Ostmann, R. Aschenbrenner, H. Reichl, Stretchable electronic systems: Realization and applications, 2009 11th Electronics Packaging Technology Conference, 2009, pp. 893-898.

- [35] B. Kneafsey, Structural adhesives, in: D.E. Packham (ed.), Handbook of Adhesion, 2nd ed. John Wiley & Sons, Bath, UK, 2005, pp. 505-508.
- [36] SFS-EN 923, Adhesives. Terms and definitions, Finnish Standards Association, Helsinki, 2015, 43 p.
- [37] E. Sancaktar, Classification of Adhesive and Sealant Materials, in: L.F.M. da Silva (ed.), A. Öchsner (ed.), R.D. Adams (ed.), Handbook of Adhesion Technology, Springer, Berlin, Heidelberg, 2011, pp. 261-290.
- [38] D. Dunn, Update on Engineering and Structural Adhesives, Smithers Rapra, Shrewsbury, 2010, 198 p.
- [39] J. Bishopp, Epoxide adhesives, in: D.E. Packham (ed.), Handbook of Adhesion, 2nd ed. John Wiley & Sons, Bath, UK, 2005, pp. 147-150.
- [40] J. Bishopp, Epoxide adhesives: curatives, in: D.E. Packham (ed.), Handbook of Adhesion, 2nd ed. John Wiley & Sons, Bath, UK, 2005, pp. 150-155.
- [41] G. Mittal, K.Y. Rhee, V. Mišković-Stanković, D. Hui, Reinforcements in multi-scale polymer composites: Processing, properties, and applications, Composites Part B: Engineering, Vol. 138, 2018, pp. 122-139.
- [42] PERMABOND® ET515 Technical Datasheet, Permabond®, 2016, 2 p. Available: <https://www.permabond.com/technical-datasheets/>.
- [43] PERMABOND® MT382 Technical Datasheet, Permabond®, 2018, 2 p. Available: <https://www.permabond.com/technical-datasheets/>.
- [44] Scotch-Weld™ EPX™ Clear Adhesive DP610 Product Data Sheet, Suomen 3M Oy, 2011, 4 p.
- [45] J. Guthrie, Cyanoacrylate adhesives, in: D.E. Packham (ed.), Handbook of Adhesion, 2nd ed. John Wiley & Sons, Bath, UK, 2005, pp. 96-99.
- [46] LOCTITE® 406 Technical Datasheet, Henkel Ltd, 2012, 3 p. Available: [http://www.henkel-adhesives.co.uk/2838\\_UKE\\_HTML.htm?no-deid=8797712023553](http://www.henkel-adhesives.co.uk/2838_UKE_HTML.htm?no-deid=8797712023553).
- [47] LOCTITE® SF 7239 Primer Technical Datasheet, Henkel Ltd, 2015, 2 p. Available: [http://www.loctite.fi/Loctite-4087.htm?no-deid=8802628272129&msdsLanguage=FI\\_FI&selectedTab=document](http://www.loctite.fi/Loctite-4087.htm?no-deid=8802628272129&msdsLanguage=FI_FI&selectedTab=document).
- [48] D.W. Aubrey, Pressure-sensitive adhesives, in: D.E. Packham (ed.), Handbook of Adhesion, 2nd ed. John Wiley & Sons, Bath, UK, 2005, pp. 363-365.

- [49] D.W. Aubrey, Pressure-sensitive adhesives – adhesion properties, in: D.E. Packham (ed.), Handbook of Adhesion, 2nd ed. John Wiley & Sons, Bath, UK, 2005, pp. 365-368.
- [50] F.C. Campbell, Pressure-Sensitive Adhesives, in: F.C. Campbell (ed.), Joining - Understanding the Basics, ASM International, Ohio, USA, 2011, p. 261.
- [51] Adhesive Transfer Tapes with Adhesive 300LSE Technical Datasheet, 3M, 2017, 5 p. Available: [https://www.3m.com/3M/en\\_US/company-us/all-3m-products/~/3M-Adhesive-Transfer-Tape-Double-Lined-8132LE/?N=5002385+3293242520&rt=rud](https://www.3m.com/3M/en_US/company-us/all-3m-products/~/3M-Adhesive-Transfer-Tape-Double-Lined-8132LE/?N=5002385+3293242520&rt=rud).
- [52] Y. Sakaniwa, M. Iida, Y. Tada, M. Inoue, Conduction path development in electrically conductive adhesives composed of an epoxy-based binder, 2015 International Conference on Electronic Packaging and iMAPS All Asia Conference (ICEP-IAAC), IEEE, 2015, pp. 252-257.
- [53] Y. Han, B. Zhang, P. Zhu, Q. Liu, Y. Hu, R. Sun, C. Wong, Preparation of highly conductive adhesives by insitu incorporation of silver nanoparticles, 2016 17th International Conference on Electronic Packaging Technology (ICEPT), IEEE, 2016, pp. 434-438.
- [54] J. Luo, Z. Cheng, C. Li, Q. Li, L. Wang, C. Yu, Y. Zhao, M. Chen, Y. Yao, Electrically conductive adhesives based on thermoplastic polyurethane filled with silver flakes and carbon nanotubes, Composites Science and Technology, Vol. 129, 2016, pp. 191-197.
- [55] M. Chae, E. Ouyang, Strip warpage analysis of a flip chip package considering the mold compound processing parameters, 2013 IEEE 63rd Electronic Components and Technology Conference, IEEE, 2013, pp. 441-448.
- [56] S. Li, X. He, J. Hao, J. Zhou, F. Xue, Investigation of properties and curing process of silver paste electrically conductive adhesives (ECAs), 2017 18th International Conference on Electronic Packaging Technology (ICEPT), IEEE, 2017, pp. 275-279.
- [57] Y. Lin, J. Zhong, A review of the influencing factors on anisotropic conductive adhesives joining technology in electrical applications, Journal of Materials Science, Vol. 43, Iss. 9, 2008, pp. 3072-3093.
- [58] tesa HAF<sup>®</sup> 8412 product information, tesa, 2017, 2 p.
- [59] Low Temperature Solder, Indium Corporation, 2016, 2 p. Available: <http://www.indium.com/technical-documents/product-data-sheets/#solar-materials>.

- [60] W.A. Hufenbach, F. Adam, T. Möbius, D. Weck, A. Winkler, Experimental Investigation of Combined Electrical and Mechanical Joints for Thermoplastic Composites, ANTEC 2014 - Proceedings of the Technical Conference & Exhibition, April 28-30, 2014, Society of Plastics Engineers, Las Vegas, Nevada, USA, pp. 592-595.
- [61] D.E. Packham, Adhesion, in: D.E. Packham (ed.), Handbook of Adhesion, 2nd ed. John Wiley & Sons, Bath, UK, 2005, pp. 14-16.
- [62] D.E. Packham, Adhesion – fundamental and practical, in: D.E. Packham (ed.), Handbook of Adhesion, 2nd ed. John Wiley & Sons, Bath, UK, 2005, pp. 16-19.
- [63] L.F.M. da Silva, A. Öchsner, R.D. Adams, Introduction to Adhesive Bonding Technology, in: L.F.M. da Silva (ed.), A. Öchsner (ed.), R.D. Adams (ed.), Handbook of Adhesion Technology, Springer, Berlin, Heidelberg, 2011, pp. 1-7.
- [64] D.E. Packham, Theories of Fundamental Adhesion, in: L.F.M. da Silva (ed.), A. Öchsner (ed.), R.D. Adams (ed.), Handbook of Adhesion Technology, Springer, Berlin, Heidelberg, 2011, pp. 11-38.
- [65] M.E.R. Shanahan, Wetting and spreading, in: D.E. Packham (ed.), Handbook of Adhesion, 2nd ed. John Wiley & Sons, Bath, UK, 2005, pp. 592-594.
- [66] J.F. Padday, Wetting and work of adhesion, in: D.E. Packham (ed.), Handbook of Adhesion, 2nd ed. John Wiley & Sons, Bath, UK, 2005, pp. 594-597.
- [67] SFS-EN 10365, Adhesives. Designation of main failure patterns, Finnish Standards Association, Helsinki, 1995, 6 p.
- [68] B. Guo, G. Liu, Rheological Models, in: B. Guo (ed.), G. Liu (ed.), Applied Drilling Circulation Systems - Hydraulics, Calculations, and Models, Elsevier, 2011, pp. 21-23.
- [69] M.M. Nir, D. Zamir, I. Haymov, L. Ben-Asher, O. Cohen, B. Faulkner, F. de la Vega, Electrically Conductive Inks for Inkjet Printing, in: S. Magdassi (ed.), Chemistry of Inkjet Inks, World Scientific, 2010, pp. 225-254.
- [70] D.E. Packham, Bonds between atoms and molecules, in: D.E. Packham (ed.), Handbook of Adhesion, 2nd ed. John Wiley & Sons, Bath, UK, 2005, pp. 60-62.
- [71] K.W. Allen, Theories of adhesion, in: D.E. Packham (ed.), Handbook of Adhesion, 2nd ed. John Wiley & Sons, Bath, UK, 2005, pp. 535-538.

- [72] R.A. Wolf, Chemical Plasma Treatment Technologies: Features and Application Benefits, in: R.A. Wolf (ed.), Plastic Surface Modification - Surface Treatment, Decoration, and Adhesion, Hanser Publishers, 2010, pp. 53-81.
- [73] G. Critchlow, General Introduction to Surface Treatments, in: L.F.M. da Silva (ed.), A. Öchsner (ed.), R.D. Adams (ed.), Handbook of Adhesion Technology, Springer, Berlin, Heidelberg, 2011, pp. 119-146.
- [74] SFS-EN 13887, Structural adhesives. Guidelines for surface preparation of metals and plastics prior to adhesive bonding, Finnish Standards Association, Helsinki, 2004, 31 p.
- [75] R.P. Wool, Polymer diffusion: reptation and interdigitation, in: D.E. Packham (ed.), Handbook of Adhesion, 2nd ed. John Wiley & Sons, Bath, UK, 2005, pp. 341-344.
- [76] R.P. Wool, Polymer-polymer adhesion: models, in: D.E. Packham (ed.), Handbook of Adhesion, 2nd ed. John Wiley & Sons, Bath, UK, 2005, pp. 347-350.
- [77] R.P. Wool, Polymer-polymer adhesion: molecular weight dependence, in: D.E. Packham (ed.), Handbook of Adhesion, 2nd ed. John Wiley & Sons, Bath, UK, 2005, pp. 350-352.
- [78] R.P. Wool, Polymer-polymer adhesion: incompatible interfaces, in: D.E. Packham (ed.), Handbook of Adhesion, 2nd ed. John Wiley & Sons, Bath, UK, 2005, pp. 344-347.
- [79] D.A. Dillard, Stress distribution: mode of failure, in: D.E. Packham (ed.), Handbook of Adhesion, 2nd ed. John Wiley & Sons, Bath, UK, 2005, pp. 496-499.
- [80] X. Lan, S. Ji, N.-A. Noda, Y. Cheng, The Effect of Geometric Configurations on the Elastic Behavior of an Edge-Cracked Bonded Strip, Advances in Materials Science and Engineering, Vol. 2017, 2017, 11 p.
- [81] D.A. Dillard, Stress distribution: stress singularities, in: D.E. Packham (ed.), Handbook of Adhesion, 2nd ed. John Wiley & Sons, Bath, UK, 2005, pp. 503-505.
- [82] D.E. Packham, Surface energy, in: D.E. Packham (ed.), Handbook of Adhesion, 2nd ed. John Wiley & Sons, Bath, UK, 2005, pp. 514-517.
- [83] J.F. Watts, Surface Characterization and its Rôle in Adhesion Science and Technology, in: L.F.M. da Silva (ed.), A. Öchsner (ed.), R.D. Adams (ed.), Handbook of Adhesion Technology, Springer, Berlin, Heidelberg, 2011, pp. 179-207.

- [84] D.E. Packham, Surface energy components, in: D.E. Packham (ed.), Handbook of Adhesion, 2nd ed. John Wiley & Sons, Bath, UK, 2005, pp. 517-520.
- [85] SFS-EN 828, Adhesives. Wettability. Determination by measurement of contact angle and surface free energy of solid surface, Finnish Standards Association, Helsinki, 2013, 12 p.
- [86] Y. Liu, Q. Sheng, S. Muftu, A. Khademhosseini, M.L. Wang, M.R. Dokmeci, A stretchable and transparent SWNT strain sensor encapsulated in thin PDMS films, 2013 Transducers & Eurosensors XXVII: The 17th International Conference on Solid-State Sensors, Actuators and Microsystems (TRANSDUCERS & EUROSENSORS XXVII), IEEE, 2013, pp. 1091-1094.
- [87] Piezobrush® PZ2 - Handheld device for universal application, Relyon Plasma GmbH, 2017, 2 p. Available: <https://www.relyon-plasma.com/relyon-plasma-products/piezobrush-pz2/?lang=en>.
- [88] D.E. Packham, Peel tests, in: D.E. Packham (ed.), Handbook of Adhesion, 2nd ed. John Wiley & Sons, Bath, UK, 2005, pp. 311-315.
- [89] B.A. Morris, Fracture Mechanics Analysis of Peel Test, in: B.A. Morris (ed.), Science and Technology of Flexible Packaging - Multilayer Films from Resin and Process to End Use, Elsevier, 2017, pp. 354-360.
- [90] M.A. Mohamed, J. Jaafar, A.F. Ismail, M.H.D. Othman, M.A. Rahman, Fourier Transform Infrared (FTIR) Spectroscopy, in: N. Hilal (ed.), A.F. Ismail (ed.), T. Matsuura (ed.), D. Oatley-Radcliffe (ed.), Membrane Characterization, Elsevier B.V., 2017, pp. 3-29.
- [91] D.A. Dillard, Stress distribution: bond thickness, in: D.E. Packham (ed.), Handbook of Adhesion, 2nd ed. John Wiley & Sons, Bath, UK, 2005, pp. 494-496.
- [92] S. Sun, M. Li, A. Liu, A review on mechanical properties of pressure sensitive adhesives, International Journal of Adhesion and Adhesives, Vol. 41, 2013, pp. 98-106.
- [93] M.M. Feldstein, E.E. Dormidontova, A.R. Khokhlov, Pressure sensitive adhesives based on interpolymer complexes, Progress in Polymer Science, Vol. 42, 2015, pp. 79-153.